THE UNIVERSITY OF CHICAGO

# AN ATOPIC MICROBIOTA MEDIATES INTESTINAL INFLAMMATION THROUGH TLR4 SIGNALING

A DISSERTATION SUBMITTED TO
THE FACULTY OF THE DIVISION OF THE BIOLOGICAL SCIENCES
AND THE PRITZKER SCHOOL OF MEDICINE
IN CANDIDACY FOR THE DEGREE OF
DOCTOR OF PHILOSOPHY

COMMITTEE ON MICRIOBIOLOGY

BY

EVELYN S. CAMPBELL

CHICAGO, ILLINOIS

AUGUST 2022

# DEDICATION

*I dedicate this thesis to my family, my ancestors, and my community.*

**Table of contents**

## List of Abbreviations

AD: atopic dermatitis

BLG: β-lactoglobulin

CMA: Cow's milk allergy

CT: Cholera toxin

DC: Dendritic cells

DMEM: Dulbecco's Modified Eagle Medium

ELISA: Enzyme-linked immunosorbent assay

FBS: Fetal Bovine Serum

GF: Germ-free

GRAF: Gnotobiotic Research Animal Facility

HDM: house dust mite

IBD: Inflammatory Bowel Disease

IEC: Intestinal epithelial cells

ILC: Innate lymphoid cells

IL: Interleukin

LPS: Lipopolysaccharide

NCCDs: Non-communicable chronic disease

PBS: Phosphate-buffered saline

PcoA: Principal Coordinate Analysis

PRR: Pattern recognition receptor

qRT-PCR: Quantitative Real Time Polymerase Chain Reaction

RT: Room Temperature

SAA: Serum amyloid A

SPF: Specific Pathogen Free

TLR: Toll-like receptor

Treg: Regulatory T cells

TSLP: Thymic stromal lymphopoietin

**List of Figures**

**List of Tables**

**Acknowledgments**

I would first like to acknowledge members of the Nagler lab, past and present, for their support throughout this journey. I of course want to thank Dr. Cathryn (Cathy) Nagler, my thesis advisor and mentor, for her guidance and support throughout this process. Through her, I've learned so many lessons that I will take with me not only in my next phase but for the rest of my life. Some of these lessons stem from a professional standpoint, like how to do thorough, rigorous work. Others stem from a personal standpoint, like how to extend empathy and patience towards other humans. Both types of lessons are extremely important in this journey of life and by meeting Cathy, I have become a stronger and more refined version of myself. I would also like to thank my colleagues from the Nagler lab. I have been extremely blessed to work with and learn from such a diverse group of people. I've expanded so much of my worldly views just through our non-scientific conversations. In these conversations, we've all been able to see each other as humans beyond the four walls of the lab with a past, present, and future that have shaped us into who we are; remembering this rudimentary, but important, fact has always reminded me to put things into perspective. I appreciate the times outside the lab hanging out with Ande Hesser, Andrea Kemter, Matt Bauer, Lisa Maccio-Marretto, and Rob Patry (and Kendra, who is pretty much an honorary Nagler lab member at this point). I also want to thank Mohamed Bashir for his support and wisdom during my time in the lab. Bottom line, I've learned so much from you all scientifically and personally, and I'm lucky to have lab mates that truly care for me the way you all have.

Next, I would like to thank my friends that I have made at UChicago over the course of these six years. I want to thank my Science Sista Elaine Kouame, who I am so grateful

to have started and ended this journey with. Watching each other grow through this process has truly been a blessing and I wouldn't have wanted to do this with anyone else. I also want to thank my other friends Michael Okoreeh, Will Wagstaff, Paul Cato, Sophia Carryl and the Micro Gals for the laughs, the cries, and the all-around good company that every one of you have been to me.

Lastly, I would like to thank Dr. Lisa Abston, Dr. Dominique Carter, Dr. Elizabeth Wayne, Dr. Celina Chatman Nelson, and Dana Bozeman for serving as mentors and role models for me and helping me see this entire process through. Dr. Abston, who served as an administrator in the earlier portion of my PhD, created a safe space for me and other black students not only to build strong communal bonds but learn from each other on how to navigate academia. These efforts were crucial for my retention earlier on in my PhD and I am so grateful to had met her. Dr. Carter and Dr. Wayne came later in my graduate school tenure and took time out of their day to talk to me for hours and help me come up with a strategy to persevere during one of the most difficult times of my PhD. Because of their efforts, I have been able to finish what I started. I also want to thank Dr. Chatman Nelson and Dana Bozeman for providing me with opportunities to explore higher education as a career and to grow as a professional.

In conclusion, it takes a village to do great things. The aforementioned people, along with my family and friends from home, and Sorors, have played an important role in my success here at UChicago, and I am grateful to have met such amazing people along the way.

**Abstract**

The increasing prevalence of food allergies has been causally associated with the depletion of allergy protective intestinal bacteria. However, few studies have investigated the role of the gut microbiota in promoting allergic responses. In a cohort of cow's milk allergic (CMA) infants, we have identified a patient with a proinflammatory and atopic microbiota. In comparison to a healthy microbiota, this CMA microbiota has increased abundance of Bacteroidetes, a Gram-negative phylum of bacteria that has been associated with increased incidence of atopy. Using this microbiota, we investigated the host-microbe interactions that mediate these intestinal inflammatory responses. To examine these interactions, we used mice with global and conditional abrogation in TLR4 signaling, as Gram-negative bacteria signal through this receptor via membrane-derived lipopolysaccharide (LPS). We show that this donor's microbiota induces serum amyloid A1 (*Saa1*) and other Th17-, B cell-, and Th2-associated genes in the ileal epithelium. Accordingly, this microbiota also induces Th17 cells, as well as regulatory T cell populations and fecal IgA. Importantly, we used both antibiotic-treated SPF and rederived germ-free mice with a conditional mutation of TLR4 in the $CD11c^+$ compartment to demonstrate that the induction of proinflammatory genes, fecal IgA, and Th17 cells is dependent on TLR4 signaling. Furthermore, metagenomic sequencing revealed that the CMA microbiota also has increased abundance of LPS biosynthesis, which is likely derived from Bacteroidetes. Lastly, upon sensitization with β-lactoglobulin, this CMA microbiota induces a TLR4-dependent mixed type 2/type 3 response in innate lymphoid cells (ILCs) during the early phases of allergic sensitization. Taken together, our results

show that a Bacteroidetes-enriched microbiota with increased abundance of LPS genes promotes a mixed Th17/Th2 response in a subset of infants with cow's milk allergy.

## Chapter 1: Introduction

### I. Increased prevalence of atopic diseases

Atopic diseases, such as asthma, atopic dermatitis (AD), allergic rhinitis, and food allergy, have increased drastically over the past thirty years and continue to be a growing public health concern. The current rate of prevalence of pediatric asthma, food allergy, and AD is estimated to be 8.1%, 7.6%, and 20% in the United States, respectively (Pate et al., 2021; Gupta et al., 2018; Nutten et al., 2015). The incidence of these diseases is spatially and temporally connected, and commonly known as the “atopic march.” The atopic march often begins with childhood AD, followed by food allergy, allergic asthma, and rhinitis in later years (Brough et al., 2022). Though connected, these diseases manifest with different symptoms. AD is characterized as an inflammatory response of the skin that often includes itchiness, swelling, and dryness. Food allergies can encompass a gastrointestinal response that includes vomiting and diarrhea, as well as other symptoms such as urticaria, angioedema, and cardiovascular collapse. Asthma and allergic rhinitis consist of responses within the airways that can including sneezing, wheezing, and conjunctivitis. Although atopy is defined as genetic tendency to develop allergic disease, all of these diseases can be triggered by environmental antigens and induce both local (mucosal barrier) and systemic responses. Furthermore, along with other non-communicable chronic diseases (NCCDs) of Western society, such as obesity, autism, and inflammatory bowel disease (IBD), atopic diseases are influenced by a multitude of genetic and environmental factors, making these diseases difficult to

diagnose, treat, and study. While atopic diseases are inherently diverse, they can all be characterized by type 2 inflammatory responses which lead to differentiation of $CD4^+$ Th2 cells and the production of IgE.

## II. Cellular mechanisms of type 2 inflammation to environmental toxins, microbes, aeroallergens, and innocuous food antigens

Classically, atopic diseases have been characterized by aberrant type 2 responses to environmental aeroallergens and innocuous food antigens mediated by antigen specific $CD4^+$ T cells (Murphy et al., 2022). Studies over the years have elucidated a more complex and collaborative network that is involved in these responses than previously appreciated. Atopic responses involve several innate effector cells, including mast cells, basophils, eosinophils, and neutrophils, as well as immunological “watchmen”, such as type 2 innate lymphoid cells (ILC2s) and dendritic cells (DCs). These immune cells are informed by the production of alarmins by nearby barrier epithelial cells, leading to the orchestration of an elegant multicellular type 2 response. Alarmins are endogenous molecules that are constitutively produced and released upon tissue insult (Chan et al., 2012). Upon exposure to stimuli or tissue damage, epithelial cells release the classical alarmins interleukin (IL)-25, IL-33, and thymic stromal lymphopoietin (TSLP) (Peterson and Artis, 2014). While these alarmins have all been implicated in promoting type 2 inflammation, they each may have unique and nonredundant roles in mediating said inflammation. For instance, in a model of allergic asthma, IL-33 was found to be important for mediating type 2 responses in the context of low-dose house dust mite (HDM)

sensitization. However, in the context of high-dose HDM sensitization, IL-25 was more important for mediating these responses, suggesting that the circumstance of antigenic stimulation mediates distinctive production of particular alarmins (Willart et al., 2012). Interestingly, for environmental (but not food) allergens, release, and processing of these alarmins has been demonstrated to be mediated by allergen-derived proteases, providing insight into how certain allergens trigger atopic responses (Cayrol et al., 2018; Snelgrove et al., 2014). Furthermore, myeloid-derived prostaglandins, eicosanoids, and leukotrienes may also serve as alarmins that notify innate immune cells to induce a type 2 inflammatory program while also helping to fine tune these responses. These molecules have been shown to mediate migration of type 2 cells, promote the production of their effector cytokines, and suppress type 2 responses in multiple animal models (Wojno etl al., 2015; Maric et al., 2019; Salimi et al., 2017; Barnig et al., 2013; Maric et al., 2018; de Los Reyes Jiménez et al., 2020; Sawada et al., 2019). Alarmins therefore serve as the initial signal to immune cells that there has been a nearby disruption in barrier homeostasis, leading to the mounting of innate and later adaptive responses.

As members of the innate arm of the immune system, mast cells, basophils, eosinophils, and neutrophils enact immediate defense mechanisms to help initiate type 2 responses. Mast cells and basophils act as immunological time bombs, readily available to release pre-formed inflammatory mediators, such as histamine, leukotrienes, and prostaglandins during allergic responses or parasitic infections (Voehringer et al., 2013). These mediators induce numerous physiological and immunological responses, including vascular leakage, smooth muscle constriction, and inflammatory cell infiltration, which mediate allergic symptoms and parasite expulsion (Barrett and Austen, 2009). Release

of these mediators can be induced by engagement of the IgE receptor (FcεRI) by crosslinked IgE bound to antigen, making for a rapid response mediated by adaptive immunity (Msallam et al, 2020; Spadaro et al., 2020). Eosinophils are circulating and tissue resident cells that facilitate type 2 inflammation in parasitic infections and allergic diseases (Weller et al., 2017). They play a major role in the pathology of eosinophilic gastrointestinal disorders, such as eosinophilic esophagitis (EoE), which can be a comorbidity of food allergies (Furuta and Katzka, 2015). In EoE, cells of the esophageal epithelium produce eotaxin-3, which recruits infiltrating eosinophils (Blanchard et al., 2006). In patients with EoE, food antigens can elicit eosinophilic production of IL-5 and IL-13 to mediate Th2 inflammation, which can result in dysphagia and food impaction (Schmid-Grendelmeier et al., 2002; Furuta and Katzka, 2015). Lastly, neutrophils mediate cytotoxic effector functions through multiple mechanisms, including phagocytosis, degranulation of proteases, and excretion of extracellular traps consisting of chromatin strands decorated in antimicrobial peptides and cytotoxic enzymes (Wills-Karp, 2018). They are recruited to inflamed tissue by IL-17 derived from $CD4^+$ T cells, and they play a part in antigen-specific allergic responses (McKinley et al., 2008; Krishnamoorthy et al., 2018). Acting as the frontline defense against pathogens and allergens, these cells play a critical role in mediating type 2 responses expeditiously.

As part of the innate immune system, ILC2s work alongside DCs (which bridge the innate and adaptive immune systems), to initiate type 2 responses after sensing alarmins in the local environment. For instance, IL-33 potently stimulates production of IL-5 and IL-13 in ILC2s and mediates their migration to the skin during allergic responses (Salimi et al., 2013). Likewise, DCs activated with TSLP can prime naïve $CD4^+$ T cells to enact a

Th2 program through the production of IL-4, IL-5, and IL-13 (Watanabe et al., 2004; Ito et al., 2005). Crosstalk between innate cells is also important for creating a microenvironment suitable for induction of type 2 immunity. ILC2-derived IL-13 promotes the induction of CCL17 in DCs, which acts as a chemoattractant for Th2 cells and leads to their migration to the skin and lung after sensitization with an allergen (Halim et al. 2016). Furthermore, IL-4 produced by basophils has been shown to activate ILC2s and DCs in a way that leads to downstream promotion of Th2 responses (Sokol et al., 2008; Tang et al., 2010; Kim et al., 2014; Motomura et al., 2014). Generalized responses by epithelial cells and innate immune cells enact an appropriate type 2 inflammatory response toward the offending allergen, which precedes more antigen-specific responses performed by the adaptive arm.

Antigen-specific responses mediated by Th2 cells are necessary for the proper resolution of some environmental insults and helminth infections. Like ILC2s, Th2 cells express the transcription factor GATA3 and elicit type 2 inflammation in response to stimuli that includes the production of IL-5 and IL-13. Th2 and T follicular helper (Tfh) cells also produce IL-4, which primes antigen-specific B cells to class switch to IgE, the hallmark antibody isotype of type 2 inflammation (Lambrecht et al., 2017). IgE mediates enhanced immunity against enteric parasites and noxious substances and plays a role in exacerbating inflammation toward innocuous dietary and aeroallergens (Obata-Ninomiya et al., 2013; Pochanke et al., 2007; King et al., 1997; Spencer et al., 2003; Gurish et al., 2004; Schwartz et al., 2014; Starkl et al., 2016; Marichal et al. 2013). IgE signaling through FcεRI mediates mast cell degranulation of histamine, proteases, and other lysosomal enzymes, and these mediators lead to the symptoms associated with allergies and

asthma (Segal et al., 1977; Gonzalez-Espinosa et al., 2003; Schwartz et al., 1987; Schwartz et al., 1981). Symptoms can be diverse, ranging from urticaria and diarrhea to more serious manifestations, such as reduced blood pressure and airway constriction (Cardona et al., 2020).

It is hypothesized that earlier in mammalian evolutionary history, type 2 responses aided in the neutralization of toxins, entrapment of mucosal parasites, and resolution of associated tissue damage (Allen and Wynn, 2011). Due to advances in medicine and technology in modern societies, our exposure and susceptibility to ailments caused by said pathogens and toxins are limited. However, in some developing countries, infection with enteropathogens, such as helminths, is endemic. Infection with intestinal helminths induces a type 2 immune response akin to what is seen in those suffering from atopic diseases. Yet, populations with higher incidence of helminth infection have been observed to have decreased prevalence of atopy (van den Biggelaar et al.; 2000; Araujo et al. 2000). This has also been corroborated by mouse studies which show that helminth infection or exposure to helminth-derived antigens reduces allergen sensitization (Bashir et al., 2002; Zaiss et al., 2015; McSorley et al., 2012). Studies examining the dynamics of immunological responses in acute and chronic helminth infection clarifies the role of type 2 inflammation in clearing infection, which, in turn, provides insight on the development of type 2 responses toward innocuous antigens.

In the early stages of helminth infection, antigenic factors, and tissue injury lead to the robust induction of a type 2 inflammatory response (Inclan-Rico et al., 2018). This helminth-induced type 2 immune response is important for controlling pathogen load, mediating worm expulsion, and initiating tissue repair. Upon infection, helminth invasion

of tissues causes barrier damage that leads to the release of alarmins such as IL-33, IL-25, and TSLP, notifying nearby immune cells of local tissue injury. As a result, local repair mechanisms are initiated through these alarmins and subsequent effector cytokines. These alarmins promote tissue repair by inducing differentiation of reparative macrophages, driving proliferation of epithelial stem cells, and promoting re-epithelialization and wound closure (Dagher et al., 2020; Lopetuso et al.; 2018, Rak et al., 2016; Molofsky et al., 2015). Interestingly, although typically described as a prototypic Th2 response, many helminths also induce an early Th17 response as they invade barrier surfaces (Ajendra et al., 2020; Steel et al., 2019). Alarmins also mediate production of the type 2 cytokines by ILC2 and $CD4^+$ T cells, which regulate reparative macrophage function, reduce epithelial damage, and promote helminth clearance through IgE (Minutti et al., 2017; Chen et al., 2012; Schwartz et al., 2014).

In chronic helminth infection, the host develops tolerance toward the pathogen. Various helminths have been shown to have tolerogenic effects through modulation of DC function and induction of regulatory T cells (Goodridge et al., 2004). Accordingly, helminth infection reduces susceptibility to allergic sensitization through similar mechanisms, which may explain the observed decrease in atopy in populations with endemic helminth infection (Wilson et al., 2005; Layland et al., 2013). Understanding this, helminths have been explored as a therapeutic approach to address allergy (Feary et al., 2010; Mortimer et al., 2006; Bager et al., 2010). However, the use of helminths in alleviating atopy has been of varying success, highlighting the complexity of the immunological responses that meditate allergic inflammation.

Similar to helminths, microbial and environmental allergens can induce tissue injury and the release of alarmins. Common allergens such as fungal extracts, toxins, and pollens induce type 2 responses by mediating alarmin release through intrinsic protease activity (Wiesner et al., 2020; Scott et al., 2018, Ramu et al., 2018; Cayrol et al., 2018). Depending on the offending allergen, such type 2 responses and subsequent physiological manifestations are not only appropriate but necessary to counter the toxic effect of the allergen. For example, survival following challenge with honeybee venom is mediated by production of IgE and binding to FcεRIα (Marichal et al., 2013). Furthermore, physiological manifestations of an allergic response, such as sneezing, tearing, scratching, and vomiting, are mechanisms by which allergens are expelled from the body (Profet, 1991). While allergic responses have evolutionary benefit, our understanding of how less harmful antigens induce these responses remains poorly understood. One hypothesis is that exposure of harmless antigens may coincide with events or antigens that induce signals associated with damage (Florsheim et al., 2021). Innocuous antigen may be mistaken as part of an inflammatory response that is induced at the time of exposure to noxious antigen. This is the basis of experimental models of atopic diseases, as exposure to innocuous antigens without an adjuvant renders a tolerogenic response (Marinaro et al., 1995, Rezende et al., 2017). With increased exposure to pollutants and noxious substances correlating to atopic disease risk (Just et al., 2012, Pénard-Morand et al., 2010), the mechanisms that drive allergic sensitization to innocuous antigens remains an active area of investigation.

Although less appreciated, type 3 inflammatory responses have been documented to contribute to type 2 responses and may play a transient role in helminth infection and

the manifestation of atopic disease. During helminth infection, IL-17 acts as an early phase effector cytokine that regulates subsequent type 2 inflammation and increases worm expulsion by promoting intestinal muscle hypercontractility (Ajendra et al., 2020; Steel et al., 2019). However, the production of IL-17 comes at a cost, as its induction during infection increases epithelial damage (Sutherland et al., 2014). In the context of allergic disease, clinical studies have found IL-17 in the serum and bronchoalveolar lavage fluid as well as increased IL-17$^+$ CD4$^+$ T cells in lung biopsies of asthmatic patients compared to non-asthmatic patients (Al-Ramli et al., 2009; Irvin et al., 2014; Doe et al., 2010). In some mouse models, IL-17 has been shown to play an active inflammatory role. For example, epicutaneous sensitization with OVA and intranasal sensitization with HDM antigens led to neutrophilic airway inflammation that was mediated by IL-17 (He et al., 2007; Brandt et al., 2013a; Chesné et al., 2015). Furthermore, there is growing evidence that IL-17 contributes to the exacerbation of allergic asthma symptoms by mediating airway smooth muscle contraction, a hallmark of an anaphylactic response (Kudo et al., 2012; Lu et al., 2015; Lajoie et al., 2010).

Type 3 inflammation may also play a role in AD pathology. A Th17 transcriptomic profile has been observed in the inflamed skin lesions of AD patients (Esaki et al., 2016; Gittler et al., 2012; Noda et al., 2015). While these studies consist of a small sample size of patients with diverse manifestations of AD, they may provide some insight on the role of Th17 immunity in a subset of patients with AD. Mouse models of AD have been shown to exhibit enhanced type 3 inflammation, paralleling observations seen in clinical studies (Kim et al., 2020; He et al., 2007). Additionally, IL-17 has been shown to induce IL-4 production in T cells, and IL-17-deficient mice have decreased numbers of IL-4$^+$ CD4$^+$ T

cells in skin draining lymph nodes and antigen-specific IgE in the serum (Nakajima et al., 2014). However, few studies have examined a role for type 3 inflammation in food allergies. In some studies, production of IL-17 has been observed to be coregulated with type 2 responses (Perrier et al., 2010; DeLong et al., 2011), but whether type 3 inflammation plays a role in food allergies remains to be explored. Overall, it is clear that atopic diseases exhibit diverse manifestations and type 2 inflammatory responses, and depending on the disease, type 3 inflammatory responses may contribute to symptoms as well.

## III. Modulation of the immune system by the microbiota

Diverse interactions between the microbiota and the immune system are important for the establishment of an “equilibrium of immunity” and maintenance of host health (Eberl 2016). These interactions are especially crucial early in life as the immune system begins to develop. In this developmental timeframe, the microbiota imprints our mucosa-associated lymphoid tissues in a way that informs immune responses later in life (Al Nabhani et al., 2019). Early imprinting of the neonatal epithelium regulates epigenetic modification of epithelial stem cells, influencing the differentiation and function of several enterocyte lineages (Yu et al., 2015). Proper development of these enterocyte lineages is further maintained by microbial stimulation and is key for upholding barrier function. For example, sensing of enteric microbes by Paneth cells increases the production of the antimicrobial peptides REG3β and REG3γ, which decreases bacterial translocation across the epithelium (Vaishnava et al., 2008).

Epithelial cells and immune cells are part of a multicellular network that regulates barrier function, initiates responses to pathogens, and mediates tolerogenic responses toward luminal antigens (Wesemann and Nagler, 2016). The effectiveness of this collaborative network is also dependent on signals from the microbiota. Intestinal DCs produce IL-23 in response to stimulation from microbial products (Kinnebrew et al., 2012). IL-23 then induces the production of IL-22 by type 3 innate lymphoid cells (ILC3s), which is important for maintaining the epithelial barrier through multiple mechanisms, such as upregulating tight junction proteins, increasing mucin and antimicrobial peptide production, and regulating epithelial turnover (Tsai et al., 2017; Layunta et al., 2021; Lindemans et al., 2015). As a result, these cytokines play an important role in suppressing expansion of gut commensals and eliminating enteric pathogens (Nagao-Kitamoto et al., 2020; Flannigan et al., 2017). Other T cells, such as CD8$\alpha\alpha^+$ intraepithelial lymphocytes and ROR$\gamma$t$^+$Foxp3$^+$ regulatory T cells (Tregs) are induced by the microbiota and specifically suppress inflammatory responses to dietary antigens (Ohnmacht, et al., 2015; Cervantes-Barragan et al, 2017; Sujino et al, 2016). Furthermore, the microbiota shapes the production and repertoire of mucosal and systemic IgA by B cells, influencing the ecology and metabolism of bacterial and fungal communities at mucosal surfaces (Li et al., 2020; Doron et al., 2021; Rollenske et al., 2021; Okai et al., 2016). These concerted efforts by numerous cell types are coordinated by the intimate mutualistic host-microbe interactions and are important to maintaining host intestinal health.

When the microbiota is perturbed early in life, the immune system can be pathologically imprinted, leading to an increase in proinflammatory responses. Aspects of the modern lifestyle factors have been shown to contribute to this disturbance of the

microbiota, including overuse of antibiotics, Caesarean birth and formula feeding, increased urbanization, and poor dietary habits (Iweala and Nagler, 2019). Epidemiological studies have found that early disturbance of the microbiota is associated with increased incidence of numerous NCCDs, including asthma, allergy, IBDs, and obesity (Metsälä et al., 2013; Arrieta et al., 2015; Wernroth et al., 2020 Hviid et al., 2011). This has been substantiated with mouse studies as well. Nearly 20 years ago, the Nagler laboratory showed that antibiotic treatment of mice prior to weaning increases their susceptibility to allergic sensitization to food antigen (Bashir et al., 2004). Since that time, others have shown that microbial perturbation during this early window increases susceptibility to inflammation in other mouse models. In a mouse model of allergic asthma, treatment of weanlings with vancomycin, which targets Gram-positive anaerobes, increases serum OVA-specific IgE, promotes eosinophilic infiltration in the lung, and exacerbates airway hyperresponsiveness (Russell et al., 2012). In a similar model using HDM as the aeroallergen, Gollwitzer et al. showed that the neonatal lung microbiota induces Tregs and PD-L1 expression in $CD11c^+$ DCs, which prevents sensitization to HDM in the airways (Gollwitzer et al., 2015). Low microbial diversity, a consequence of early microbial perturbation, has been shown lead to increased susceptibility to oral anaphylaxis (Cahenzli et al., 2013). In a different inflammatory model, microbial colonization of GF neonates, but not GF adult mice, leads to protection from oxazalone-induced colitis that is dependent on invariant natural killer T cells (Olszak et al., 2015). Another group using this same colitis model showed that $ROR\gamma t^+$ Tregs induced by the microbiota prior to weaning also contributed to this protection (Al Nabhani

et al., 2019). Early dysbiosis and the associated dysregulation of the immune system have profound implications for host health and susceptibility to inflammatory diseases.

## IV. TLR signaling in atopic diseases

Toll-like receptors (TLRs) are a type of Pattern Recognition Receptor (PRR) that recognizes common, evolutionarily conserved motifs (Iwasaki and Medzhitov, 2010). TLRs play a major role in initiating innate immunity and mediating subsequent adaptive responses. They are expressed on a variety of cell types, particularly, epithelial cells, antigen presenting cells (APCs), B cells, and T cells and dictate immunological phenotypes based on TLR ligation as well as the local cytokine microenvironment (O'Neill et al., 2013). Humans express ten different TLRs, and these receptors recognize a wide variety of non-self, conserved epitopes, such as nucleic acids and membrane-derived products from bacteria, fungi, and viruses (O'Neill et al., 2013). Host sensing of microbially-derived products through TLRs can initiate a vast signaling pathway that dictates appropriate immune responses. These signaling pathways are initiated by several adapters, such as MyD88, MAL, TRIF, and TRAM, as well as numerous kinases to induce proinflammatory cytokines and Type I Interferons (O'Neill et al., 2013).

Detection of microbial products by host TLRs has been shown to have implications in regulating type 2 responses in models of allergic disease. Because TLRs can sense different microbial products, stimulation with certain TLRs can have protective or proallergic affects depending on the context of their stimulation. For instance, TLR9 recognizes cytosolic unmethylated DNA containing CpG motifs. Ligation of TLR9 initiates

a proinflammatory program in response to intracellular bacterial or viral infection (Volpi et al., 2013). When TLR9 is stimulated in the context of allergen exposure, it can drive Th1 rather than Th2 inflammation, generating a tolerogenic response (Bashir et al., 2004). This response can mediate protection against allergic inflammation by decreasing the production of the epithelial alarmin IL-33, decreasing type 2 cytokines production in ILC2s, inhibiting B cell class switching to IgE and IgG1, inducing Type I Interferon in pDCs, and reducing *Gata3* expression in $CD4^+$ T cells (Thio et al., 2019; Liu et al., 2003; Volpi et al., 2013). Interestingly, global knockout of TLR9 can be protective or proallergic depending on the allergen and mechanism of sensitization, highlighting the importance of the context of allergen exposure and PRR stimulation (Volpi et al., 2013, Berin and Wang, 2013).

Other TLRs that recognize microbial components that may be associated with food or aeroallergens can be important for meditating allergic inflammation. HDM, a common aeroallergen, consists of several fungal and bacterial-derived TLR ligands and induces allergic inflammation in the airways. β-glucan, a component of fungal cell walls, is abundant in HDM extracts and is recognized by TLR2. Treatment of HDM with β-glucanase, an enzyme that degrades glycan structures, or administration of HDM to TLR2-deficient mice, attenuates HDM-induced type 2 inflammation in cervical lymph nodes, which drain the upper airways (Ryu et al., 2013). TLR2 mediates allergic inflammation in the airways by inducing expression of TSLP, leading to downstream activation of basophils and DCs (Lv et al., 2018).

Bacterial flagellin, which signals through TLR5, can act as an adjuvant to induce allergic sensitization to food antigen in a dose-dependent manner. This inflammation can

be alleviated in *Tlr5*$^{-/-}$ mice or by abrogation of MyD88 signaling in CD11c$^{+}$ cells (Wilson et al., 2012). However, TLR5-mediated allergic inflammation is context dependent. In an asthma model that used a different allergen, concomitant exposure to flagellin and allergen reduced type 2 cytokines in the bronchoalveolar lavage fluid and allergen specific IgE in the serum (Shim et al., 2016). Differences in the ability of TLR5 signaling in regulating allergic inflammation could be attributed to the genetic background of the host, (C57BL/6 vs. BALB/c), method of sensitization and challenge (oropharyngeal vs. intraperitoneally/intranasally), or the antigen itself (HDM vs. OVA) (Shim et al., 2016; Wilson et al., 2012).

One the of the most well-studied TLRs in the context of allergic disease is TLR4. TLR4, the first Toll described in humans, is a host receptor for bacterial LPS (Medzhitov, et al. 1997; Chow et al., 1999). The TLR4/LPS signaling axis involves several soluble, membrane-bound, and intracellular adapters that dictate downstream signaling and cytokine production. LPS binding to TLR4 is mediated by soluble LPS-binding protein (LBP) and CD14, which can be in soluble or membrane forms (Schumann et al., 1990; Wright et al., 1990; Bazil et al, 1989). A ternary complex of LBP, CD14, and LPS can then bind TLR4/MD-2 dimers on host cell membranes. TLR4/MD-2 dimers then recruit adapter proteins that bind to TLR4's intracellular Toll/Interleukin-1 Receptor (TIR) domain, initiating signaling cascades. TLR4 can initiate signaling through MyD88 and TRIF adapters. MyD88 initiates immediate signaling through NF-κB, inducing production of TNF-α, IL-6, and IL-12 (Wesche et al., 1997; Yamamoto et al., 2002). TRIF can also mediate expression of NF-κB and proinflammatory cytokines including IFN-β, although through a delayed mechanism that includes IRF3 (Yamamoto et al., 2003; Fitzgerald et

al., 2003; Cheng et al., 2015). While these signaling pathways are distinct and can differentially activate immune cells, both adapters have been shown to be important for regulating type 2 responses (Shen et al., 2008; Hsia et al., 2015; Piggott et al., 2005).

In animal models of atopic disease, TLR4 has been shown to contribute to allergic inflammation through various mechanisms. In models of atopic dermatitis and food allergies, TLR4 signaling has been observed to have protective, non-protective, and null effects (Jeon et al., 2021; Bashir et al., 2004; Gertie et al., 2022). In animal models of allergic asthma, the most well-studied atopic disease, TLR4 has been shown to regulate type 2 responses under specific circumstances. For example, numerous studies have observed that intranasal, low-dose exposure to LPS, particularly in neonates, promotes allergic inflammation, while high doses are protective (Garcia et al., 2020, Wang and McCusker, 2006, Bachus et al., 2019, Gao et al., 2021, Eisenbarth et al., 2002, Radermecker et al., 2019). Furthermore, TLR4 expression in specific cell types elicits distinct allergic responses (Hammad et al., 2009; Tan et al., 2010; McAlees et al., 2015). Depending on the allergen, TLR4 signaling can even promote allergic inflammation (Trompette et al., 2009). As data in human studies describe various and sometimes conflicting findings about the role of TLR4 in atopy (Gehring et al., 2008; Thorne et al., 2005), coupled with the diverse manifestations of allergic disease in humans and in animal models, defining a role for TLR4 in atopy has been, and remains, controversial. However, the flexibility of TLR4 to initiate an assortment of immune responses speaks to the evolutionary advantage that multiple pathways can offer in response to the many structural variants of LPS and at various mucosal sites (Schwarzer et al., 2017; Martin et al., 2001).

As described above, the manifestation of allergic diseases involves the interaction of multiple factors, including genetics, the environment, and the microbiota. Importantly, at the interface between genetics and the microbiota lies crucial host-microbe interactions that dictate immunological responses toward environmental antigens. Using mouse models of food allergy, our lab has studied how these interactions play a role in mediating immune responses that protect against allergic sensitization to dietary antigens. However, our understanding of how these interactions may initiate immune responses that *promote* allergic sensitization toward food antigens is currently limited. In this thesis, we utilize the microbiota from a severely cow's milk allergic infant to investigate its role in mediating intestinal immune responses that contribute to allergic sensitization β-lactoglobulin, a major cow's milk allergen. This work highlights a previously unappreciated role for the microbiota in contributing to food allergy through mediating type 2 and type 3 inflammation.

## Chapter 2: Methods

### I. Recruitment of infant participants

As previously reported (Feehley et al., 2019), fecal samples from healthy infants that had no risk or history of atopic disorders were obtained from participants in a vaccination program at the University of Naples Federico II. Fecal samples from cow's milk allergic infants were obtained following diagnosis at a tertiary pediatric allergic center (Pediatric Allergy Program at the Department of Translational Medical Science of the University of Naples Federico II); Participation of infants in this study was in compliance with the Declaration of Helsinki and approved by the ethics committee of the University of Naples Federico I. Written informed consent was obtained from the parent(s) or guardian(s) of all children involved.

### II. Collection and preparation of human fecal samples

Fresh fecal samples were collected in the clinic in sterile stubs, weighed, and mixed with 2 mL of 30% glycerol in Luria-Bertani broth per 100-500 mg of feces (Feehley et al., 2019). These samples were aliquoted into sterile cryovials and immediately stored at -80 °C. Samples were shipped from Naples, Italy to the University of Chicago on dry ice, where they were stored at -80 °C until homogenization. For colonization of mice, frozen fecal samples were thawed in an anaerobic chamber. Thawed feces were mixed with 3 mm borosilicate glass beads in a sterile 50 mL tube with 2.5 mL of pre-reduced 0.05% Tween in 1X PBS cysteine and vortexed gently to dissociate. The resulting homogenate was filtered through a 100 μm filter for a total of four times. The final filtrate

was mixed with an equal volume of 30% glycerol/0.05% cysteine. The solution was aliquoted into Balch tubes with rubber stoppers and introduced into the gnotobiotic isolator. The remaining fecal homogenate was frozen in aliquots at -80 °C.

III. Mouse husbandry and care

All mice used in these experiments were housed and bred at the University of Chicago of Animal Resource Center in a specific-pathogen free (SPF) facility or the Gnotobiotic Research Animal Facility (GRAF) under a 12-hour light/dark cycle. Mouse cages were autoclaved and bedded with pine-shavings. Mice maintained in the GRAF were housed in Trexler-style flexible film isolators (Class Biologically Clean) with Ancare polycarbonate mouse cages (catalog number: N10HT). Gnotobiotic mice were fed an autoclaved diet (5K67, Purina Lab Diets; sterilized at 121 °C for 30 min) and were provided sterile infant formula (Enfamil) or water (USP grade, pH 5.2) *ad libitum* (Feehley et al., 2019). Cage bedding for gnotobiotic mice was changed daily or every other day due to leakage of formula from the bottles.

Sterility of each isolator was confirmed using culture-dependent and culture-independent methods on a weekly basis. Collected fecal pellets were homogenized and cultured in Brain-Heart Infusion, Nutrient, and Sabouraud broth at 37 °C and 42 °C under aerobic and anaerobic conditions, respectively, for 96 hours. DNA isolated from collected fecal pellets was analyzed for the presence of the 16S gene using PCR. Reaction mixtures were made using 40 μL of water, 0.5 μL of dNTP mix, (Thermo Scientific), 1 μL of 8F primer, 1 μL of 1492R primer, 0.5 μL of DreamTaq polymerase (Thermo Scientific), 5 μL of 10X DreamTaq Buffer (Thermo Scientific), and 2 μL of DNA per 50 μL reaction.

Cycling conditions for the reaction mixture entailed an activation stage at 95°C for 2 min; 40 cycles of a 30 sec hold at 95°C, a 30 sec hold at 48°C, and a 1 min hold at 72°C; and a final stage at 72°C for 10 min followed by an infinite hold at 4°C. Upon rederivation or acquisition of new animals into the gnotobiotic colony, all mice were screened for parasites, full serology profile, and/or PCR, bacteriology, and gross and histological analysis of major organs through IDEXX Radil or Charles River Lab using an Axenic Profile Screen. Specific-pathogen free mice were fed an irradiated standard chow diet (Teklad 2916, Envigo) and provided autoclaved acidified water *ad libitum*. All experiments were performed in compliance with the University of Chicago Animal Care and Use Protocols (Protocol #72039 and #72114).

IV. Mouse lines

Specific-pathogen free C57BL/6 *CD11c*$^{cre}$ and C56BL/6 *Tlr4*$^{fl/fl}$ mice were purchased from Jackson Labs. *CD11c*$^{cre}$ and *Tlr4*$^{fl/fl}$ mice were bred inhouse to obtain a *CD11c*$^{cre}$*Tlr4*$^{fl/fl}$ colony. Specific-pathogen free WT *Foxp3*$^{GFP}$ and *Tlr4*$^{-/-}$*Foxp3*$^{GFP}$mice, both on a C57BL/6J background, were bred in-house. *Foxp3*$^{GFP}$ mice, were crossed with *Tlr4*$^{-/-}$ mice (originally from Jackson Labs) to create a homozygous mutant colony. These mice were rederived by Kathy McCoy at the University of Calgary International Microbiome Center (Calgary, Alberta, CA) by two-cell embryo transfer into germ-free pseudo-pregnant recipient females and bred and maintained in flexible-film isolators. Germ-free C3H/HeN mice were provided by Tatyana Golovkina as an in-house transfer through the GRAF.

V. Colonization of experimental mice with the human infant gut microbiota

Human infant microbiota repository mice were created by gavaging 3-6-week-old C3H/HeN mice with 500 μL of prepared human infant fecal homogenate. The repository mice for each donor were housed in separate isolators to avoid microbial cross-contamination. Fecal samples from both repository and experimental mice were routinely examined through 16S rRNA sequencing analysis, which demonstrated that mouse-to-mouse transfer from repository to experimental mice by gavage was highly reproducible and stable over time. To aid in the transfer of the human infant microbiota, repository mice colonized with the healthy microbiota (Donor 1 or Donor 2) were maintained on Enfamil Infant formula (Mead Johnson Nutrition), while CMA repository mice colonized with the Donor 5 microbiota initially received Nutramigen I formula (Mead Johnson Nutrition) *ad libitum* (that is, the formula the CMA infants consumed) but were switched to Enfamil for the duration of the experiments reported in this thesis.

For colonization experiments, feces from these repository mice were collected and homogenized in 1 mL of sterile PBS. For colonization of germ-free mice with the CMA Donor 5 or healthy Donor 1 or Donor 2 microbiotas, mice were gavaged at weaning with 250 μL of freshly homogenized feces obtained from CMA or healthy repository mice. Prior to colonization, mice were fed Enfamil formula at a 1:4 dilution in water for 4 hours to aid in the transfer of the human infant microbiota. After colonization, CMA-colonized and healthy-colonized mice were housed in specialized isolators, fed standard chow, and were provided with diluted infant formula. On day 7 post-colonization, mice were sacrificed and fecal, cecal, and ileal contents were collected and stored at -20 °C.

For SPF mice, littermates were treated intragastrically with 100 µL of an antibiotic cocktail of kanamycin sulfate (4 mg/mL), gentamycin sulfate (0.35 mg/mL), colistin sulfate (8500 U/mL), metronidazole (2.15 mg/mL), and vancomycin hydrochloride (0.45 mg/mL) daily for 7 days prior to weaning. At weaning, mice were colonized by intragastric gavage with 250 µL of freshly homogenized feces obtained from CMA or healthy repository mice. SPF littermate experimental controls followed the same antibiotic treatment regimen but were left uncolonized at weaning. They were provided sterile acidified water. Mice colonized with the human infant microbiota followed the same experimental timeline as their germ-free counterparts and were sacrificed 7 days post-colonization. Intestinal contents were stored as previously described.

VI. Sensitization of mice with β-lactoglobulin (BLG)

At weaning, mice were either colonized with the human infant microbiota or left uncolonized as GF controls. On day 7 post-colonization, mice were fasted for 3 hours. Following this fast, mice were gavaged with 200 µL of sterile 0.2 M sodium bicarbonate in Ultrapure water (Gibco). The mice were allowed to rest for 30 minutes and then each mouse was gavaged with 200 µL of sterile BLG (20 mg) + cholera toxin (CT, 10µg) in 1X PBS. The food was replaced, and this procedure was repeated on day 14 post-colonization. Mice were sacrificed on day 21 post-colonization.

VII. Growth of bacterial isolates

*Parabacteroides distasonis* (DFI.1.37) was streaked from a frozen stock solution onto Anaerobic LKV Blood Agar plates (Thermo Fisher). These plates were grown for 5 days anaerobically at 37 °C. Colonies were then picked and inoculated into 5-7mL of

cooked/chopped meat broth supplemented with glucose (3g/L, Anaerobe Systems), Peptone Yeast Extract broth supplemented with glucose (10g/L, Anaerobe Systems), and Yeast Casitone Fatty Acids broth (Anaerobe Systems). These cultures were allowed to grow for 2 days. A portion of this sample was used for quantification of colony forming units (CFU) using serial dilutions on Brucella Agar supplemented with 5% sheep's blood, hemin, and vitamin K (Remel). The rest of the culture was used to create stock solutions, which were stored at -80 °C.

*Bacteroides thetaiotaomicron* (DFI.1.69), *Bacteroides vulgatus* (DFI.1.45), *Bacteroides dorei* (DFI.5.24), and *Parabacteroides distasonis* (DFI.1.37) were obtained from the Symbiotic Bacterial Strain Bank of the Duchossois Family Institute. Each bacterial strain streaked out from a frozen stock solution into 5 mL of Brain-Heart Infusion media supplemented with L-cysteine (0.5 mg/ml), menadione (10 ng/mL), and hemin (1 ng/mL). Cultures were grown for 3-5 days anaerobically at 37°C. Stocks were made from these cultures and were stored at -80 °C. The remaining volumes of these cultures were used to make subcultures by adding 200 μL of each culture to a vial of cooked/chopped meat broth supplemented with glucose. Frozen *P. distasonis* stocks were inoculated into these cultures using an inoculation loop. These subcultures were then allowed to grow overnight. Stocks of these subcultures were made and frozen at -80°C until used for colonization of germ-free mice. At weaning, mice were colonized with 200 μL of the Bacteroidetes consortium stock solution or a single *P. distasonis* stock solution.

VIII. Ileal epithelial cell isolation

At sacrifice, whole terminal ileum tissue (measured 10 cm proximal to the cecum) was carefully removed, being sure to keep the tissue fully intact. Ileal tissues were cleaned, inverted, and inflated with enough air to expand the tissue but not rupture it (Nik et al., 2013). Peyer's patches were not removed. Intestinal epithelial cells were collected from the inflated inverted tissue in Cell Recovery Solution (Corning) by agitating the tissue every 5 minutes for 30 minutes on ice. Cells were centrifuged at 800 g for 5 min, lysed in 1 mL of TRIzol Reagent (ThermoFisher), and stored at -80 °C for at least 24 hours.

RNA was extracted using the PureLink RNA Mini Kit (Invitrogen). Samples in 1 mL of Trizol were slowly thawed on ice, then incubated at RT for 5 min. Following incubation, 200 μL of chloroform was added, and each sample was shaken vigorously for 15 seconds. Samples were then incubated at RT for 3 min and centrifuged at 12000 x g for 15 min at 4 °C. Approximately 600 μL of the colorless upper phase was transferred to a new RNAse-free tube. An equal volume of 70% ethanol was added, and the sample was vortexed. The sample was transferred to a spin column and spun at 12000 x g for 30 sec until the whole sample was processed. The column was washed once with 700 μL of wash buffer (Wash Buffer I), followed by two 500 μL washes of wash buffer containing 70% ethanol (Wash Buffer II). The spin column was centrifuged at 12000 x g for 1 min to dry the membrane. For elution of RNA, 50 μL of RNAse-free water was added to the membrane, and the column was allowed to incubate for 1 minute at RT. The spin column was transferred to a new tube and spun at 12000 x g for 2 min at RT. RNA quality and quantity was immediately determined using Nanodrop One (Thermo Scientific). Samples were stored at −80 °C until utilized for cDNA synthesis or RNA sequencing.

IX. Lymphocyte isolation from ileal tissue

Ileal lymphocytes were isolated according to previous protocols, with some modification (Gracz, et al., 2012; Moro et al., 2015). At sacrifice, ileal tissue was cleaned with 1X PBS with mesenteric fat removed and cut longitudinally. The whole tissue was placed into 4 mL of 30 mM EDTA and 1.5 mM dithiothreitol in 1X PBS for 20 minutes on ice. The tissue was then transferred to 4 mL of 30 mM EDTA in 1X PBS and placed into an incubator for 10 minutes at 37 °C, followed by gentle shaking for 30 seconds. Tissues were then transferred to a 6 well plate and washed with 10 ml of 1X PBS to remove remaining epithelial cells. In initial studies for samples being analyzed for T cell subsets, tissues were transferred to a 3 mL digest solution of 4% fetal bovine serum (FBS) in Dulbecco's Modified Eagle Medium (DMEM) containing 0.5 mg/ml collagenase D (Roche), 0.5 mg/ml dispase (Roche) and 40 µg/ml DNAse (Sigma). In later studies for samples being analyzed for both T cell and innate lymphoid cell (ILC) populations, tissues were transferred to a 3 mL digest solution of 4% FBS in RPMI containing 0.05 mg/mL liberase (Roche) and 40 µg/ml DNAse (Sigma). The tissue was minced finely in the digest solution with surgical scissors and placed into a shaking incubator for 30 minutes at 37°C, 200 rpm.

Following digestion, the cell suspensions were poured over a 70-micrometer cell strainer into a 50 mL conical tube and washed with 20 mL PBS. The cell suspension was spun at 800 g for 5 minutes and resuspended in 4 mL of 4% FBS in DMEM. Four milliliters of 80% Percoll (36 mL of Percoll, 10 mL of 1X PBS, and 4 mL of 10X PBS per 50 mL) was added to the suspension, and the suspension was gently overlaid onto 5 mL of 80% Percoll. The Percoll gradient was centrifuged at 1200 x g for 35 minutes with 0 brake

acceleration and 0 brake deceleration. Cells were collected at the interface of the Percoll layers and washed with 30 mL of 4% FBS in DMEM. The cells were then centrifuged at 800g for 5 min, resuspended in cold 4% FBS in DMEM, and counted for viability with trypan blue.

X. Cell stimulation and staining for flow cytometry

For the staining of T cell subsets, ileal lymphocytes from WT and TLR4 KO mice were plated at a concentration of $10^6$ viable cells per milliliter in a stimulation solution containing 50 ng/mL of phorbol myristate acetate (PMA, Sigma) and 750 ng/mL ionomycin (Sigma) in the presence of Brefeldin A (10µg/mL, Sigma). Cells were incubated for four hours at 37°C, 10% $CO_2$. After stimulation, cells were centrifuged at 800 g for 5 minutes and washed in 200 µL of 1X PBS supplemented with 4% FBS for staining in a 96-well round bottom plate. For ILCs, lymphocytes were directly transferred into a 96-well round bottom plate for staining immediately after isolation from ileal tissue and washed with 200 µL of 1X PBS supplemented with 4% FBS.

Following the wash, cells were incubated in Fc block for 10 minutes on ice, followed by surface staining on ice in the dark for 30 min. Cells were washed and then stained for viability 30 minutes on ice in the dark using Live/Dead Fixable Aqua (Life Technologies) at a 1:500 dilution. Cells were then fixed using the Foxp3/Transcription Factor Staining Buffer Set (eBioscience), with prepared solutions according to manufacturer's protocol, for 40 minutes on ice. Fixed cells were then stained intracellularly for 40 minutes at room temperature in the dark. Data was collected on the Fortessa 4-15 (BD Biosciences) or

Aurora spectral flow cytometer (Cytek) and analyzed using FlowJo software (v10.3.2, Becton Dickinson and Company). Antibodies used in these experiments are listed below.

**Table 1**: Antibodies and flow cytometry reagents used in this study

| Antibody | Color | Manufacturer | Catalog Number |
|---|---|---|---|
| Live Dead Aqua | - | Invitrogen | L34966 |
| CD4 (clone RM4-5) | BV605, PE-Cy7 | Biolegend | 100548 |
| CD45 (clone 30-F11) | BUV395 | Biolegend | 103151 |
| CD3e (clone 145-2C11) | AF750 | Biolegend | 100362 |
| RORγt (clone Q31-378) | PE | Biolegend | 562607 |
| Foxp3 (clone FJK-16s) | PE-Cy7 | Invitrogen | 25-5773-82 |
| IL-17A (clone TC11-18H10.1) | AF647, FITC | Biolegend | 506911, 506907 |
| RORγt (clone B2D) | AF488 | Thermo Fisher | 53-6981-82 |
| Gata3 (clone L50-823) | AF647 | BD | 560068 |
| TCRβ (clone H57-597) | AF750 | Biolegend | 1009246 |
| CD45 (clone 30-511) | BUV395 | BD | 564279 |
| CD90 (clone 30-H12) | BUV737 | BD | 741702 |
| KLRG1 (clone 2F1/KLRG1) | BV785 | Biolegend | 138345 |
| Lineage | PE | Biolegend | 78035 |
| CD4 (clone PC61.5) | PE-Cy7 | eBioscience | 25-0251-82 |
| InVivoMAb anti-mouse CD16/CD32 (clone 2.4G2) | Fc Block | BioXCell | BE0307 |

XI. ELISAs

Venous blood samples (3 mL) were collected from CMA and healthy patients at the University of Naples Federico I. Serum was obtained by centrifugation for 15 min and stored at -80°C. IgE specific for the nBos d 5 epitope on BLG was quantified using the ThermoFisher Scientific ImmunoCAP system and was expressed as kilounits per liter (kUA/L). Serum SAA-1 levels were determined with a Human Serum Amyloid A ELISA Kit (AbCam) with a range of 0.41 ng/mL - 300 ng/mL.

For qualification of fecal IgA, ELISA plates were coated overnight with 2 μg/mL of goat-anti mouse IgA-UNLB (Southern Biotech), 50 μL per well. The next day, plates were

washed 4x with 300 μL of 1X PBS-0.05% Tween and blocked with 200 μL of 3% BSA/PBS for at least 2 hours at RT. Fecal pellets were weighed and placed into 0.01% NaN3 in 1X PBS (1 mL/100 mg of feces). Pellets were vortexed for 5 minutes at top speed and centrifuged for 15 minutes at 10,000 rpm. The supernatant was collected and diluted 1:8 or as needed for IgA quantification. Excess sample was stored at -80 °C. A nine-point standard curve was made by conducting serial 1:1 dilutions of 200 ng/mL stock solution of mouse IgA UNLB (BD Pharmigen). Following the 2-hour incubation period, 50 μL of each sample and standard was applied to the wells overnight. The following day, plates were washed 4x with 300 μL of 0.05% Tween in 1X PBS. 50 μL of diluted secondary antibody (1:2500) was applied to each well and incubated for 1 hour at RT. Following incubation, the plate was washed 4x with 300 μL of 0.05% Tween in 1X PBS Tween. Developer (KPL) was applied to the plate, 100 μL per well, and was allowed to develop for up to 30 minutes. Development was stopped with 100 μL per well of 5% EDTA in water.

XII. Quantitative Real Time PCR (qRT-PCR)

Complementary DNA was synthesized from isolated RNA using the iScript cDNA Synthesis kit from BioRad using a normalized quantity of RNA for each sample (500ng – 1500ng). Depending on the desired quantity of RNA, the reaction mixture was scaled up or down accordingly. For each 20 μL reaction, 4 μL of 5x Reaction Mix and 1 μL of RT enzyme was used along with an appropriate amount of water depending on sample RNA concentration. Reaction mixtures were placed in a thermocycler and underwent the following conditions to synthesize cDNA: 1) 5 min at 25°C, 2) 20 min at 46°C, 3) 1 min at

95°C, 4) held at 4°C indefinitely. Samples were used right away for qRT-PCR analysis or stored at -20°C for future use.

cDNA reaction mixes were made using the QuantiNova SYBR Green Kit (Qiagen) or PowerUp SYBR Green system (Applied Biosystems). For the QuantiNova Kit, reaction mixtures consisted of 10 μL of 2x SYBR Green PCR Master Mix, 0.1 μL of QN ROX Reference Dye, 1 μL of forward primer, 1 μL of reverse primer, 5.9 μL of RNAse-free water, and 2 μL of cDNA for a total of 20 μL. For the PowerUp kit, reaction mixtures consisted of 10 μL of PowerUP SYBR Green, 1 μL of forward primer, 1 μL of reverse primer, 6 μL of RNAse-free water, and 2 μL of cDNA for a total of 20 μL. Samples were run in duplicate to determine the average cycle for which each sample reached a set threshold (0.2). Primers used in the reaction mixes are listed in **Table 2**. Expression was measured with the QuantStudio 3 instrument by Applied Biosystems. The cycling conditions for the reaction mixture entailed an activation cycle of 50°C for 2 min followed by one cycle of 95°C for 10 min and 40 cycles at 94°C for 20 s, 55 °C for 20 s and 72 °C for 50 s. The fluorescent probe was detected in the last step of the cycle. A melt curve was performed at the end of the PCR reaction to confirm the specificity of the PCR product. Relative expression was calculated by determining the ΔCt based on expression of the endogenous housekeeping gene (*Hprt*), followed by normalization to the control group (GF or antibiotic-treated SPF) within each genotype.

**Table 2**: Primers used in this study

| Gene | Sequence | Reference |
|---|---|---|
| Hprt | F -tgaagagctactgtaatgatcagtcaac<br>R - agcaagcttgcaaccttaacca | Upadhyay et al., 2012 |
| Saa1 | F - tgttcacgaggctttccaag<br>R - cccgagcatggaagtatttg | Atarashi et al., 2015 |
| Reg3b | F - atggctcctactgctatgcc<br>R - gtgtcctccaggcctcttt | Upadhyay et al., 2012 |
| Jchain | F - gaactttgtataccatttgtcagacg<br>R - ctgggtggcagtaacaacct | Campos-Rodríguez et al., 2016 |
| Igha | F - cgtccaagaattggatgtga<br>R - agtgacaggctgggatgg | Campos-Rodríguez et al., 2016 |
| Il25 | F - gagttggacagggacttgaa<br>R - aggtggtgagcatgactaag | Liu et al., 2017 |
| Il33 | F - tatgagtctccctgtcctgcaa<br>R - ctcatgttcaccatcaccttcttc | Judd et al., 2015 |

XIII. Bulk RNA sequencing and analysis

RNA libraries for total RNA from ileal epithelial cells were prepared and sequenced at the University of Chicago Functional Genomics Core. Libraries were prepared using a TruSeq Stranded Total Library Preparation Kit with Ribo-Zero Human/Mouse/Rat (Illumina). Samples were sequenced using 50-bp single-end reads chemistry on the HiSeq2500 instrument. Raw reads were assessed for quality, counted, and aligned to the mm10 reference genome using the R-subread package (Liao et al., 2019). All samples had a Phred score of at least 30. Normalization and differential expression analysis between healthy- and CMA-colonized were performed using the edgeR package (Chen et al., 2016). Read counts for each gene were fit to a negative binomial generalized log-linear model. Multiplicity correction was performed by applying the Benjamini-Hochberg method on the *P*-values to control for the false discovery rate (FDR = 0.1). Genes with an FDR of <0.05 and a fold change >1.5 or <-1.5 were plotted as significant. Gene ontology

pathways for genes expressed in $CD11c^{WT}$ and $CD11c^{\Delta TLR4}$ CMA-colonized mice were determined using Metascape (Zhou et al., 2019).

XIV. Single-cell RNA sequencing

Following ileal lymphocyte isolation, cell suspensions were filtered through a 40μm Flowmi™ Cell Strainer (Research Products International) to remove epithelial debris. Two samples were pooled per genotype, per colonization condition. Cells were centrifuged for 5 min at 800g and resuspended in 1X PBS supplemented with 4% FBS for counting. Following counting, scRNA-seq libraries were prepared following the Chromium Single Cell 3' Reagent Kits User Guide (v3.1 Chemistry) from 10X Genomics at the University of Chicago Functional Genomics Core. The cell suspension was prepared with a mastermix solution to yield 10,000 cells per reaction. PCR cleanup was performed using SPRIselect reagents (Beckman Coulter), 10% Tween 20 (Bio-Rad), and Qiagen Buffer EB. Rainin 200 μL LTS filter tips (Cat# 30389240) and 20 μL LTS filter tips (Cat # 3038922) were used for the handling of all cell suspensions and reagents. The 10X libraries were sequenced on a Novaseq XP instrument (Illumina). The Cell Ranger Single-Cell Software Suite (10X Genomics) was used for demultiplexing, assignment of barcodes, and quantification of unique molecular identifier (UMI) using the mm10 reference genome (Genome Reference Consortium Mouse Build 38) for read alignment.

Normalization and scaling were performed using the Seurat default pipeline. The optimal number of principal components used for clustering was determined by using the ElbowPlot function, which was determined to be 50. Clusters were determined using the FindNeighbors and FindClusters functions (algorithm = 2, resolution = 1) to create UMAP

projections. Clusters were annotated using canonical markers for epithelial cells, macrophages, dendritic cells, B cells, T cells, tuft cells, enterocytes, Paneth cells, stem cells, goblet cells, regulatory T cells, Th17 cells, ILC2s, and ILC3s. These cells were defined using the following markers:

Epithelial cell: Cd24a, Itga6, Ceacam1, Itgb4

Macrophage: Mrc1, Itgax, Itgam, Adgre1

Dendritic cell: Klrb1c, Cd19, Cd14

B cell: Cd79a, Cd79b, Ms4a1, Cd19, Ptprc

T cell: Cd3d, Cd3e, Cd3g, Ptprc

Tuft (Brush) cell: Avil, SiglecF, Cdhr2, Espn

Enterocyte: Slc10a2, Alpi, Rnf186, Klf5, Cldn15, Aldob, Cd36

Paneth cell: Ctnnb1, Defa5, Tlr5

Stem cell: Itgb1, Prom1

Goblet cell: Muc2, Muc5ac, Krt7, Galnt12, Atoh1

Tregs: Cd3d, Cd3e, Cd3g, Ptprc, Cd4, Foxp3

ILC2: Gata3, Rora, and Id2. (Il4 and Il13 can be used, but may be lowly expressed)

ILC3: Rorc, IL17a, Il23r, Il22, Ahr

Th17: Cd3d, Cd3e, Cd3g, Ptprc, Cd4, Il21r, Il17a, Stat3, Rorc

Cluster condensing was determined based on the extent of expression of these markers in various clusters. Low or no expression of certain markers (i.e., ILC2 and ILC3 markers) resulted in condensing of clusters expressing these markers into a more general annotation (i.e., ILC). Final annotations used for clusters are described in **Table 6**. The

FindMarkers function was used to generate a table of differentially expressed features (p_val_adj = 0.1, all other arguments set to default).

## XV. DNA extraction from fecal and ileal contents

DNA was extracted using the QIAamp PowerFecal Pro DNA kit (Qiagen). Samples were suspended in PowerBead tubes along with lysis buffer and loaded on a Bead Mill 24 Homogenizer (Thermo Fisher) or taped to a vortex. Tubes were agitated at maximum speed for 10 minutes at RT to dissociate the fecal pellet. PowerBead tubes were then centrifuged at 10,000 x g for 30 seconds at RT. Isolation of released DNA was then conducted according to the manufacturer's protocol. DNA was purified routinely using a spin column filter membrane and quantified using the Qubit 4 Fluorometer (Thermo Fisher). Ileal contents were subjected to DNA isolation using the PowerSoil® DNA Isolation Kit (MoBio) or the QIAamp PowerFecal Pro DNA kit (Qiagen), according to the manufacturer's protocol.

## XVI. 16S Sequencing and analysis

Isolated DNA was sequenced at the Argonne National Laboratory Sequencing Facility or the Duchossois Family Institute (DFI) at the University of Chicago. For samples sequenced at Argonne, 16S rRNA gene amplicon sequencing was performed on an Illumina MiSeq instrument. Paired-end reads (151 bp) were generated with 12-bp barcodes. The V4 region of the 16S rRNA gene was amplified using 515F and 806R primers that included sequencer adapter sequences used in the flow cell. Raw

multiplexed reads were provided by the facility and were demultiplexed using qiime2 (v.2018.4, Bolyen E et al., 2019).

For samples sequenced at the Duchossois Family Institute, sequencing was performed on the Illumina MiSeq platform in the Functional Genomics Facility at the University of Chicago using 2×250 Paired End reads, generating 5,000-10,000 reads per sample. The V4-V5 region within 16S rRNA gene was amplified using the universal bacterial primers – 563F (5'-nnnnnnnn-NNNNNNNNNNNN-AYTGGGYDTAAA- GNG-3') and 926R (5'-nnnnnnnn-NNNNNNNNNNNN-CCGTCAATTYHT- TTRAGT-3'), where 'N' represents the barcodes, 'n' are additional nucleotides added to offset primer sequencing. Amplicons were then purified using a spin column-based method (Qiagen), quantified, and pooled at equimolar concentrations. Illumina sequencing-compatible Unique Dual Index (UDI) adapters were ligated onto the pools using the QIAseq 1-step amplicon library kit (Qiagen). Library quality control was performed using Qubit 4 Fluorometer (Thermo Fisher) and Tapestation (Agilent) and sequenced on Illumina MiSeq platform to generate 2x250bp reads.

For 16S analysis, Dada2 (v1.14, Callahan, et al., 2016) was used for processing raw 16S rRNA reads. The first 180 bp for both forward and reverse reads were trimmed to remove low quality nucleotides. Taxonomic analysis was determined using the RDP database (Wang et al., 2007) with a minimum bootstrap confidence score of 50. Multiple sequence alignment was performed using msa (v1.18.0, Bodenhofer et al., 2015) and ape (v5.3). Alpha and beta diversity were calculated using Dada2.

XVII. Shotgun metagenomics:

Libraries were prepared using 100 ng of genomic DNA using the QIAseq FX DNA library kit (Qiagen). DNA was fragmented enzymatically into smaller fragments and desired insert size was achieved by adjusting fragmentation conditions. Fragmented DNA was end repaired and polyA tails were added to the 3' ends to stage inserts for ligation. During the ligation step, Illumina compatible Unique Dual Index (UDI) adapters were added to the inserts and the prepared library was PCR amplified. Amplified libraries were cleaned up, and QC was performed using a Tapestation (Agilent). Sequencing runs were performed on the Illumina NextSeq platform in the Functional Genomics Facility at at the University of Chicago using the 2×150 paired-end reads cassette.

For metagenomic analysis, quality reads were used in Kraken2 (v.2.1.1) for taxonomic classification and to assemble contigs via Megahit (v1.2.9, Li et al., 2015a). Genes were annotated using Prodigal (v.2.6.3, Hyatt et al., 2010), and functional annotations were perform using eggnog-emapper (v.2.0.1b, Cantalapiedra et al., 2021). Wilcoxon rank sum test was performed on MAGs identified in healthy-colonized and CMA-colonized mice to determine differentially abundant species.

Statistical Analysis

Statistical analyses were performed using GraphPad Prism version 9.3.0. The test details are indicated in the figure legends.

## Chapter 3. The Donor 5 microbiota induces a unique proinflammatory response in the ileum that is dependent on TLR4 signaling

### I. The CMA Donor 5 microbiota induces intestinal inflammation

Within the last century, there has been a concurrent increase in the prevalence of food allergies and dysbiosis of the human microbiome (Gupta et al., 2018; Brough et al., 2021). Many factors contributing to this dysbiosis are rooted in features of a modern lifestyle, including overuse of antibiotics, poor dietary habits, and increased Cesarean birth, which have been correlated with food allergy (Iweala and Nagler, 2019). A number of studies have highlighted mechanisms by which the gut microbiota regulates allergic responses to food (Stefka et al., 2014; Abdel-Gadir et al., 2019). Recently, we investigated the role of the microbiota in regulating food allergy using fecal samples from human infant donors (Feehley et al., 2019). The premise of this work is based on unpublished findings from the experiments performed in Feehley et al., 2019. In that study, we examined the role of the gut microbiota of four healthy infants (Donors 1 - 4) and four cow's milk allergic (CMA) infants (Donors 5 - 8) in mediating food allergic responses. We found that mice colonized with the healthy infants' microbiota were protected against an anaphylactic response to β-lactoglobulin (BLG), a major cow's milk allergen, while both germ-free (GF) mice, and mice colonized with the CMA infants' microbiota were susceptible. In the absence of a microbiota, GF mice spontaneously produce increased amounts of IgE (Cahenzli et al., 2013; Stefka et al, 2014). Although GF and CMA-colonized mice both develop anaphylaxis after sensitization and challenge

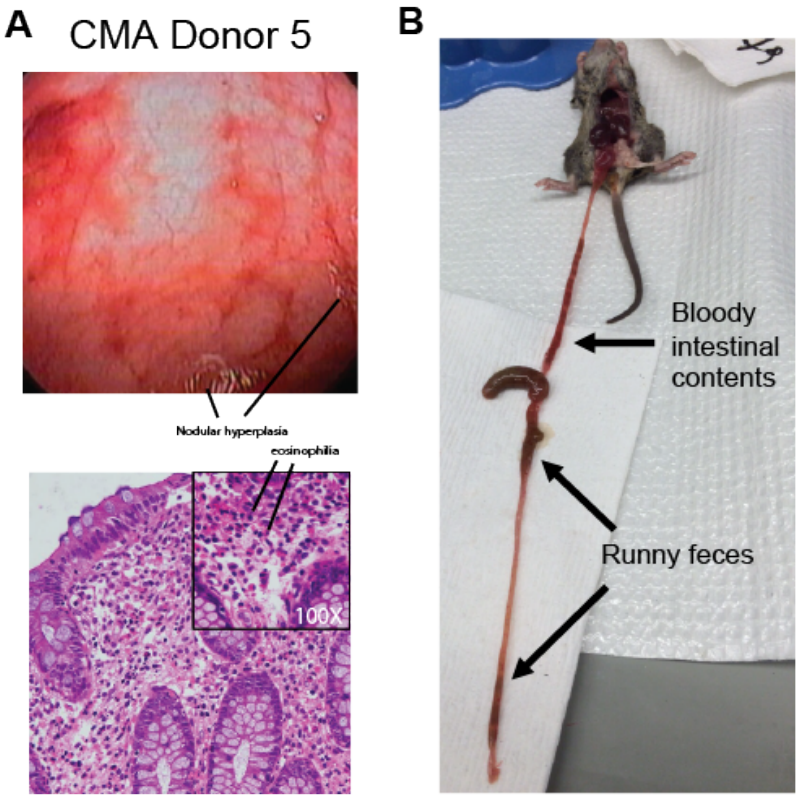


**Figure 1**: The CMA Donor 5 microbiota induces intestinal inflammation. **A)** Colonoscopy and histology images of the gastrointestinal tract of CMA donor 5 minutes after feeding. **B)** A C3H/HeN mouse colonized with the CMA Donor 5 for one week.

with food allergen, CMA-colonized mice have an increased antigen-specific response in comparison to both GF and healthy-colonized mice, suggesting that the CMA microbiota plays a role in *promoting* the allergic response (Feehley et al., 2019). In the present study, we focused initially on one CMA infant donor that exhibited more severe symptoms upon consumption of cow's milk compared to other CMA infant donors within this cohort. This donor, CMA Donor 5, experienced abdominal pain, diarrhea, and urticaria within minutes after feeding with cow's milk. CMA Donor 5 also exhibited blood within the stool. A colonoscopy was thus performed to rule out other sources of gastrointestinal bleeding. Examination of the gastrointestinal tract through colonoscopy revealed localized inflammation, as observed by nodular hyperplasia on the intestinal walls of the rectum (**Figure 1A**). To investigate the inflammation further, the tissue was biopsied for

histological analysis. Histological results revealed eosinophilic infiltration within the gastrointestinal tissue, supporting an immunological basis for the symptoms experienced by CMA Donor 5 (**Figure 1A**).

Stool samples from CMA Donor 5 were used to colonize GF mice to examine the role of the microbiota in mediating allergic sensitization BLG. In response to the initial colonization with the CMA Donor 5 microbiota, some mice appeared to be lethargic and exhibited diarrhea and crusted fecal matter around the anus. Upon euthanasia of mice colonized with the CMA Donor 5 microbiota for one week, some mice were observed to have bloody intestinal contents in the ileum and loose stool pellets in the colon (**Figure 1B**). In the original publication, ileal and colonic tissue was collected from mice colonized with feces from each of the eight infant donors at sacrifice after sensitization with BLG plus cholera toxin (CT) and at 5-6 months post colonization. The tissues were fixed in formalin and stained with hematoxylin and eosin (H & E) or placed in Carnoy's fixative for periodic acid-Schiff (PAS) staining. A gastrointestinal pathologist examined the stained sections in a blinded fashion and found no evidence of pathology, ruling out an infectious etiology (Feehley et al., 2019, Extended Data Figs. 1 and 2). The similarity of the symptomatic manifestations observed in both CMA Donor 5 and in mice colonized with the Donor 5 microbiota led to the hypothesis that this microbiota may be contributing to food allergic responses by inducing transient intestinal inflammation.

II. The CMA Donor 5 microbiota induces a proinflammatory signature that includes the induction of *Saa1* in the ileum epithelium

In the context of food allergies and other atopic diseases, the epithelium acts not only as a barrier between exogenous antigens and the immune system, but also receives signals from these exogenous antigens through innate receptors and relays information about said antigens to local immune cells. This surveillance feature of the epithelium is important for mounting appropriate immune responses to allergens and noxious substances (Iweala and Nagler, 2019). To more broadly understand how the CMA Donor 5 microbiota influences the gut mucosa, bulk RNA sequencing was performed on intestinal epithelial cells (IECs) of the ileum in GF mice, mice colonized with the CMA Donor 5 microbiota, and mice colonized with the microbiota of healthy infants (Donors 1 -4). The data presented in **Fig. 2** and **Tables 3** and **4** is a reanalysis of this subset of donors from Feehley et al., 2019. These samples were taken one-week post-colonization. Analysis of this data for differentially expressed genes between Donor 5-colonized mice and the four healthy-colonized mice revealed 169 genes that were significantly different between these two groups, some of which are involved in immunological processes (**Table 3**). When comparing differentially expressed genes between Donor 5-colonized mice and GF mice, 2921 were identified to be significantly different. Interestingly, several of these genes are involved in regulation of the epithelial barrier in response to bacterial colonization (*Defa17*, *Defa23*, *Il18*, *Il15*), APC function (*Cd8a*, *Cd83*), B cell function (*Jchain*, *Fcgrt*) and type 2 responses (*Il13ra1*, *Il33*) (Harrison et al., 2015; Ganz et al., 2003; Nowarski et al., 2015, Campbell et al., 2021) (**Table 4**).

**Table 3**: Selected genes that are differentially expressed between CMA Donor 5-colonized mice and healthy Donor 1-colonized mice

| Gene Symbol | Description | Adjusted P-value |
|---|---|---|
| Acot12 | acyl-CoA thioesterase 12 | 0.00757309 |
| Acot6 | acyl-CoA thioesterase 6 | 0.00623227 |
| Apobec1 | apolipoprotein B mRNA editing enzyme, catalytic polypeptide 1 | 0.07476772 |
| Bcl2l15 | BCLl2-like 15 | 0.07259898 |
| Cyp2c29 | cytochrome P450, family 2, subfamily c, polypeptide 29 | 1.17E-07 |
| Cyp2j13 | cytochrome P450, family 2, subfamily j, polypeptide 13 | 0.00206117 |
| Cyp3a59 | cytochrome P450, family 3, subfamily a, polypeptide 59 | 0.06645415 |
| Fgfr3 | fibroblast growth factor receptor 3 | 0.00845 |
| Fut2 | fucosyltransferase 2 | 0.00623227 |
| Gpr17 | G protein-coupled receptor 17 | 0.05619717 |
| Gprc5a | G protein-coupled receptor, family C, group 5, member A | 0.08050387 |
| Gsdmc4 | gasdermin C4 | 0.07011188 |
| Hdac8 | histone deacetylase 8 | 0.07866151 |
| Hist2h3c1 | H3 clustered histone 14 | 0.09696993 |
| Itgax | integrin alpha X | 0.07153791 |
| Jchain | immunoglobulin joining chain | 0.00206117 |
| Mptx2 | mucosal pentraxin 2 | 0.05181688 |
| Mx1 | MX dynamin-like GTPase 1 | 0.04033043 |
| Notch1 | notch 1 | 0.07011188 |
| Olfr147 | olfactory receptor 147 | 0.08823171 |
| Ptpn22 | protein tyrosine phosphatase, non-receptor type 22 (lymphoid) | 0.09017347 |
| Ptprc | protein tyrosine phosphatase, receptor type, C | 0.0572275 |
| Rdh16 | retinol dehydrogenase 16 | 0.03954212 |
| Reg3g | regenerating islet-derived 3 gamma | 0.01827653 |
| Saa1 | serum amyloid A 1 | 0.00243493 |
| Shroom1 | shroom family member 1 | 0.0532847 |
| Slc30a10 | solute carrier family 30, member 10 | 0.09124464 |
| Slc37a3 | solute carrier family 37 (glycerol-3-phosphate transporter), member 3 | 0.05616279 |
| Slc40a1 | solute carrier family 40 (iron-regulated transporter), member 1 | 0.03538343 |
| Slc44a2 | solute carrier family 44, member 2 | 0.09696993 |
| Slc4a7 | solute carrier family 4, sodium bicarbonate cotransporter, member 7 | 0.04033043 |
| Slc6a14 | solute carrier family 6 (neurotransmitter transporter), member 14 | 0.00206117 |
| Slc6a18 | solute carrier family 6 (neurotransmitter transporter), member 18 | 0.03954212 |
| Tgfbr3 | transforming growth factor, beta receptor III | 0.06441447 |

**Table 4**: Selected genes that are differentially expressed between CMA Donor 5-colonized mice and GF mice

| Gene Symbol | Description | Adjusted P-value |
|---|---|---|
| Cd160 | CD160 antigen | 0.06947858 |
| Cd177 | CD177 antigen | 0.08047643 |
| Cd24a | CD24a antigen | 0.04445793 |
| Cd302 | CD302 antigen | 0.04805503 |
| Cd320 | CD320 antigen | 0.04053096 |
| Cd36 | CD36 molecule | 0.08813624 |
| Cd38 | CD38 antigen | 0.0540062 |
| Cd3eap | CD3E antigen, epsilon polypeptide associated protein | 0.05288883 |
| Cd3g | CD3 antigen, gamma polypeptide | 0.00861828 |
| Cd44 | CD44 antigen | 0.06065537 |
| Cd46 | CD46 antigen, complement regulatory protein | 0.03639436 |
| Cd55 | CD55 molecule, decay accelerating factor for complement | 0.00801274 |
| Cd7 | CD7 antigen | 0.07327333 |
| Cd83 | CD83 antigen | 0.02296515 |
| Cd8a | CD8 antigen, alpha chain | 0.00429624 |
| Cd9 | CD9 antigen | 0.01162222 |
| Defa17 | defensin, alpha, 17 | 0.06422669 |
| Defa23 | defensin, alpha, 23 | 0.06245495 |
| Dock10 | dedicator of cytokinesis 10 | 0.05807853 |
| Fcgrt | Fc fragment of IgG receptor and transporter | 0.00394739 |
| Igbp1 | immunoglobulin (CD79A) binding protein 1 | 0.0671521 |
| Il10rb | interleukin 10 receptor, beta | 0.04695145 |
| Il13ra1 | interleukin 13 receptor, alpha 1 | 0.02205206 |
| Il15 | interleukin 15 | 0.0059675 |
| Il18 | interleukin 18 | 0.0210679 |
| Il1rap | interleukin 1 receptor accessory protein | 0.04343139 |
| Il33 | interleukin 33 | 0.00218614 |
| Il6ra | interleukin 6 receptor, alpha | 0.00463023 |
| Ildr1 | immunoglobulin-like domain containing receptor 1 | 0.08842589 |
| Ilf2 | interleukin enhancer binding factor 2 | 0.02370086 |
| Jchain | immunoglobulin joining chain | 0.01865222 |
| Mif | macrophage migration inhibitory factor (glycosylation-inhibiting factor) | 0.01439386 |
| Saa1 | serum amyloid A1 | 0.003403449 |
| Saa3 | serum amyloid A3 | 0.054006204 |

Additionally, several genes that have been previously described to be associated with a proinflammatory Th17 signature were found to be significantly upregulated in Donor 5-colonized mice compared to healthy-colonized mice (Atarashi et al., 2015; Haberman et al., 2014). These genes include *Saa1*, *Saa3*, *Slc6a14*, *Fut2*, *Reg3b*, and *Reg3g* (**Figure 2A, Table 3**). *Saa1* was of particular interest because it is well known as an acute-phase protein expressed by hepatocytes during injury and infection (Sun and Ye, 2016). In the clinic, SAA-1 has been used as a biomarker of systemic inflammation for patients with Crohn's disease as well as asthmatics (Yarur et al., 2016; Bich et al., 2022; Ozseker et al., 2006). More recently, it has been shown be induced in the intestinal and bronchial epithelium and can regulate type 2 and type 3 inflammation at those sites (Lee et al., 2020; Smole et al, 2020). Furthermore, *Saa1* can be induced in the terminal ileal epithelium by Segmented Filamentous Bacteria (SFB), *Citrobacter rodentium*, *Escherichia coli* O157, and other epithelial-adherent bacteria (Atarashi et al., 2015).

Because *Saa1* has this documented affiliation with inflammatory responses and mice colonized with the CMA Donor 5 microbiota exhibit transient intestinal inflammation, we hypothesized that *Saa1* induced by the Donor 5 microbiota may be a biomarker for a subset of patients with food allergies. To determine if *Saa1* upregulation was induced by the microbiota of other CMA infants, GF mice were colonized with repository feces from CMA Donors 5-8, as well as repository feces from healthy Donors 1-4. Mice were sacrificed one-week post-colonization. Although Quantitative Real Time Polymerase Chain Reaction analysis (qRT-PCR) showed that expression of *Saa1* was induced by colonization with all donor microbiotas compared to GF controls, mice colonized with the Donor 5 microbiota exhibited significantly higher expression of *Saa1* compared to all other

CMA donors, all healthy donors, and GF mice (**Figure 2B**). To determine the relevance of SAA-1 to human infants, we quantified SAA-1 in the serum, as well as antibodies specific for n Bos d 5, an epitope of BLG, in a larger cohort of healthy and CMA patients. As expected, CMA infants had significantly higher levels of antibodies against nBos d 5, a diagnostic indicator of cow's milk allergy, in comparison to healthy infants. Surprisingly, these infants also had significantly greater levels of serum SAA-1 compared to healthy infants (**Figure 2C-D**). This cohort of infants had great variability in their quantity of serum SAA-1, some with quantities comparable to that found in healthy infants. Accordingly, the quantity of serum SAA-1 was not significantly correlated with n Bos d 5-specific IgE (**Figure 2E**). In summary, SAA-1 can be used as an inflammatory biomarker to identify a subset of CMA infants. CMA Donor 5 exhibits a unique microbiota that can induce upregulation of *Saa1* in the ileal epithelium, which the microbiotas from other CMA infants fail to do. The Donor 5 microbiota also induces a proinflammatory response in the ileum epithelium that includes the upregulation of Th2- and Th17-related genes.

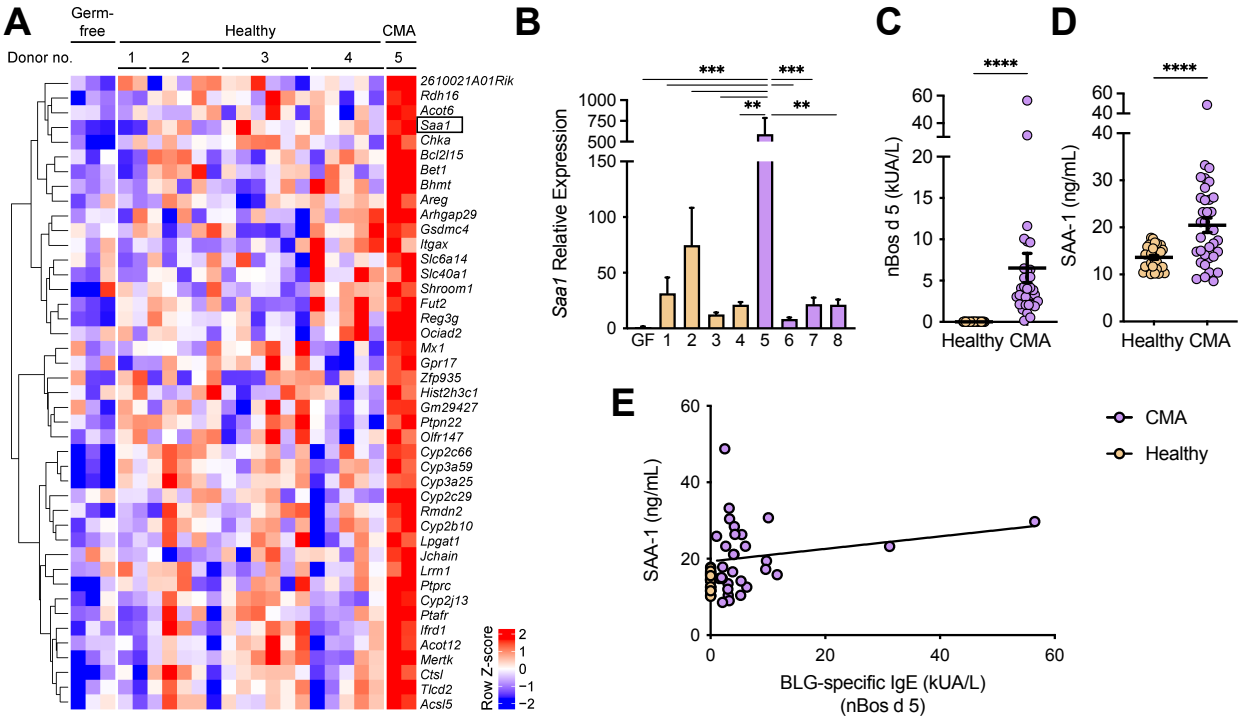


**Figure 2**: The Donor 5 microbiota induces expression of *Saa1* in ileal IECs. **A)** Heatmap of relative abundance of gene transcripts significantly upregulated in C3H/HeN mice colonized with the CMA Donor 5 microbiota compared to GF and mice colonized the microbiota from healthy donors 1 – 4. **B)** qRT-PCR analysis of *Saa1* relative expression in GF mice and mice colonized with the microbiota from healthy donors (donors 1 – 4) and CMA donors (5 – 8). **C)** Serum concentrations of IgE specific for the nBos d 5 epitope of BLG and **D)** SAA-1 from age and sex-matched healthy and CMA patients. **E**) Correlation of serum SAA-1 with nBos d 5. Symbols represent individual patients, bars represent mean ±S.E.M, n=30 patients per group. For B, 2-way ANOVA with multiple testing using the Benjamini, Krieger, and Yekutili method was performed. For C-D, Wilcoxon rank sum test was performed between both conditions. Expression was analyzed one week post-colonization $^{**}P < 0.01$, $^{***}P < 0.001$, $^{****}P < 0.0001$

## III. *Saa1* induction in the ileum epithelium of Donor 5-colonized mice is regulated by TLR4 signaling

After observing microbially induced upregulation of *Saa1* in the ileal epithelium of Donor 5-colonized mice, we hypothesized that intestinal inflammatory responses mediated by SAA-1 might contribute to food allergy. Therefore, we next sought to understand the host-microbe interactions that mediate this phenotype. Analysis of fecal samples from healthy and CMA infant donors revealed that the microbial signature associated with healthy infants that were protected from food allergy consisted of enrichment of Clostridial species, particularly *Lachnospiraceae* (Feehley et al., 2019). In contrast, the microbial signature of CMA infants was highly enriched in Bacteroidetes. Interestingly, SAA-1 has been previously correlated with *Bacteroides* species in a multi-omic analysis examining transcriptomic and microbial sequencing data from intestinal biopsies taken from IBD patients (Tang et al., 2017). Furthermore, a previous study found Bacteroidetes to be enriched in two cohorts of infants with increased prevalence of allergy and autoimmunity compared to a genetically similar cohort with decreased prevalence of these diseases (Vatanen et al., 2016). Moreover, this study showed that lipopolysaccharide (LPS) from several Bacteroidetes species was hypoimmunogenic and was not protective against the onset of diabetes in a mouse model, as opposed to LPS from *Escherichia coli* which was hyperimmunogenic and protective. As described in the Introduction, bacterial LPS is sensed by host Toll-like receptor 4 (TLR4). TLR4 has been shown to regulate allergic inflammation in multiple models of atopic disease through various mechanisms (Eisenbarth et al., 2002; Bashir et al., 2004; McAlees et al., 2015). Thus, we looked at the

role of TLR4 in inducing ileal expression of *Saa1*, our reproducible biomarker in the Donor 5-colonized mice (**Fig. 2B**) as well as the larger cohort of CMA infants (**Fig. 2D**). We used GF C57BL/6 mice with TLR4 sufficiency and deficiency to examine the induction of *Saa1* in ileal IECs. These mice were colonized at weaning with the CMA Donor 5 microbiota or the healthy Donor 1 microbiota and were sacrificed one week later.

Expression analysis showed that *Saa1* was significantly upregulated in mice colonized with the CMA Donor 5 microbiota compared to GF mice and mice colonized with the healthy Donor 1 microbiota in TLR4-sufficient, but not TLR4-deficient mice (**Figure 3A)**. Along with *Saa1*, *Reg3b* has previously been shown to be associated with a Th17 signature induced by bacterial adherence to the ileal epithelium (Atarashi et al., 2015). Thus, we examined the expression of *Reg3b* in CMA Donor 5-colonized and healthy Donor 1-colonized mice as well. We observed that colonization of mice with the Donor 5 microbiota and the Donor 1 microbiota induced significant upregulation of *Reg3b* compared to GF and healthy-colonized mice (**Figure 3B)**. However, in the global absence of TLR4 signaling, mice colonized with the Donor 5 microbiota did not have significant upregulation of *Reg3b* compared to GF mice. Interestingly, Donor 1-colonized mice still exhibited significant upregulation of *Reg3b* compared to GF and Donor 5-colonized mice. These results show that TLR4 signaling regulates the expression of *Saa1* and *Reg3b* induced by the Donor 5 microbiota.

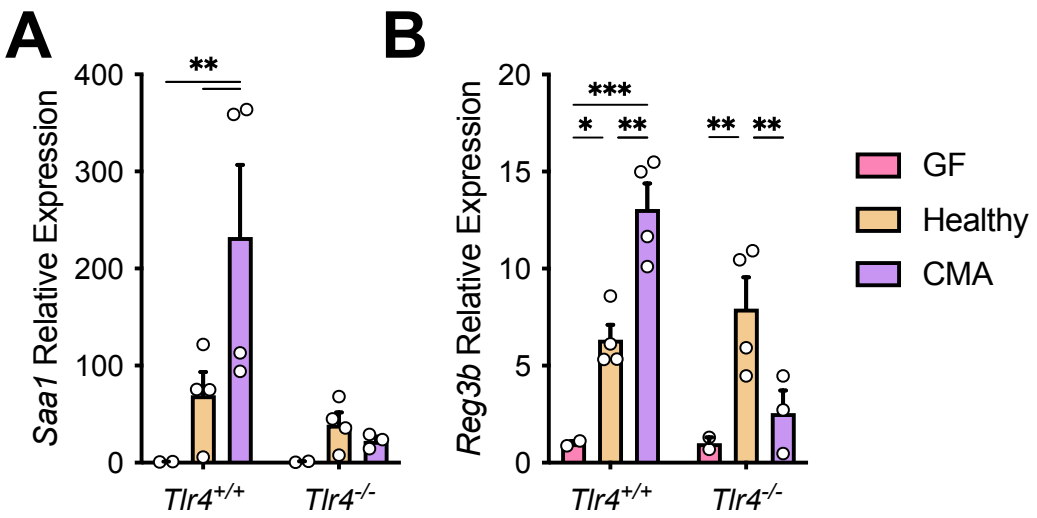


**Figure 3**: *Saa1* and *Reg3b* expression in ileal IECs is regulated by TLR4 signaling
**A)** Relative expression of *Saa1* and **B)** *Reg3b* in ileal IECs from GF, healthy Donor 1-colonized or CMA Donor 5-colonized *Tlr4*$^{+/+}$ and *Tlr4*$^{-/-}$ mice one-week post-colonization. For A-B, 2-way ANOVA with multiple testing using the Benjamini, Krieger, and Yekutili method was performed. *$P$ < 0.05, **$P$ < 0.01, ***$P$ < 0.001

IV. Ileal regulatory T cells and Th17 cells are induced by the Donor 5 microbiota in a TLR4-dependent manner

Because SAA-1 has been previously implicated in regulating type 2 and type 3 inflammation (Smole et al., 2020, Lee et al., 2020), the induction of *Saa1* in a TLR4-dependent manner would suggest that TLR4 also regulates immunological responses. Therefore, we examined Foxp3$^{+}$ regulatory T cells (Tregs), RORγt$^{+}$ Foxp3$^{+}$ Tregs, and IL-17A$^{+}$ RORγt$^{+}$ Th17 cells in TLR4 sufficient and deficient mice (**Figures 5A-D** and Figure **6A-B**)

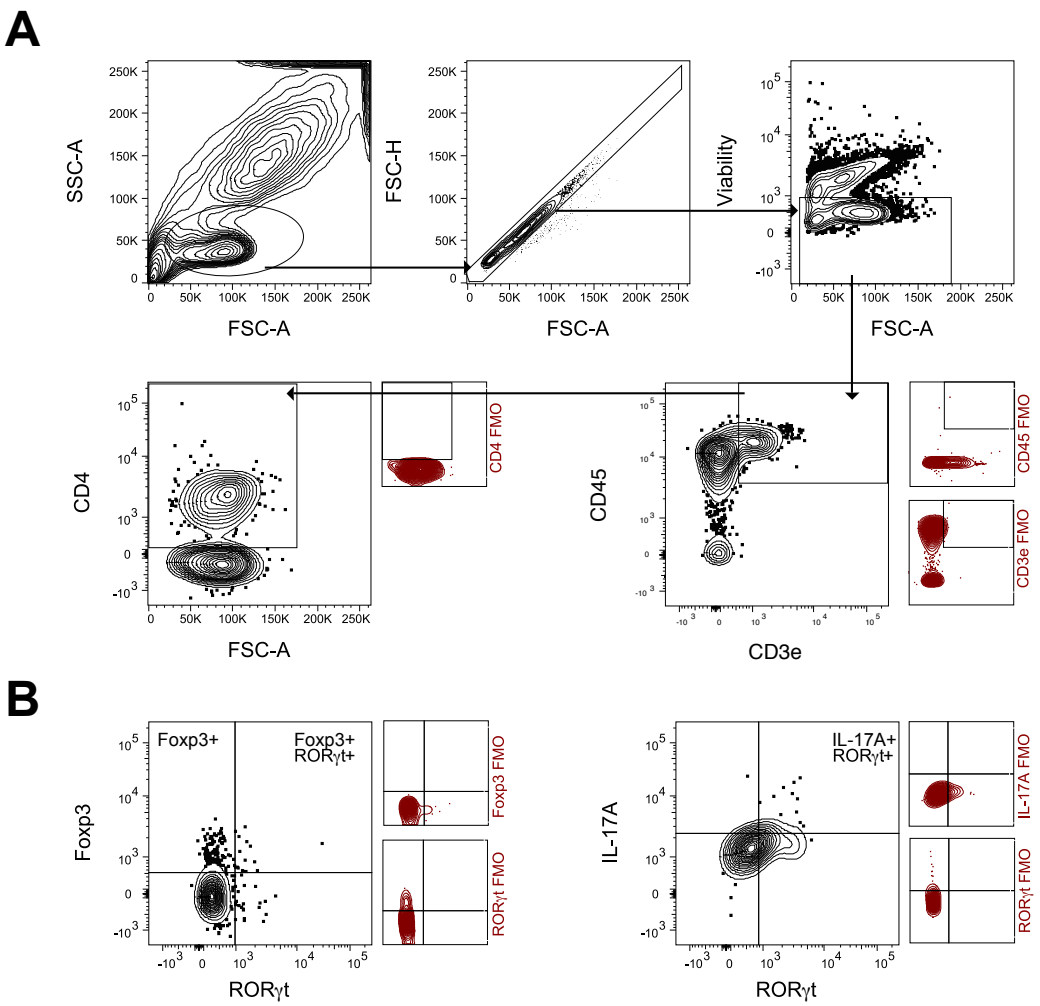


**Figure 4**: Gating strategy for the identification of Tregs and Th17 cells
**A**) Gating strategy for the identification of CD4$^+$ T cells. **B)** Gating strategy to identify Foxp3$^+$Tregs, Foxp3$^+$ RORγt$^+$Tregs, and IL-17A$^+$ RORγt$^+$ Th17 cells within the CD4-positive gate

Regulatory T cells are important for suppressing intestinal inflammation and are identified by the expression of the transcription factor Foxp3 (Bae et al., 2016). Foxp3$^+$ Tregs that develop extrathymically are specifically induced by the microbiota and express the transcription factor RORγt (Sefik et al., 2015). RORγt$^+$ Foxp3$^+$ Tregs have been found to be especially important for the suppression of type 2 inflammation in several mouse models (Abdel-Gadir et al., 2019; Ohnmacht et al., 2015; Josefowicz et al., 2012). Thus, we examined the proportion and absolute numbers of Foxp3$^+$ Tregs and RORγt$^+$Foxp3$^+$

Tregs in the ileum of mice colonized with the CMA and healthy microbiotas. GF C57BL/6 TLR4-sufficient and TLR4-deficient mice were colonized with the CMA Donor 5 microbiota or healthy Donor 2 microbiota at weaning. These mice were then sacrificed one week later to isolate lymphocytes from the ileal lamina propria. Using the gating strategy shown in **Figure 4**, flow cytometric analysis revealed that, in TLR4-sufficient, but not TLR4-deficient, mice, both the frequency and numbers of Foxp3$^+$ Tregs was significantly increased in CMA Donor 5-colonized mice compared to healthy Donor 2-colonized mice and GF mice (**Figure 5A- B).**

For RORγt$^+$ Foxp3$^+$ Tregs, there was an increase in frequency in CMA Donor 5-colonized mice compared to healthy Donor 2-colonized mice and GF mice when TLR4 signaling was sufficient (**Figure 5C**). Furthermore, TLR4 deficiency resulted in a nearly significant decrease in the frequency of this population in CMA-colonized mice. The absolute number of RORγt$^+$Foxp3$^+$ Tregs was significantly higher in TLR4-sufficient, CMA-colonized mice compared to GF mice of the same genotype (**Figure 5D**). There

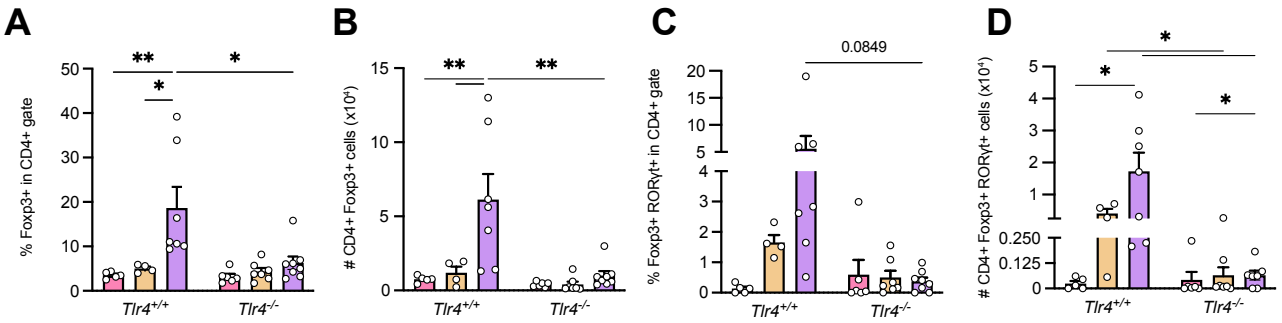


**Figure 5**: Induction of Foxp3$^+$ and RORγt$^+$ Foxp3$^+$ Tregs in the ileum of CMA-colonized mice is regulated by TLR4. Frequency and absolute numbers of **A-B**) Foxp3$^+$ Tregs and **C-D**) Foxp3$^+$ RORγt$^+$ Tregs in the ileal lamina propria of *Tlr4*$^{+/+}$ and *Tlr4*$^{-/-}$ GF (pink), healthy Donor 2-colonized (yellow), and CMA Donor 5-colonized (purple) mice one week post-colonization. Summary of at least two independent experiments per condition. Statistics were calculated using 2-way ANOVA with multiple testing using the Benjamini, Krieger, and Yekutili method. *$P$ < 0.05, **$P$ < 0.01, ***$P$ < 0.001

was also significant reduction in the absolute number of RORγt$^{+}$Foxp3$^{+}$ Tregs in TLR4-deficient, CMA-colonized mice compared to their wildtype counterparts. This population was also significantly reduced in healthy-colonized mice.

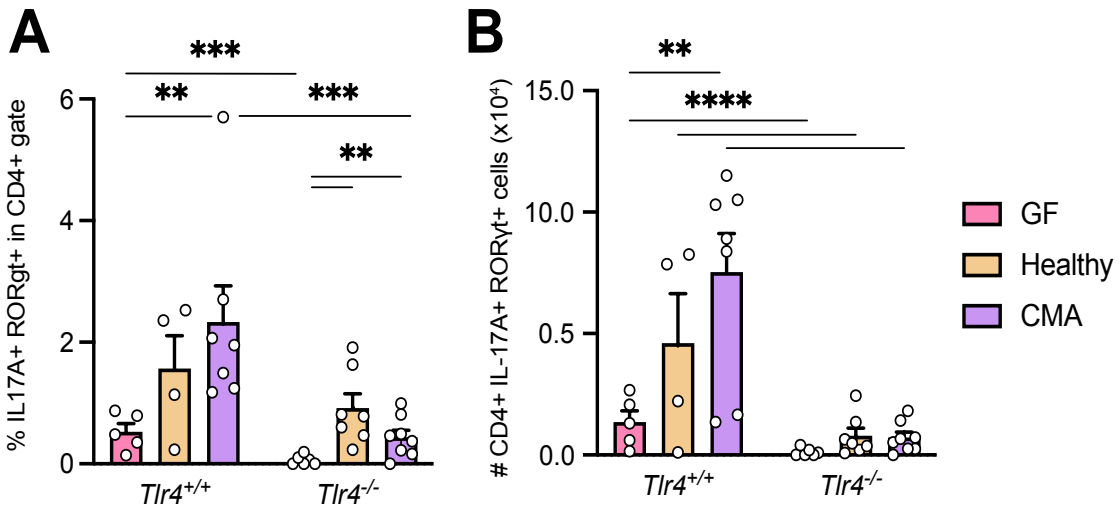


**Figure 6**: Th17 cells are induced in the ileum of CMA-colonized mice in a TLR4-dependent manner. Frequency and absolute numbers of **A-B**) IL-17A$^{+}$ RORγt$^{+}$ Th17 cells in the ileal lamina propria of *Tlr4*$^{+/+}$ and *Tlr4*$^{-/-}$ GF, healthy-colonized, and CMA-colonized mice. **C**) Total CD4$^{+}$ cell numbers in GF, healthy Donor 2-colonized, and CMA Donor 5-colonized mice. **D)** Ratio of the percentage of Th17 cells over Foxp3$^{+}$ Tregs. Data is pooled from at least two independent experiments per condition. Experiments were performed one week post-weaning Statistics were calculated using 2-way ANOVA with multiple testing using the Benjamini, Krieger, and Yekutili method. *$P$ < 0.05, **$P$ < 0.01, ***$P$ < 0.001, ****$P$ < 0.0001

Examining Th17 cell populations, both the frequency and number of Th17 cells was significantly increased in TLR4-sufficient, but not TLR4 deficient, CMA-colonized mice compared to GF mice (**Figure 6A-B**). Importantly, the frequency and numbers of Th17 cells was significantly decreased in TLR4-deficient mice colonized with the CMA microbiota compared to their TLR4-sufficient counterparts. Furthermore, in TLR4-deficient mice, there was a significantly higher frequency of Th17 cells in healthy-colonized and CMA-colonized mice compared to GF mice. The absolute number of Th17

cells was also significantly reduced in TLR4-deficient GF and healthy-colonized mice compared to their WT counterparts. Overall, these data show TLR4 regulates the induction of Th17 cells and Tregs in mice colonized with the microbiota from CMA Donor 5. In agreement with what has been observed in the literature, *Saa1* and *Reg3b* expression is coregulated with the induction of Th17 cells (Atarashi et al., 2015, Sano et al., 2015; Lee et al., 2020).

V. Epithelial TLR4 signaling regulates *Saa1* induction in antibiotic-treated mice colonized with the Donor 5 microbiota

The observation that TLR4 signaling not only regulates the induction of *Saa1* expression by the Donor 5 microbiota but also Th17 and Treg subsets suggests that it may regulate intestinal inflammation that could promote allergic responses to food. It has been well documented that TLR4 signaling in various cellular compartments differentially contributes to regulating atopic inflammation. In a model of allergic asthma, TLR4 signaling in radioresistant epithelial cells contributes to eosinophilic inflammation upon HDM sensitization while TLR4 signaling in the hematopoietic compartment contributes to neutrophilic inflammation (Hammad et al., 2009; McAlees et al., 2015). Furthermore, DCs have specifically been shown to regulate T cell and B cell responses through binding of retinol-SAA-1 complexes in the intestine (Bang et al., 2021). Thus, we examined the role of TLR4 signaling in the epithelial compartment and in the hematopoietic $CD11c^{+}$ compartment, which includes macrophages and DCs.

To do this, we used mice with a conditional knockout of TLR4 in epithelial cells (Villin$^{cre}$TLR4$^{fl/fl}$) and CD11c$^{+}$ cells (CD11c$^{cre}$TLR4$^{fl/fl}$). Because these mice were housed under specific-pathogen free (SPF) conditions, we first depleted their microbiota by treating pups with antibiotics by intragastric gavage for seven days prior to weaning. At weaning, these pups were colonized with the CMA Donor 5 microbiota or the healthy Donor 1 microbiota or left uncolonized as SPF controls. Mice were then sacrificed one week later to examine gene expression in ileal IECs. All experiments were littermate controlled.

Conditional abrogation of TLR4 in epithelial cells revealed interesting results. *Saa1* expression was nearly significantly upregulated in CMA Donor 5-colonized mice compared to healthy Donor 1-colonized mice and SPF controls when TLR4 signaling was sufficient in epithelial cells (Villin$^{WT}$) (**Figure 7A**). In mice with TLR4 deficiency in epithelial cells (Villin$^{\Delta TLR4}$), *Saa1* was no longer upregulated in CMA-colonized mice compared to

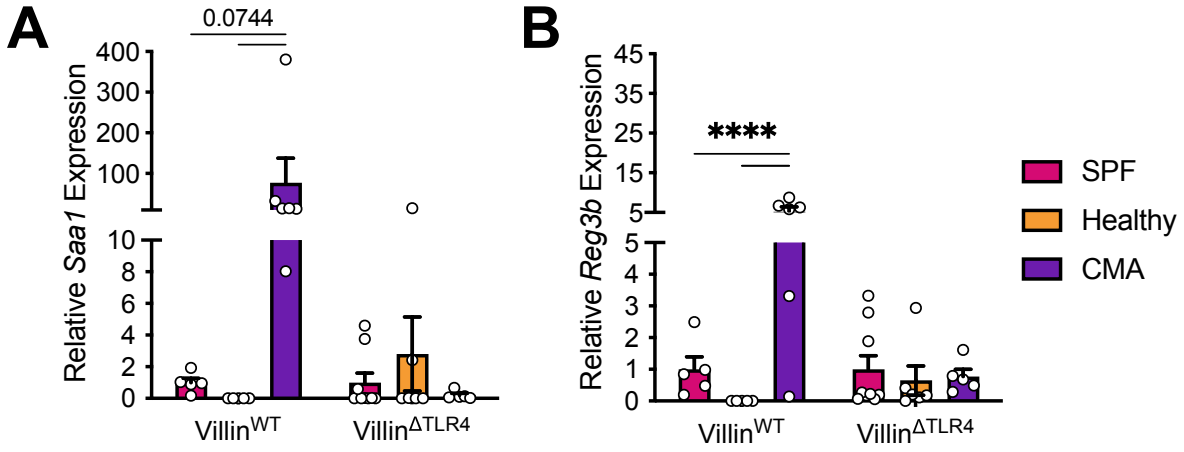


**Figure 7**: Epithelial TLR4 signaling regulates *Saa1* and *Reg3b* expression in ileal IECs in CMA-colonized mice. **A)** Relative expression of *Saa1* and **B)** *Reg3b* in antibiotic-treated SPF mice colonized with the CMA Donor 5 microbiota, healthy Donor 1 microbiota, or left uncolonized after treatment one week post-weaning. Statistics were calculated using 2-way ANOVA with multiple testing using the Benjamini, Krieger, and Yekutili method. ****$P < 0.0001$

SPF controls and healthy-colonized mice. Furthermore, *Reg3b* was significantly upregulated in CMA-colonized mice compared to SPF controls and healthy-colonized mice when TLR4 signaling was sufficient in epithelial cells (**Figure 7B**). However, when TLR4 signaling was abrogated in the epithelial compartment, this gene was no longer significantly upregulated in CMA-colonized mice. In healthy-colonized mice, however, both *Saa1* and *Reg3b* expression were decreased compared to SPF controls, although not significantly. This was somewhat unexpected, as our previous data showed that the healthy Donor 1 microbiota significantly induces expression *Saa1* and *Reg3b* compared to GF mice (**Figure 2B**, **Figure 3**). However, interference from the SPF microbiota may contribute to this result that was not observed in a GF colonization model. Overall, these data show that TLR4 signaling in epithelial cells does regulate *Saa1* and *Reg3b* expression in ileal IECs of Donor 5-colonized mice.

VI. TLR4 signaling in CD11c$^{+}$ cells regulates the expression of Th17 genes, B cell genes, and alarmins in the ileum epithelium of Donor 5-colonized mice

In mice with a conditional mutation of TLR4 in CD11c$^{+}$ cells, we observed changes in gene expression that were similar to those seen in global TLR4 knockout mice. In CD11c$^{WT}$ mice, both *Saa1* and *Reg3b* were significantly upregulated in CMA Donor 5-colonized mice compared to healthy Donor 1-colonized mice and SPF controls (**Figure 8 A-B**). However, in their CD11c$^{\Delta TLR4}$ littermates, this upregulation was no longer observed. To get a better understanding of the immunological responses that may be mediated by ileal IECs in CMA-colonized mice, we also examined the expression of B cell related

genes and alarmins, which were observed to be upregulated in CMA-colonized mice in our previous RNA sequencing results (**Tables 3** and **4**). IgA is the most abundant immunoglobulin secreted at mucosal surfaces and is important for regulating microbial pathogens and commensal ecology (Okai et al., 2016; Nakajima et al., 2018). IgA is dimerized by joining-chain (J-chain) after secretion by plasma cells and then transcytosed from the basolateral side of the epithelium to the apical surface and into the intestinal lumen (Campbell et al., 2021). We observed that *Igha*, the gene for IgA, and *Jchain* were both significantly upregulated in Donor 5-colonized, $CD11c^{WT}$ mice but not in their $CD11c^{\Delta TLR4}$ littermates (**Figure 9A-B**). These observations correlated with observable differences in fecal IgA, which was significantly reduced in $CD11c^{\Delta TLR4}$ mice compared to

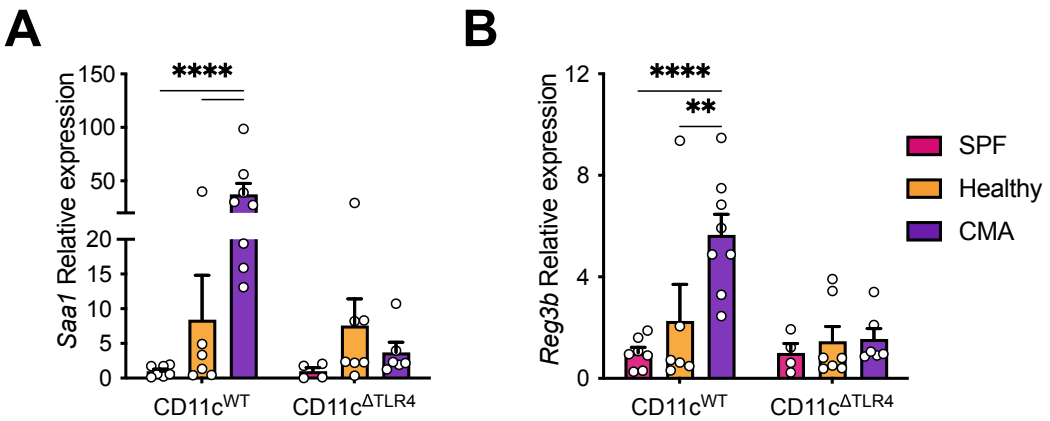


**Figure 8**: CMA-dependent upregulation of *Saa1* and *Reg3b* is dependent on TLR4 signaling in $CD11c^{+}$ cells. **A)** Relative expression of *Saa1* and **B)** *Reg3b*, in antibiotic-treated SPF mice colonized with the CMA Donor 5 microbiota, healthy Donor 1 microbiota, or left uncolonized after treatment one week post-weaning. Statistics were calculated using 2-way ANOVA with multiple testing using the Benjamini, Krieger, and Yekutili method $^{**}P < 0.01$, $^{***}P < 0.001$, $^{****}P < 0.0001$

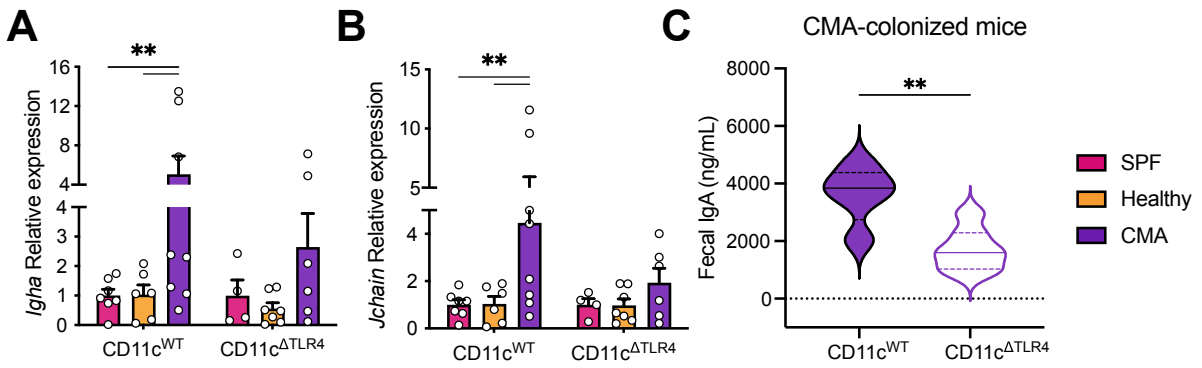


**Figure 9**: Fecal IgA is regulated by TLR4 signaling in CD11c+ cells. **A)** Relative expression of I*gha* and **B)** *Jchain*. **C)** Measurement of fecal IgA in CD11c$^{WT}$ and CD11c$^{\Delta TLR4}$ mice colonized with the CMA microbiota. Experiments were performed one week post-weaning. For A-B, 2-way ANOVA with multiple testing using the Benjamini, Krieger, and Yekutili method. For C, Wilcoxon rank sum test was performed between both genotypes. $^{**}P < 0.01$

CD11c$^{WT}$ mice colonized with the CMA-microbiota (**Figure 9C**). These results suggest that TLR4 may also shape mucosal bacterial communities by regulating IgA production.

We also examined the expression of the epithelial alarmins *Il25*, *Il33*, and *Tslp*, which play a role in mediating type 2 inflammation in response to damage and sensitization with an allergen (Peterson et al., 2014). *Il25* and *Il33* appeared to be regulated in a reciprocal manner. In CD11c$^{WT}$ mice, *Il33* was nearly significantly upregulated in CMA-colonized mice compared to both healthy-colonized mice and SPF

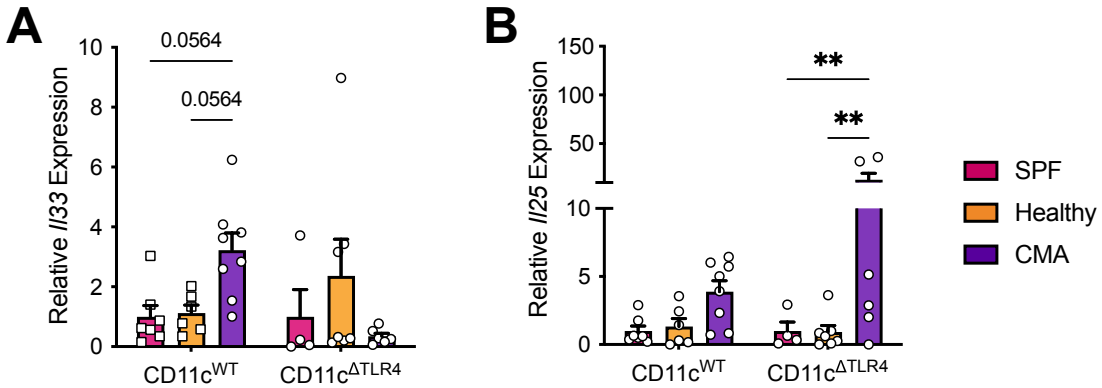


**Figure 10**: TLR4 signaling in CD11c$^{+}$ cells reciprocally regulates alarmins **A)** Relative expression of *IL33* and **B)** *Il25* in antibiotic-treated SPF mice colonized with the CMA Donor 5 microbiota, healthy Donor 1 microbiota, or left uncolonized after treatment one week post-weaning. Statistics were calculated using 2-way ANOVA with multiple testing using the Benjamini, Krieger, and Yekutili method. $^{**}P < 0.01$

mice, which was not seen in CD11c$^{\Delta TLR4}$ littermates (**Figure 10A**). Conversely, *Il25* was not observed to be upregulated in CD11c$^{WT}$ mice colonized with the CMA microbiota (**Figure 10B**). However, in CD11c$^{\Delta TLR4}$ mice, *Il25* was upregulated significantly in CMA-colonized mice compared to both healthy-colonized mice and SPF controls. *Tslp* was not expressed in any mice (data not shown). These results suggest that TLR4 signaling in CD11c$^{+}$ cells may regulate type 3 responses, type 2 responses, and B cell responses in the ileum of Donor 5-colonized mice. This RT-qPCR analysis validates the results obtained from the bulk RNA sequencing data performed in ex-GF mice (**Tables 3** and **4**).

VII. Expression of genes involved in various immunological pathways is regulated by TLR4 signaling in CD11c$^{+}$ cells

To better understand how TLR4 signaling in CD11c$^{+}$ cells regulates gene expression in the ileal mucosa of CMA Donor 5-colonized mice, bulk RNA sequencing was conducted on RNA isolated from ileal IECs of antibiotic-treated CD11c$^{WT}$ and CD11c$^{\Delta TLR4}$ mice that were uncolonized SPF controls, colonized with the CMA microbiota, or colonized with the healthy microbiota. Differential expression analysis between CD11c$^{WT}$ mice colonized with the CMA microbiota and the healthy microbiota revealed several genes to be specifically upregulated in each group. Some of the genes upregulated in this dataset were upregulated in our previous RNA sequencing dataset which analyzed ileal IEC gene expression in ex-GF mice colonized with each of the 4 healthy infant donors compared to CMA Donor 5 (see **Tables 3** and **4**). Specifically, the expression of *Saa1* was upregulated, along with other previously identified Th17-associated genes, such as *Reg3b* and *Reg3g*, (**Figure 11A**, **Table 5**). Other genes

involved in epithelial-induced proinflammatory responses and barrier function such as *Il18* and *Il18bp* were also upregulated. Many genes related to B cell responses were also upregulated, including *Igha*, *Jchain*, and numerous immunoglobulin genes (note that our method for isolation of IECs does not include excision of Peyer's patches – see Methods). The type 2 alarmin *Il33* was also found to be upregulated in CMA-colonized mice compared to healthy-colonized mice, in agreement with the qRT-PCR results (**Table 5, Figure 10**). This also agrees with our previous RNA sequencing data, which showed *Il33* to be upregulated in CMA Donor 5-colonized ex-GF mice (**Table 4**).

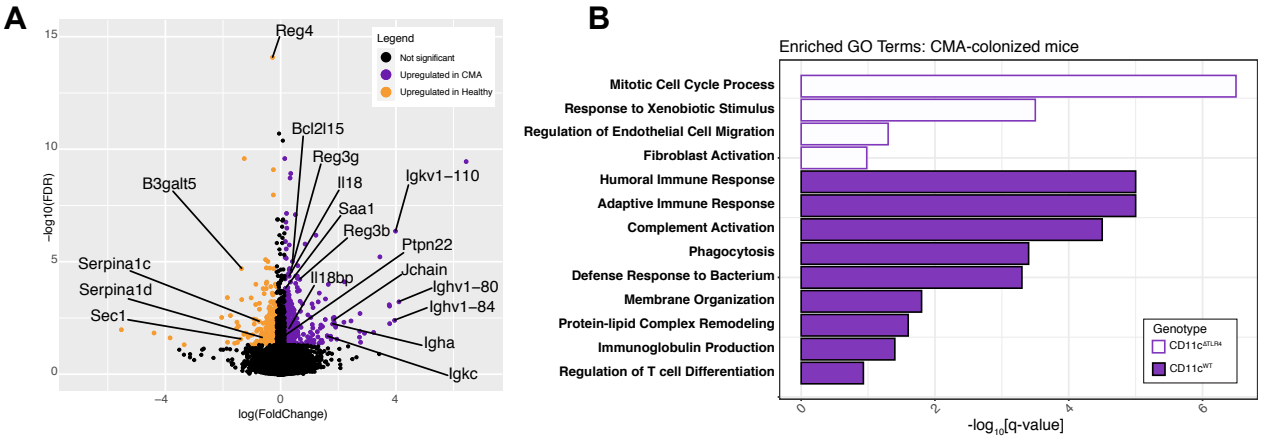


**Figure 11**: TLR4 signaling in CD11c$^+$ cells regulates gene expression in IECs from CMA-colonized mice. **A)** Volcano plot of significantly upregulated genes in CD11c$^{WT}$ antibiotic-treated SPF mice colonized with the CMA Donor 5 or healthy Donor 1 microbiotas one week following colonization **B)** Identified gene ontology (GO) pathways significantly enriched in ileal IECs of CMA-colonized CD11c$^{WT}$ and CD11c$^{\Delta Tlr4}$ mice.

Next, pathway analysis was conducted on CD11c$^{WT}$ and CD11c$^{\Delta TLR4}$ mice colonized with this the Donor 5 microbiota. Results showed that many genes upregulated in CD11c$^{WT}$ mice were involved in immunological processes. In agreement with the differential expression analysis and qRT-PCR data, genes involved in humoral immune responses and immunoglobulin production were highly significantly upregulated (**Figure 11B**). Genes involved in regulation of T cell differentiation were also significantly

upregulated, in agreement with our previous data showing global TLR4 signaling regulates several T cell subsets in Donor 5-colonized mice (**Figures 5-6**). Interestingly, genes involved in defense against bacteria were also upregulated, suggesting that members of the Donor 5 microbiota may be antigenically proinflammatory in nature. In CD11c$^{\Delta TLR4}$ mice, these immunological pathways were not upregulated. Instead, the pathways upregulated were more aligned with homeostatic regulation of the epithelium.

To get an understanding of the bacterial communities that induce these genes in CMA-colonized and healthy-colonized mice, 16S sequencing was performed on samples of ileal contents acquired from these mice at sacrifice. We are aware that because these mice originated from a SPF colony and were treated with antibiotics, the gut microbiota will consist of an amalgamation of bacteria originating from the SPF mouse facility and human-derived bacteria from the infant donors. Therefore, we performed a basic, holistic analysis of alpha and beta diversity to assess the ecological dynamics of the commensal microbiota and determine the fidelity of transfer of the human infant microbiota. The

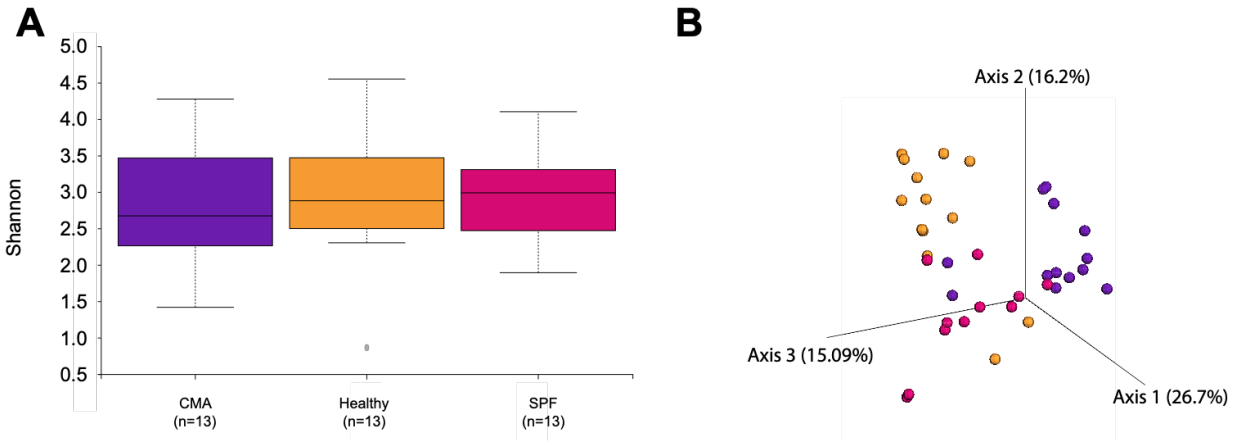


**Figure 12**: Antibiotic-treatment of SPF mice allows for engraftment of the human infant microbiota. **A)** Alpha diversity of each colonization condition (CMA Donor 5, Healthy Donor 1, and SPF) as measured by the Shannon diversity index. **B)** Principal Coordinate Analysis (PCoA) of beta diversity (Bray-Curtis) showing Euclidean distances between antibiotic-treated SPF mice colonized with an infant microbiota (CMA or healthy) or left uncolonized after treatment (SPF). Sequencing and analysis were performed on ileal samples from mice one week post-weaning.

Shannon index was used to calculate diversity within each sample. Analysis of each sample by group determined that the average diversity within each sample was not significantly different between colonization status (**Figure 12A**). To determine the fidelity of transfer, beta diversity was determined using the Bray-Curtis index of dissimilarity. Analysis between groups showed that there were significant differences between microbial communities based on colonization status (**Figure 12B**). This suggests that the transfer of the human infant gut microbiota was successful following antibiotic treatment of SPF mice and that differences in gene expression observed in CMA-colonized mice and healthy-colonized mice were due to the infant microbiota. Together, these data show that in our antibiotic-treated SPF model, the phenotypic upregulation of *Saa1* and *Reg3b* (as well as numerous immune system genes) in isolated IEC and the production of fecal IgA, is most likely due to the engraftment of the Donor 5 microbiota despite these mice being of SPF origin.

In this chapter, we show that a microbiota from an infant with a severe allergy to cow's milk (CMA Donor 5) promotes ileal inflammatory responses upon transfer to GF mice and antibiotic-treated SPF mice. This inflammatory response includes the upregulation of genes involved in type 2 and type 3 responses (e.g., *Saa1*, *Reg3b*, *Il33*), induction of Tregs and Th17 cells, and increased production of intestinal IgA. Moreover, this inflammatory response is regulated by TLR4 signaling.

Elevated SAA in serum and other bodily secretions has been associated with a number of diseases and specifically induces differentiation of naïve T cells into Th17 cells (Bourgonje et al., 2019; Yarur et al., 2017; Bich et al., 2022; Ozseker et al., 2006; Ivanov et al., 2009). Additionally, in models of allergic disease, it has been shown to contribute

to type 2 and type 3 inflammatory responses (Lee et al., 2020; Ather et al., 2011). In agreement with the literature, induction of *Saa1* by the CMA microbiota is coregulated with *Il33* expression and induction of IL-17 by Th17 cells (Smole et al., 2020). As *Il33* is an epithelial-derived alarmin (Peterson and Artis, 2014), the induction of *Il33* by the Donor 5 microbiota suggests that the microbiota itself may have adjuvant-like properties and can orient the ileal mucosa toward type 2 inflammatory responses. Moreover, reciprocal regulation of *Il33* and *Il25* by TLR4 further implies that the Donor 5 microbiota induces a type 2 inflammatory microenvironment through distinct pathways and that microbial sensing by TLR4 regulates type pathway by which said inflammation is induced. Microbial-derived products can influence allergic sensitization when administered with adjuvants and allergens (Hadebe et al., 2015; Zhang et al., 2017). Thus, it would be expected that sensitization with food antigen and a strong adjuvant, like CT, would exacerbate the type 2 inflammation that the CMA microbiota already promotes. Although this work doesn't investigate effector functions of type 2 responses prior to sensitization, examination of type 2 immune cells, such as ILC2s, in future experiments could reveal information about the inflammatory status of Donor 5-colonized mice. All in all, the data presented supports previous findings that *Saa1* is a hallmark of a mixed type 2/type 3 inflammatory profile.

Along with inflammatory gene expression, we show that T cell and B cell responses are regulated by TLR4 signaling in Donor 5-colonized mice. TLR4 signaling has been shown to be required for optimal activation of APCs and thus T cell effector function in allergic mouse models of asthma (Dabbagh et al., 2002; Cho et al., 2018). Additionally, induction of $Foxp3^+$ Tregs and $ROR\gamma t^+$ $Foxp3^+$ Tregs in response to gut inflammation

induced by Gram-negative bacteria requires TLR4 signaling (Liu et al., 2022; Jia et al., 2017). Thus, the high induction of Tregs specifically in CMA-colonized mice is likely due to immune mechanisms aimed at addressing inflammatory responses induced by the microbiota. Additionally, production of secretory IgA is associated with decreased inflammatory responses following allergen sensitization and challenge (Schwarze et al., 1998; Smits et al., 2009; Bonnegarde-Bernard et al., 2014). Furthermore, IgA can be differentially induced in the gut by LPS based on the bacterial source (Shibata et al., 2018). Regulation of inflammatory gene expression and IgA by TLR4 signaling in specific cellular compartments suggests that multiple cell types are involved in the response to the proinflammatory Donor 5 microbiota. As TLR4 signaling in epithelial cells and hematopoietic cells regulate eosinophilic and neutrophilic allergic inflammation respectively (McAlees et al., 2015; Hammad et al., 2009), the cellular effectors that respond to the CMA microbiota may be very diverse. Re-deriving both conditional knock out strains as GF and examining these specific granulocyte populations could give insight to how TLR4 signaling in these compartments contributes to the overall inflammatory response induced by the CMA microbiota. Therefore, microbial sensing through TLR4 can regulate the immune system’s concerted effort to regain homeostatic balance in the face of local inflammatory responses. data described highlights a previously unappreciated multicellular axis by which an atopic microbiota promotes intestinal inflammation.

**Table 5**: Differentially expressed genes upregulated in IEC from CMA Donor 5-colonized mice compared to healthy Donor 1-colonized mice that have been treated with antibiotics prior to weaning

| Gene Symbol | Description | Adjusted P-value |
|---|---|---|
| Bcl2l15 | BCLl2-like 15 | 9.87E-06 |
| C1qa | complement component 1, q subcomponent, alpha polypeptide | 0.03130316 |
| C1qb | complement component 1, q subcomponent, beta polypeptide | 0.08882121 |
| Ccl22 | chemokine (C-C motif) ligand 22 | 0.03165497 |
| Cd180 | CD180 antigen | 0.03800273 |
| Clec4n | C-type lectin domain family 4, member n | 0.00763022 |
| Dnase1l3 | deoxyribonuclease 1-like 3 | 0.00653161 |
| Hif3a | hypoxia inducible factor 3, alpha subunit | 0.02816113 |
| Igha | immunoglobulin heavy constant alpha | 0.00589532 |
| Ighj2 | immunoglobulin heavy joining 2 | 0.00811764 |
| Ighj3 | immunoglobulin heavy joining 3 | 0.00297253 |
| Ighv1-11 | immunoglobulin heavy variable V1-11 | 0.02267783 |
| Ighv1-5 | immunoglobulin heavy variable V1-5 | 0.00320737 |
| Ighv1-75 | immunoglobulin heavy variable 1-75 | 3.56E-10 |
| Ighv1-80 | immunoglobulin heavy variable 1-80 | 0.00060879 |
| Ighv1-84 | immunoglobulin heavy variable 1-84 | 0.00405857 |
| Igkc | immunoglobulin kappa constant | 0.02100662 |
| Igkj2 | immunoglobulin kappa joining 2 | 7.86E-05 |
| Igkj4 | immunoglobulin kappa joining 4 | 0.02771162 |
| Igkv1-110 | immunoglobulin kappa variable 1-110 | 4.38E-07 |
| Igkv1-117 | immunoglobulin kappa variable 1-117 | 6.11E-06 |
| Igkv1-122 | immunoglobulin kappa chain variable 1-122 | 0.01392853 |
| Igkv2-137 | immunoglobulin kappa chain variable 2-137 | 0.01513843 |
| Iglv2 | immunoglobulin lambda variable 2 | 0.02046588 |
| Il18 | interleukin 18 | 4.41E-05 |
| Il18bp | interleukin 18 binding protein | 0.00944632 |
| Il33 | interleukin 33 | 0.01594795 |
| Jchain | immunoglobulin joining chain | 0.00404739 |
| Mt1 | metallothionein 1 | 0.00200604 |
| Mt2 | metallothionein 2 | 0.00082159 |
| Mt4 | metallothionein 4 | 0.00566028 |
| Ptpn22 | protein tyrosine phosphatase, non-receptor type 22 | 0.01973732 |
| Reg3b | regenerating islet-derived 3 beta | 6.08E-05 |
| Reg3g | regenerating islet-derived 3 gamma | 2.57E-05 |
| Siglech | sialic acid binding Ig-like lectin H | 0.0913945 |
| Saa1 | serum amyloid A 1 | 0.000152846 |
| Slc35f4 | solute carrier family 35, member F4 | 0.04296241 |
| Tnfrsf26 | tumor necrosis factor receptor superfamily, member 26 | 0.03722319 |

## Chapter 4. The Donor 5 microbiota is enriched with Bacteroidetes and primes an early type 2/type 3 response that is TLR4-dependent

### I. Th17- and B cell-associated genes are regulated by TLR4 signaling in CD11c$^+$ cells in ex-GF mice colonized with the CMA microbiota

We have shown that global and conditional expression of TLR4 in CD11c$^+$ cells regulates ileal IEC gene expression in CMA-colonized mice in both GF and antibiotic-treated colonization models, respectively. Furthermore, global TLR4 signaling regulates the induction of Tregs and Th17 cells, while TLR4 signaling in CD11c$^+$ cells regulates intestinal IgA induction. In order get an understanding of members of the Donor 5 microbiota that may contribute to these immune responses, we proceeded to rederive SPF CD11c$^{WT}$ and CD11c$^{\Delta TLR4}$ mice as GF. The experiments that were performed in the antibiotic-treated model were repeated using these GF mice. In repeating these experiments, we followed a protocol similar to that utilized for the global TLR4 knockout mice. These mice were colonized at weaning with the Donor 5 or Donor 2 microbiota and sacrificed one-week post-colonization to isolate RNA from ileal IECs and examine *Saa1* expression.

Expression analysis showed results that were strikingly similar to those observed in global and CD11c conditional knockout mice. *Saa1* and *Reg3b* were significantly upregulated in CMA-colonized mice compared to healthy-colonized and GF mice (**Figure 13A-B**). However, in mice with a conditional mutation in TLR4 in CD11c$^+$ cells, these genes were no longer upregulated in CMA-colonized mice. When looking at B cell-related

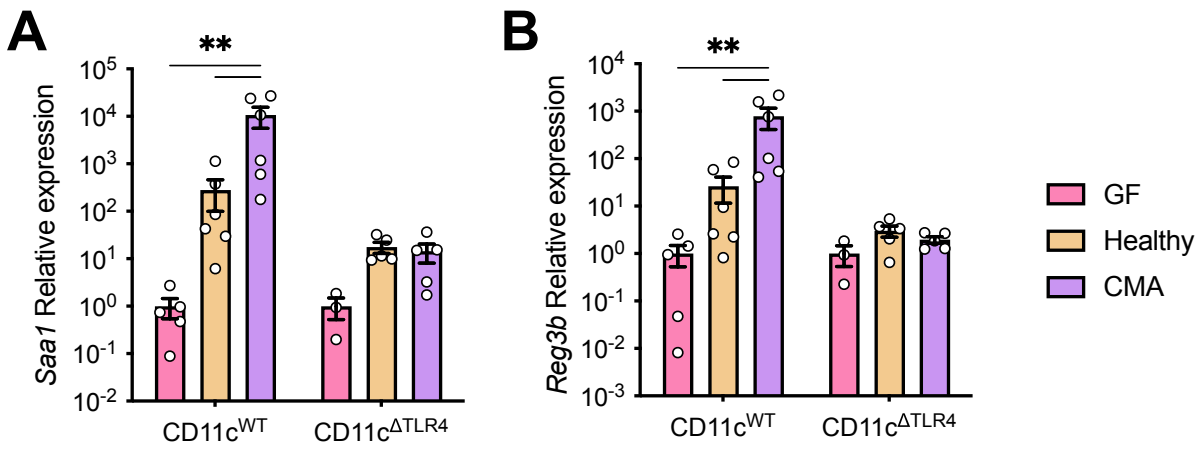


**Figure 13**: *Saa1* and *Reg3b* expression is regulated by TLR4 signaling in CD11c$^+$ cells in ex-GF mice colonized with the CMA microbiota **A)** Relative expression of *Saa1*, **B)** *Reg3b* in ex-GF CD11c$^{WT}$ and CD11c$^{\Delta TLR4}$ mice colonized with the CMA Donor 5 microbiota, the healthy Donor 2 microbiota or left GF for one-week post-weaning. Statistics were calculated using 2-way ANOVA with multiple testing using the Benjamini, Krieger, and Yekutili method. $^{**}P < 0.01$

genes, a similar pattern was observed. Expression of *Igha* and *Jchain* was higher in CMA-colonized mice compared to healthy-colonized and GF mice, which was regulated by TLR4 signaling in CD11c$^+$ cells (**Figure 14 A-B**). This translated to differences in the production of fecal IgA. In CD11c$^{WT}$ mice, fecal IgA was significantly higher in CMA-colonized mice compared to healthy-colonized and GF mice. In CD11c$^{\Delta TLR4}$ mice, there was significantly higher fecal IgA in CMA-colonized and healthy-colonized mice compared to GF mice. Interestingly, there was a significant reduction in fecal IgA in CMA-colonized CD11c$^{WT}$ mice compared their CD11c$^{\Delta TLR4}$ littermates (**Figure 14C**). This significant reduction was not observed between CD11c$^{WT}$ and CD11c$^{TLR4}$ mice colonized with the healthy microbiota nor CD11c$^{WT}$ and CD11c$^{\Delta TLR4}$ GF mice. These data show that TLR4 signaling in CD11c$^+$ cells regulate the expression of *Saa1* and *Reg3b* in ileal IECs of Donor 5-colonized mice in both the GF and antibiotic-treated colonization models.

Furthermore, in Donor 5-colonized mice, TLR4 signaling in CD11c$^{+}$ cells regulates B cell responses, and intestinal IgA production.

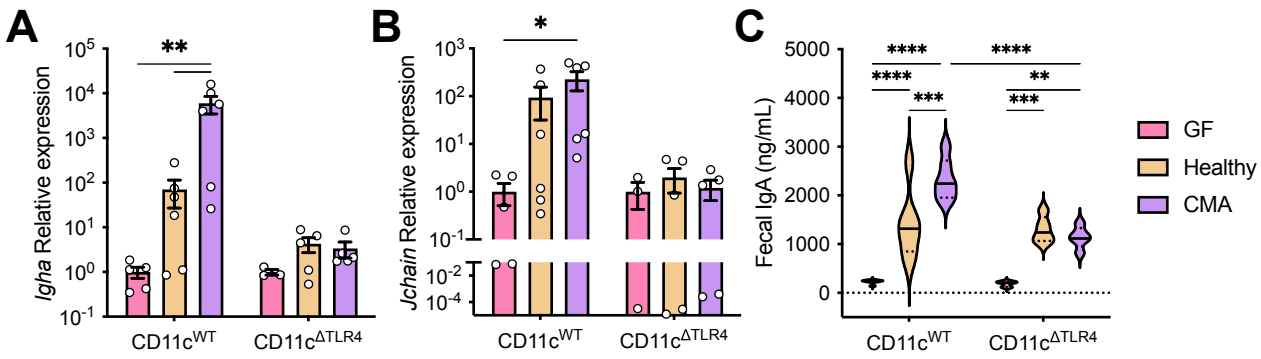


**Figure 14**: Intestinal IgA production is regulated by TLR4 signaling in CD11c$^{+}$ cells in ex-GF mice colonized with the CMA microbiota **A)** Relative expression of *Igha* and **B)** *Jchain* in ex-GF CD11c$^{WT}$ and CD11c$^{\Delta TLR4}$ mice colonized with the CMA Donor 5 microbiota, the healthy Donor 2 microbiota or left GF for one-week post-weaning. **C)** Quantified IgA in fecal pellets from these mice. Statistics were calculated using 2-way ANOVA with multiple testing using the Benjamini, Krieger, and Yekutili method. *$P$ < 0.05, **$P$ < 0.01, ***$P$ < 0.001, ****$P$ < 0.0001

II. TLR4 signaling in CD11c$^{+}$ cells regulates Th17 populations but not Treg populations in the ileum of Donor 5-colonized mice

Because similar gene expression results were seen in ex-GF mice with TLR4 globally knocked out, we proceeded to examine whether TLR4 signaling in CD11c$^{+}$ cells regulated T cell populations in a similar fashion. We observed that TLR4 signaling in CD11c$^{+}$ cells did not regulate T cell populations in the same way that global TLR4 signaling did. Both CMA and healthy-colonized mice had significantly more frequent Foxp3$^{+}$ Tregs compared to GF mice when TLR4 signaling was sufficient in CD11c$^{+}$ cells (**Figure 15A**). The absolute number of Foxp3$^{+}$ Tregs was also significantly higher in CD11c$^{WT}$, CMA-colonized mice compared to their GF counterparts (**Figure 15B**). The frequency of allergy

suppressive RORγt$^{+}$ Foxp3$^{+}$ Tregs was also increased in CD11c$^{WT}$ mice colonized with the CMA microbiota compared to GF mice (**Figure 15C**). However, the frequency and absolute number of both Foxp3$^{+}$ Tregs and RORγt$^{+}$Foxp3$^{+}$ Tregs was not different between CD11c$^{WT}$ and CD11c$^{\Delta TLR4}$ littermates in all colonization conditions (**Figure 15D**). This suggests that TLR4 signaling in another cellular compartment regulates the induction of Treg populations that are induced by the Donor 5 microbiota.

Examining Th17 populations, we observed that in CD11c$^{WT}$ mice, there were significantly higher frequencies in healthy and CMA-colonized mice compared to GF mice (**Figure 16A**). Furthermore, the frequency of this population was significantly reduced in CD11c$^{\Delta TLR4}$ mice colonized with the CMA microbiota compared to their wildtype littermates. This reduction was also observed in the absolute numbers of Th17 cells and

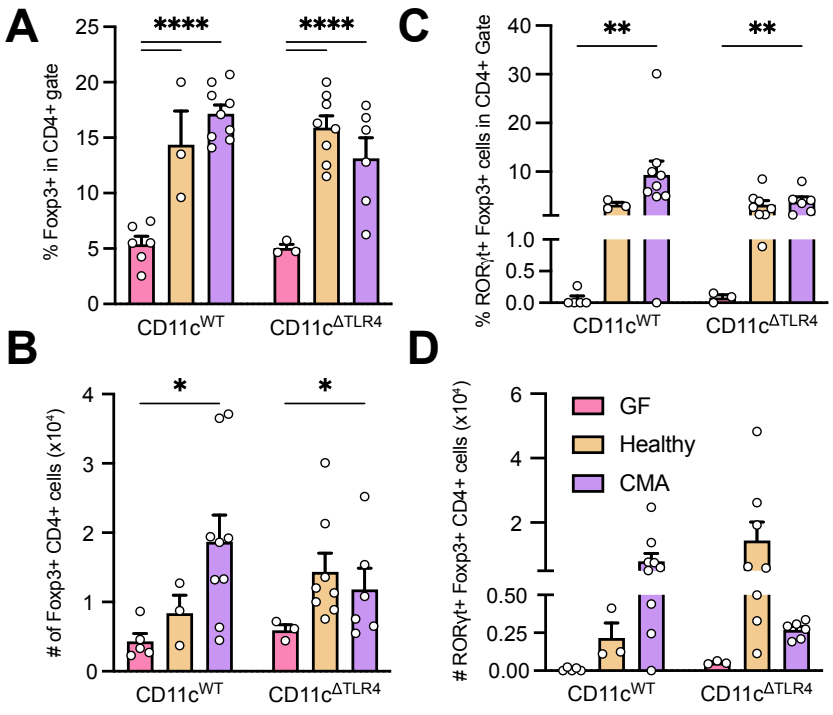


**Figure 15**: Ileal Treg populations are not regulated by TLR4 signaling in CD11c$^{+}$ cells in CMA-colonized mice. Frequency and absolute numbers of **A-B)** Foxp3$^{+}$ (SP) Tregs and **C-D)** Foxp3$^{+}$ RORγt$^{+}$ (DP) Tregs in the ileal tissue of GF, healthy Donor 2-colonized, and CMA Donor 5-colonized CD11c$^{WT}$ and CD11c$^{\Delta TLR4}$ mice one week post-weaning. Summary of at least 2 independent experiments per condition. Summary of at least 2 independent experiments per condition. Statistics were calculated using 2-way ANOVA with multiple testing using the Benjamini, Krieger, and Yekutili method. *$P$ < 0.05, **$P$ < 0.01, ****$P$ < 0.0001

was nearly significant (**Figure 16B**). The absolute number of Th17 cells in CMA-colonized mice was also greater compared to healthy-colonized mice and GF mice when TLR4 signaling was sufficient in CD11c$^{+}$ cells. In CD11c$^{\Delta TLR4}$ mice, the frequency and absolute number of Th17 cells was significantly higher in CMA-colonized mice compared to GF mice (**Figure 16A-B**). These results show that in CMA-colonized mice, TLR4 signaling in CD11c$^{+}$ cells regulates Th17 but not Treg populations. This agrees with previous findings that SAA induces Th17 differentiation only in the presence of CD11c$^{+}$ DCs from the lamina propria (Ivanov et al., 2009). Together, these data show that while global TLR4 signaling regulates the induction of Tregs and Th17 cells in Donor 5-colonized mice, TLR4 signaling in CD11c$^{+}$ cells specifically regulates the induction of Th17 cells.

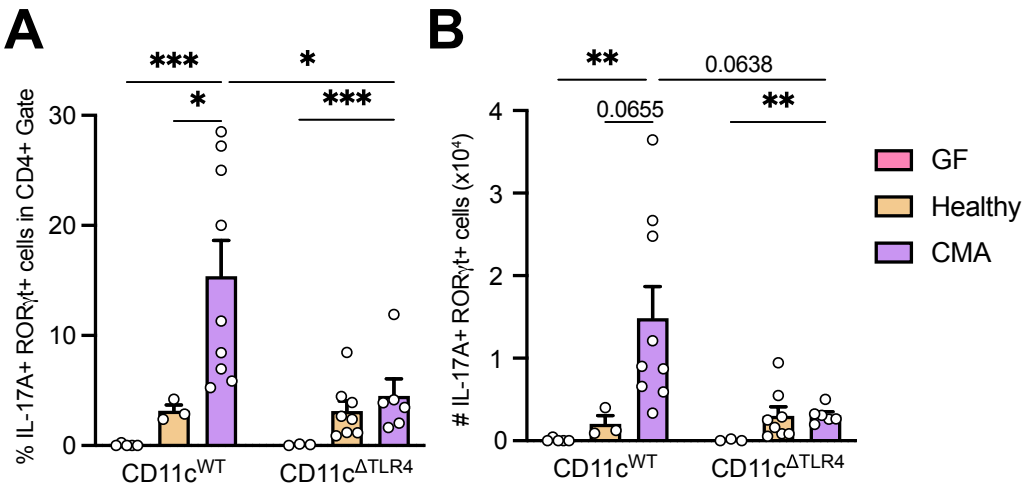


**Figure 16**: TLR4 signaling in CD11c$^{+}$ cells regulate Th17 populations in the ileum of CMA-colonized mice. **A-B)** Frequency and absolute numbers of IL-17A$^{+}$ RORγt$^{+}$ Th17 cells in the ileal tissue of GF, healthy Donor 2-colonized, and CMA Donor 5-colonized CD11c$^{WT}$ and CD11c$^{\Delta TLR4}$ mice one week post-weaning. Summary of at least 2 independent experiments per condition. Summary of at least 2 independent experiments per condition. Statistics were calculated using 2-way ANOVA with multiple testing using the Benjamini, Krieger, and Yekutili method. *$P$ < 0.05, **$P$ < 0.01, ***$P$ < 0.001, ****$P$ < 0.0001

III. Expression of antimicrobial genes by multiple immune cell populations is induced by the Donor 5 microbiota and is regulated by TLR4 signaling in $CD11c^+$ cells

So far, our data shows that TLR4 signaling in $CD11c^+$ cells regulates the expression of the Th17-associated genes *Saa1* and *Reg3b*, as well as B cell-associated genes *Igha* and *Jchain*. Accordingly, Th17 populations are also regulated by TLR4 signaling in $CD11c^+$ cells. To get a more global understanding of how TLR4 signaling in $CD11c^+$ cells regulate other immune cell phenotypes, we conducted single cell RNA sequencing on lymphocytes isolated from the ileum of CMA-colonized mice. Single cell transcriptomic analysis showed that between $CD11c^{WT}$ and $CD11c^{\Delta TLR4}$ mice, similar populations of immune cells are represented in the ileum (**Figure 17A**). These cell types were determined by examining the expression of prototypical marker genes of each cell type within each cluster (**Figure 17B, Table 6**).

**Table 6**: Gene markers used to identify cell clusters

| **Cell type** | **Markers** |
|---|---|
| Epithelial cell | Cd24a, Itga6, Ceacam1, Itgb4 |
| Macrophage | Mrc1, Itgax, Itgam, Adgre1 |
| B cell | Cd79a, Cd79b, Ms4a1, Cd19, Ptprc |
| T cell | CD8, Cd3d, Cd3e, Cd3g, Ptprc, Cd4, Il21r, Il17a, Stat3, Rorc |
| Tuft (Brush) cell | Avil, Siglecf, Cdhr2, Espn |
| Paneth cell | Ctnnb1, Defa5, Tlr5 |
| Stem cell | Itgb1, Prom1 |
| Goblet cell | Muc2, Muc5ac, Krt7, Galnt12, Atoh1 |
| Tregs | Cd3d, Cd3e, Cd3g, Ptprc, Cd4, Foxp3 |
| ILC | Gata3, Rora, Id2, Rorc, IL17a, Il23r, Il22, Ahr |

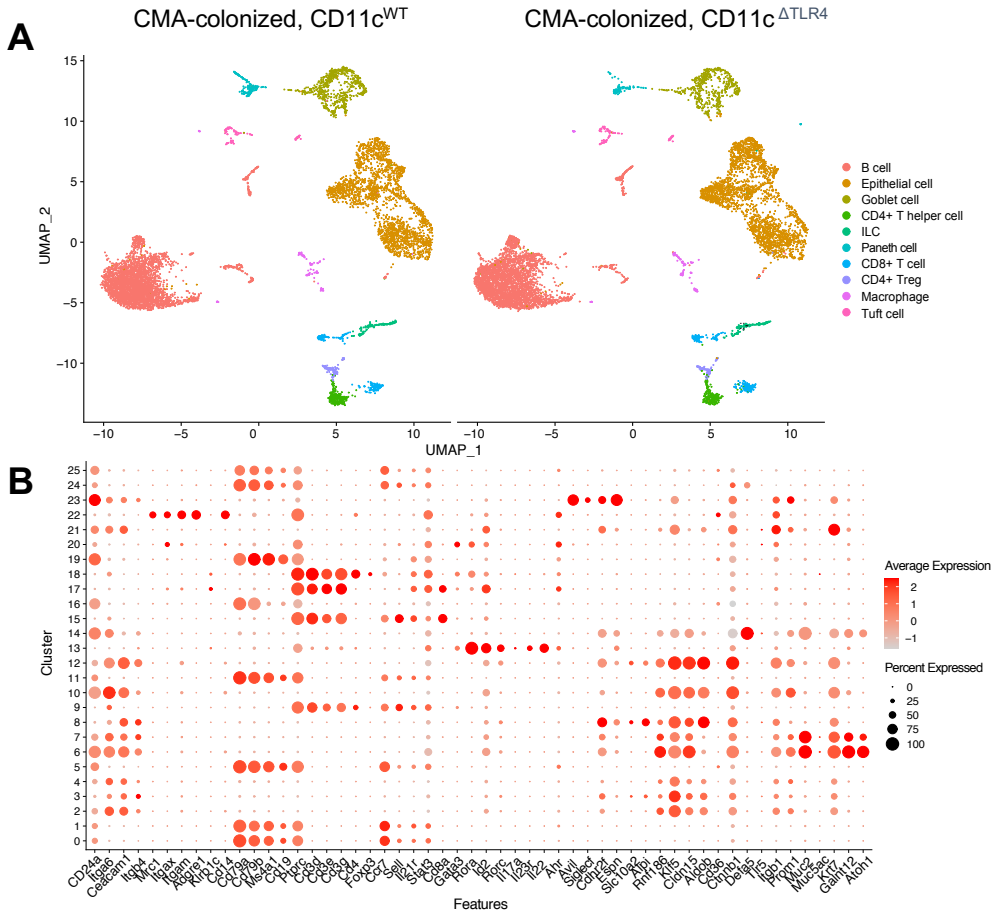


**Figure 17**: Immune cells of the ileum of CMA Donor 5-colonized mice. **A)** UMAP projections of isolated ileal cells from CMA-colonized CD11cWT and CD11c mice. **B)** Expression matrix of canonical markers used to annotate cell clusters.

After identifying each cluster, differential expression analysis was conducted between each genotype for each cluster. In this analysis, we found that several antimicrobial defense genes were upregulated in CD11c$^{WT}$ mice, but down regulated in CD11c$^{\Delta TLR4}$ mice in comparison. Note that we also saw that defensin genes (*Defa17* and *Defa23*) were upregulated in IEC in response to colonization with the CMA microbiota in WT C57BL/6 mice in comparison to GF mice in the bulk RNAseq analysis presented in **Table 4**. Single cell transcriptomic analysis showed that antimicrobial genes were upregulated in ILCs, CD4$^{+}$ Tregs, CD8α$^{+}$ T cells, and CD4$^{+}$ T helper cells in CD11c$^{WT}$ mice colonized with the CMA microbiota (**Figure 18A-D**). These data suggest that TLR4

signaling in CD11c$^+$ cells regulates multiple T cell subsets, as well as ILCs. While TLR4 signaling in CD11c$^+$ cells does not regulate the induction of Tregs, it may regulate their effector function. Furthermore, the CMA microbiota induces an antimicrobial transcriptional profile in CD8α$^+$ T cells, ILCs, and CD4$^+$ helper cells that is dependent on TLR4 signaling in the CD11c$^+$ compartment.

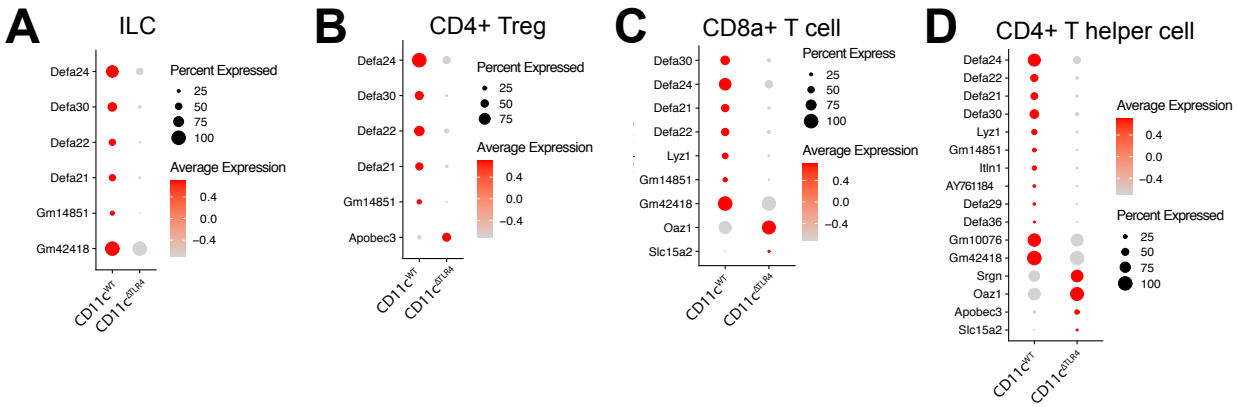


**Figure 18**: Antimicrobial genes in CMA Donor 5-colonized mice are regulated by TLR4 signaling in CD11c$^+$ cells. Percent and average expression of antimicrobial defense genes in **A)** ILCs, **B)** CD4$^+$ Tregs, **C)** CD8α$^+$ T cells and **D)** CD4+ T helper cells.

IV. Donor 5-colonized mice have higher representation of Bacteroidetes in their ileal contents

To reiterate, GF rederivation of mice with TLR4 conditionally knocked out in CD11c$^+$ cells allowed us to determine microbial contributors to *Saa1* expression that our previously utilized antibiotic-treatment model would not have allowed. Thus, to determine microbial contributors to the observed TLR4-dependent phenotypes, we conducted 16S sequencing on ileal samples of CMA and healthy-colonized CD11c$^{WT}$ and CD11c$^{\Delta TLR4}$ mice. Through analysis of these sequences, we determined that multiple taxa were differentially abundant between healthy and CMA-colonized mice. As expected,

colonization of GF mice with the CMA or healthy microbiota were observed to be distinct according to beta-diversity metrics (**Figure 19**). In healthy-colonized mice several Clostridial taxa were significantly more abundant, including *Lachnospiraceae* and Clostridium XIVa, which we have previously reported to be barrier protective Clostridia (Stefka et al., 2014; Feehley et al., 2019) (**Figure 20**). Importantly, all Gram-negative bacteria that were identified as differentially abundant were significantly higher in CMA-colonized mice compared to healthy-colonized mice (**Figure 21**).

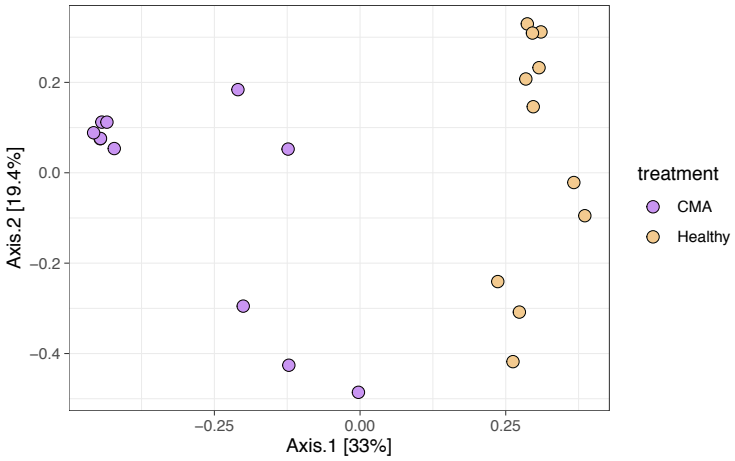


**Figure 19**: GF mice colonized with the healthy and CMA microbiotas have distinct microbial communities. Beta diversity of healthy Donor 2-colonized and CMA Donor 5-colonized mice using the Bray-Curtis metric. Sequencing was performed on ileal samples from mice one week post-weaning.

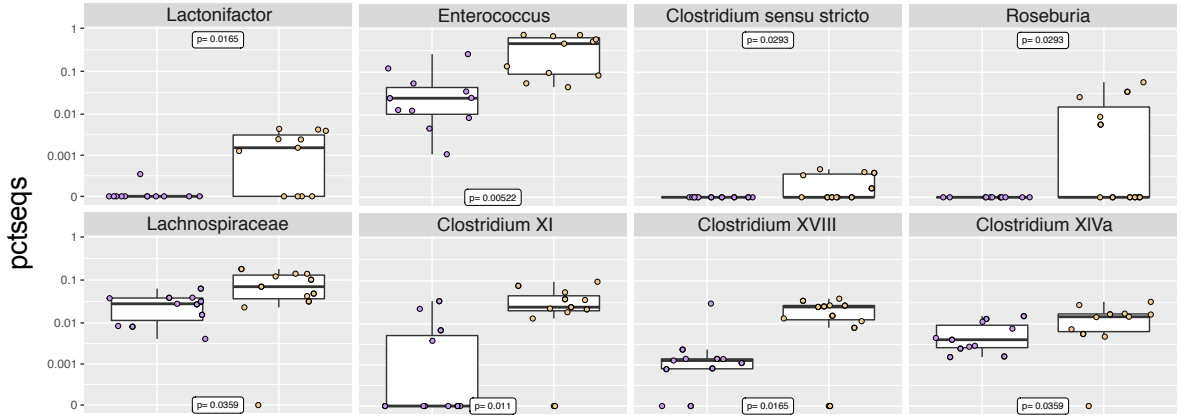


**Figure 20**: Healthy-colonized mice have increased abundance of Clostridia. Relative abundance of taxa significantly enriched in ileal samples from Donor 2-colonized mice compared to Donor 5-colonized mice one week post-weaning. 16S rRNA amplicon reads were processed using the dada2 pipeline and ASVs were assigned using the RDP database. Statistical analysis was performed using the Kruskal-Wallis test with a Benjamini-Hochberg correction.

After obtaining these results, we followed up with shotgun metagenomic sequencing of DNA from the same samples to get a more resolved understanding of which species were differentially abundant between healthy Donor 2-colonized and CMA-Donor 5 colonized mice. Taxonomic analysis showed that the bacterial communities in Donor 2-colonized, and Donor 5-colonized mice were vastly different (**Figure 22**). In agreement with the 16S data, CMA Donor 5-colonized mice had an expansion of Gram-negative bacteria, such as Proteobacteria and Bacteroidetes. Healthy-colonized mice had a higher abundance of *Enterococcus* and *Lachnospiraceae*, which was also in agreement with the 16S data.

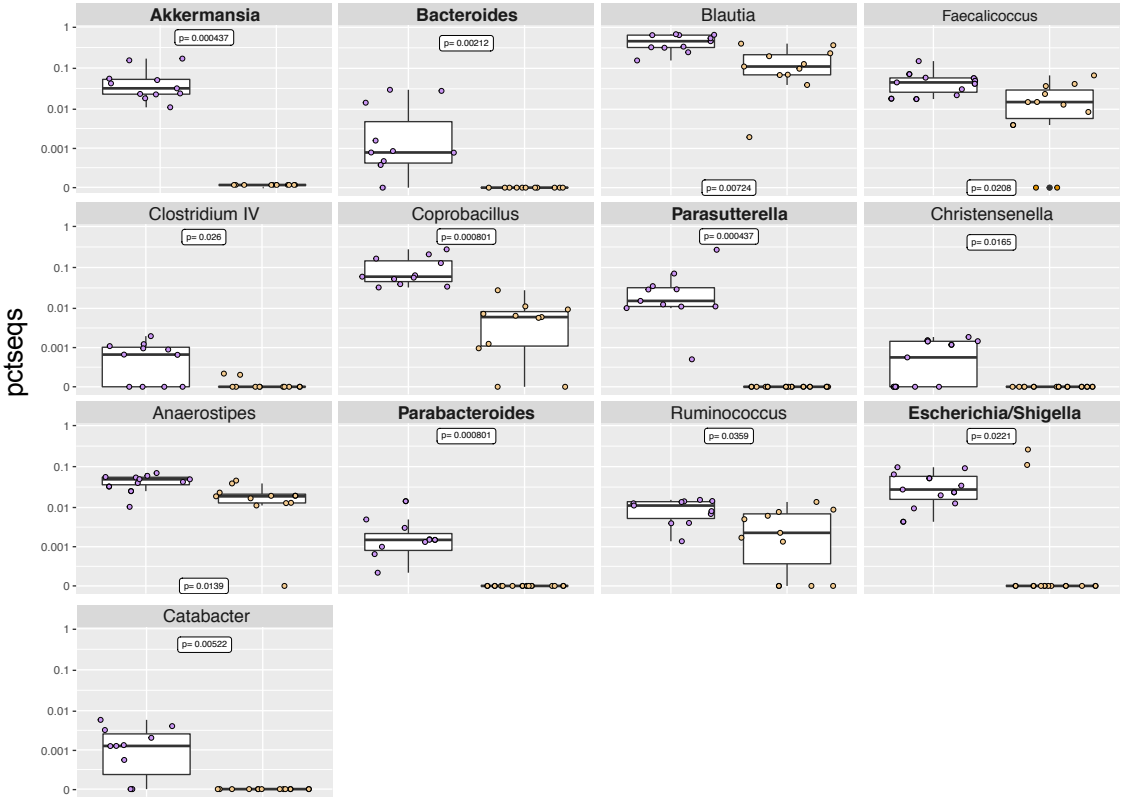


**Figure 21**: Gram-negative bacteria are enriched in CMA-colonized mice. Relative abundance of taxa significantly enriched in ileal contents from CMA Donor 5-colonized mice compared to healthy Donor 2-colonized mice one week post-weaning. 16S rRNA amplicon reads were processed using the dada2 pipeline and ASVs were assigned using the RDP database. Gram-negative taxa are depicted with bold lettering. Statistical analysis was performed using the Kruskal-Wallis test with a Benjamini-Hochberg correction.

Differential abundance analysis of shotgun metagenomic sequences revealed numerous bacterial species to be differentially abundant between healthy Donor 2-colonized and CMA Donor 5-colonized mice. Interestingly, we again saw that all Gram-negative species were significantly more abundant in CMA Donor 5-colonized mice than healthy Donor 2-colonized mice, which agreed with the 16S sequencing data we previously collected (**Figure 23**). Specifically, CMA Donor 5-colonized mice had an increase in Bacteroidetes compared to healthy-colonized mice.

The Bacteroidetes are a phylum of bacteria that produce hypoimmunogenic LPS and have previously been associated with allergy (Vatanen et al., 2016). Knowing this, we analyzed the representation of LPS synthesis and LPS modification genes in these samples. We saw that all genes analyzed were significantly more represented in CMA-colonized mice, with exception to *lpxE*, which was significantly higher in healthy-colonized mice (**Figure 24**). Together, these data show that the Donor 5 microbiota has higher abundance of Gram-negative bacteria, particularly, Bacteroidetes in comparison to the Donor 2 microbiota. Accordingly, the Donor 5 microbiota also has increased representation of LPS genes that are likely derived from Bacteroidetes.


**Figure 22**: CMA-colonized and healthy-colonized mice have distinct microbial communities in the ileum. Taxonomic classification of bacteria in ileal samples collected from CD11c$^{WT}$ and CD11c$^{\Delta TLR4}$ mice colonized with the healthy Donor 2 and CMA Donor 5 microbiotas one week post-weaning. Classification of metagenomic reads was done using kraken2.

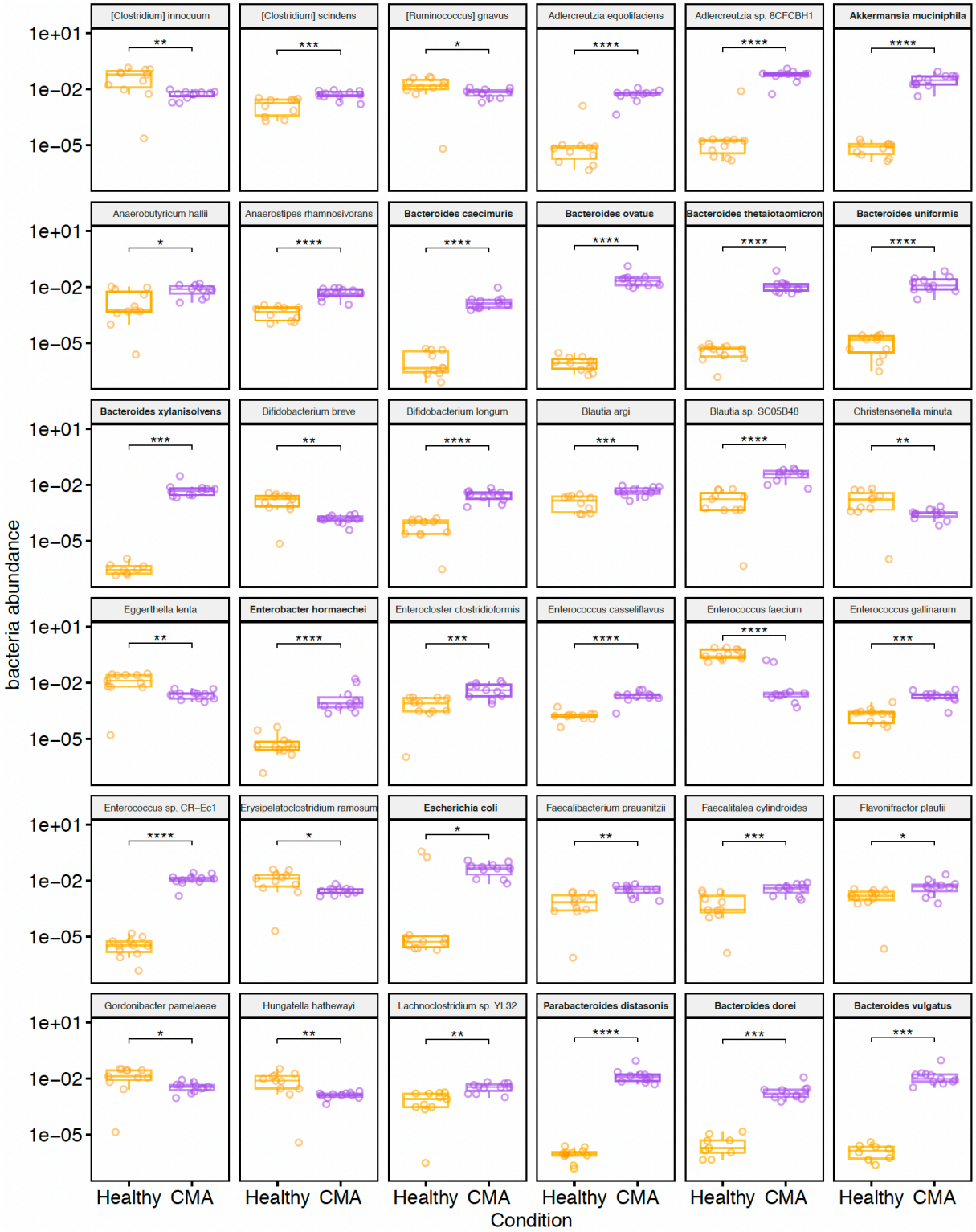


**Figure 23**: CMA-colonized mice have increased abundance of Gram-negative species, particularly, Bacteroidetes. Differentially abundant bacterial species in ileal samples from healthy Donor 2-colonized and CMA Donor 5-colonized mice one week post-weaning. Bacterial species were determined through assembly of metagenomic reads using megahit, followed by annotation using prodigal. Statistical analysis was performed using the Kruskal-Wallis test with a Benjamini-Hochberg correction. *$P$ < 0.05, **$P$ < 0.01, ***$P$ < 0.001, ****$P$ < 0.0001

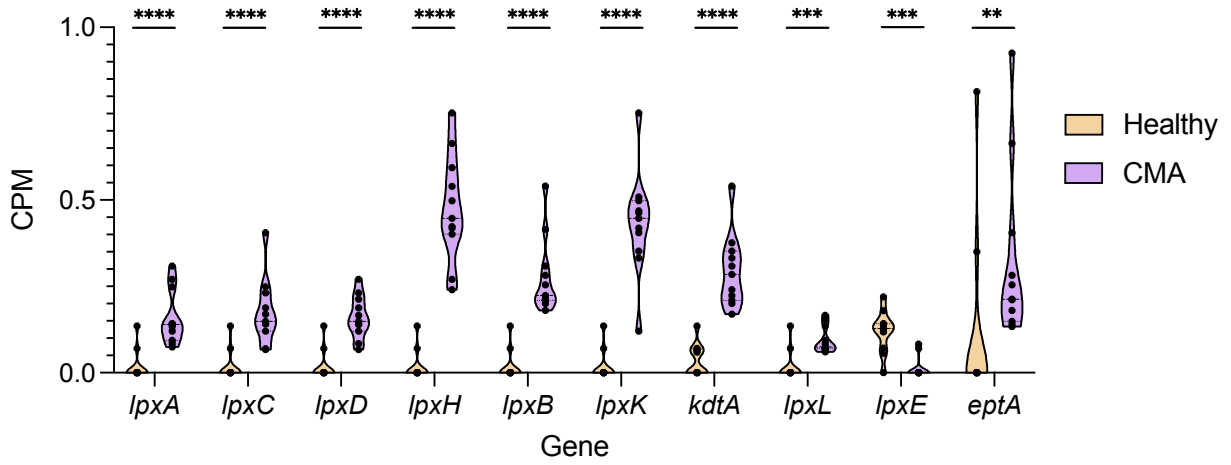


**Figure 24**: CMA-colonized have higher abundance of LPS synthesis genes. Counts per million of genes involved in KEGG pathways related to KDO2-lipid A biosynthesis (M00060 and M00866) and modification (M00867) in ileal samples from mice colonized with the CMA Donor 5 and healthy Donor 2 microbiotas one week post-weaning. Statistics determined using Wilcoxon rank sum test was performed between both colonization conditions. $^{**}P < 0.01$, $^{***}P < 0.001$, $^{****}P < 0.0001$

V. *Saa1* is not induced in ileal IECs by a small consortium of Bacteroidetes or monocolonization with a *Parabacteroides distasonis*

Because Bacteroidetes have been associated with allergy and are enriched in CMA Donor 5-colonized mice, we wanted to determine the role that these bacteria may play in inducing *Saa1* expression in the ileum. To further investigate this, we performed monocolonization experiments using a representative Bacteroidetes to determine the level of *Saa1* induction relative to healthy-colonized mice. We chose *Parabacteroides distasonis* as a representative Bacteroidetes because it was observed to be more abundant in the microbiota of CMA infants compared to healthy infants in an independent study (De Filippis et al., 2021). We colonized wildtype mice with a human-derived *P. distasonis* strain obtained from the DFI biobank (**Figure 25A-B**). Colonization of wildtype mice with *P. distasonis* did not induce appreciable *Saa1* in ileal IECs. Gavaging mice

twice with a *P. distasonis* stock slightly increased *Saa1* expression, but not significantly (**Figure 25A**).

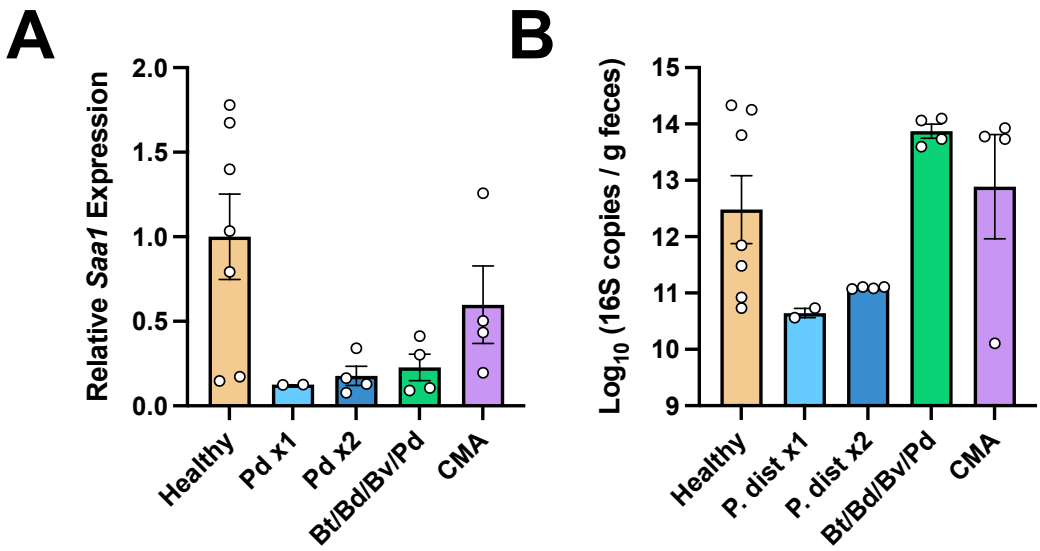


**Figure 25**: Monocolonization with *P. distasonis* or a small consortium of Bacteroidetes does not induce *Saa1* expression in ileal IECs. **A)** Relative expression of *Saa1* in healthy Donor 2-colonized mice, CMA Donor 5-colonized mice, mice that received one dose (x1) of *P. distasonis*, mice that received two doses (x2) of *P. distasonis*, and mice colonized with a consortium consisting of *Bacteroides thetaiotaomicron* (Bt), *Bacteroides dorei* (Bd) , *Bacteroides vulgatus* (Bv), and *Parabacteroides distasonis* (Pd). For mono-colonization with *P. distasonis*, mice received one oral gavage of 3.9 x$10^8$ CFU *P. distasonis* at weaning (x1) or received an oral gavage of *P. distasonis* at weaning, followed by a second gavage 3 days later (x2). **B)** Bacterial load of these mice. Experiments were performed on week post-weaning

Seeing these results, we next made a small consortium of Bacteroidetes to see if multiple species could induce *Saa1* expression in the ileum epithelium. This consortium consisted of *Bacteroides thetaiotaomicron* (Bt), *Bacterodes vulgatus* (Bv), *Bacteroides dorei* (Bd), and *Parabacterodes distasonis* (Pd). All of these Bacteroidetes are known to be common members of the human gut, and some have been documented to be associated with intestinal inflammation or disease. *B. thetaiotaomicron* is a common commensal of the mammalian intestine (Donaldson et al., 2016) and *B. vulgatus* has been associated with intestinal inflammation in IBD (Mills et al., 2022). *B. dorei* was previously found to be correlated with *Saa1* expression and Th17 induction (Atarashi et al., 2015).

Using this consortium, we colonized wildtype mice to examine *Saa1* induction one-week post-colonization. We observed that colonization with this small consortium of Bacteroidetes also did not induce expression of *Saa1* compared to CMA-colonized and healthy-colonized mice (**Figure 25A**). The bacterial load of mice colonized with the consortium was also similar to that of mice colonized with the human infant gut microbiotas (**Figure 25B**). Together, these data suggest that colonization with just one or four bacteria representative of the CMA microbiota is not sufficient to induce *Saa1* expression. Donor 5-specific strains or a more complex microbial community may be needed to induce appreciable expression of *Saa1* in ileal IECs.

### VI. TLR4 regulates type 2 and type 3 T cells and ILCs during early development of an allergic response in CMA-colonized mice

Cumulatively, the Donor 5 microbiota induces immunological responses in the ileum that are proinflammatory in nature. In response to the Donor 5 microbiota, compensatory defense mechanisms are enacted through the induction of IgA and antimicrobial peptides, and these responses are regulated by TLR4 in $CD11c^+$ cells. As these responses are induced by a microbiota originating from an infant with a severe allergy to cow's milk, one question that remains is the role of this microbiota in inducing allergic inflammation through TLR4-dependent mechanisms. To investigate this, we sensitized TLR4-sufficient and TLR4-deficient mice colonized with the Donor 5 microbiota, the Donor 2 microbiota, or GF controls. Using a model where mice are sensitized twice with BLG plus CT, we looked at ileal ILC and T helper cell populations in

the early development of an allergic response. Specifically, using the gating strategy presented in **Figure 26**, we examined ILC2 and Th2 cells to examine mediators of type 2 inflammatory responses, as well as ILC3s and Th17 cells to examine mediators of type 3 inflammation. Following this sensitization protocol, we observed that in TLR4-sufficient mice, there was no significant difference in the percentage or number of ILCs in GF, healthy Donor 2-colonized, and CMA Donor 5-colonized mice. (**Figure 27A**). In TLR4-deficient mice, the frequency of ILCs was significantly increased in healthy-colonized mice compared to GF and CMA-colonized mice. The total number of ILCs was observed to be significantly higher in TLR4-deficient healthy-colonized mice compared to GF and CMA-colonized mice of the same genotype as well as healthy-colonized WT mice (**Figure 27B**).

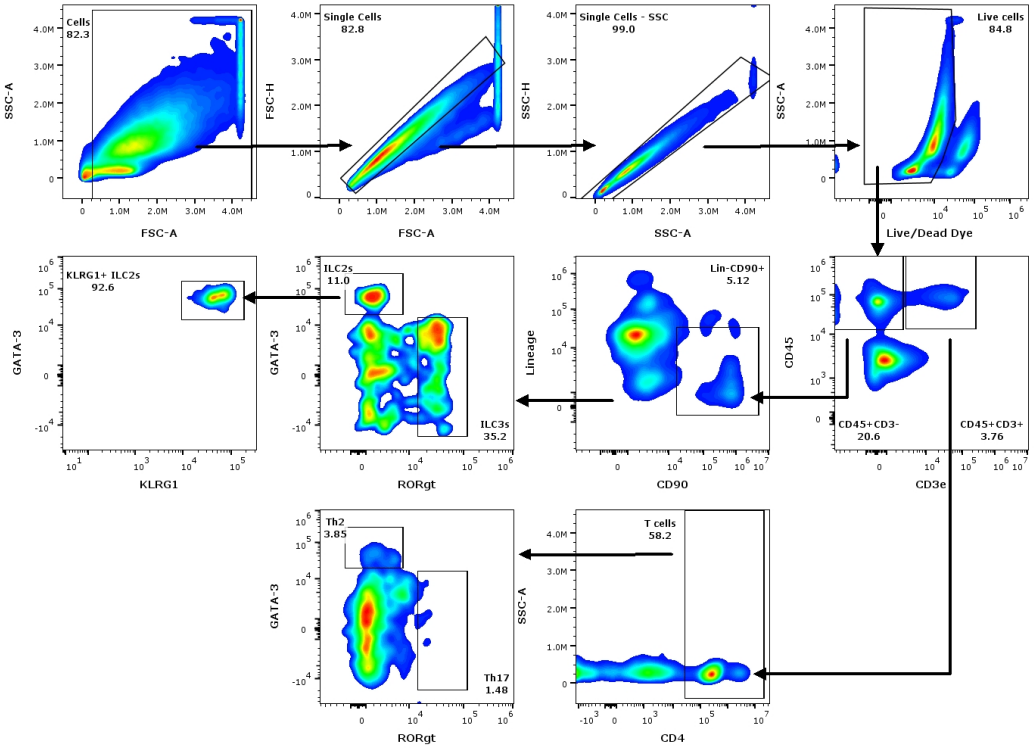


**Figure 26**: Gating strategy for the identification of ILC2s/Th2 and ILC3/Th17 populations in mice sensitized with BLG. Representative flow plots depicting the gating strategy used to identify ILC and T cell subsets in the ileum lamina propria of GF, CMA-colonized, and healthy-colonized mice

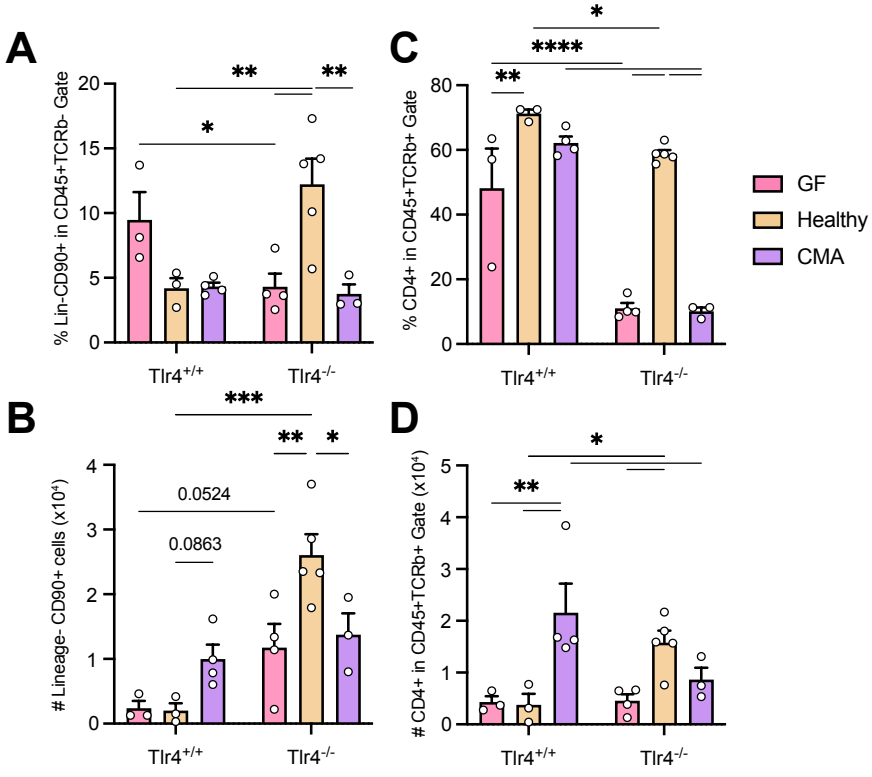


**Figure 27**: TLR4 signaling regulates total T cell populations but not total ILC populations in sensitized CMA-colonized mice. Frequency and absolute numbers of **A-B)** total ILCs and **C-D)** total T cells in the ileal tissue of GF, healthy Donor 2-colonized, and CMA Donor 5-colonized *Tlr4*$^{+/+}$ and *Tlr4*$^{-/-}$ mice one week post-weaning. Summary of at least 2 independent experiments per condition. Summary of at least 2 independent experiments per condition. Statistics were calculated using 2-way ANOVA with multiple testing using the Benjamini, Krieger, and Yekutili method. *$P$ < 0.05, **$P$ < 0.01, ****$P$ < 0.0001

Examining total T cells, we observed that all colonization statuses had a reduction in the frequency of T cells when TLR4 signaling was deficient compared to when it was sufficient (**Figure 27C**). In TLR4-deficient mice, healthy-colonized mice had a higher frequency of T cells compared to both GF and CMA-colonized mice. For absolute numbers of T cells, CMA-colonized mice had more T cells compared to healthy-colonized mice and GF mice when TLR4 signaling was sufficient (**Figure 27D**). This number was significantly reduced in CMA-colonized TLR4-deficient mice.

In TLR4 sufficient mice, we saw that after two sensitizations, GF and CMA Donor 5-colonized mice had a greater frequency of ILC2s compared to healthy colonized mice (**Figure 28A**). This was also observed in TLR4-deficient mice. This agrees with previous

findings that both GF and CMA-colonized mice are more susceptible to allergic sensitization than healthy-colonized mice (Feehley et al., 2019). Interestingly, the frequency of ILC2s in both GF and CMA-colonized mice was significantly increased in TLR4-deficient mice compared to TLR4-sufficient mice while the frequency in healthy Donor 2-colonized mice did not increase. The absolute number of ILC2s increased in all colonization statuses when TLR4 was deficient compared to their WT counterparts (**Figure 28B**). For Th2 cells, there was an increased frequency in all colonization statuses in TLR4-deficient mice compared to their WT counterparts (**Figure 28C**). The absolute number of Th2 cells was observed to be increased TLR4-deficient healthy-colonized mice compared to their WT complements (**Figure 28D**).

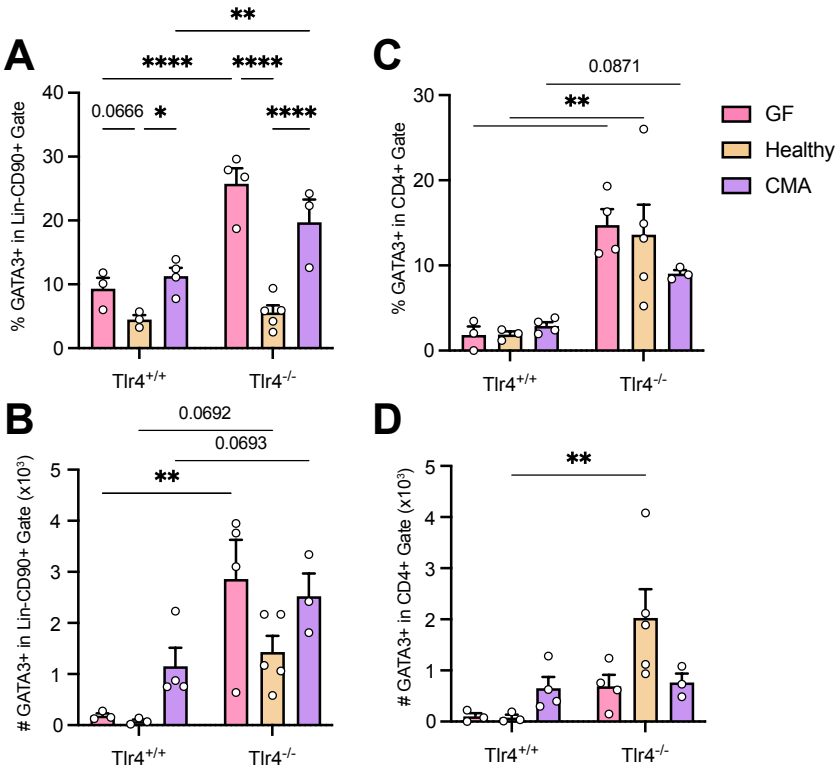


**Figure 28**: Early type 2 innate immune responses are regulated by TLR4 in sensitized CMA-colonized mice. Frequency and absolute numbers of **A-B)** ILC2s and **C-D)** Th2 cells in the ileal tissue of GF, healthy Donor 2-colonized, and CMA Donor 5-colonized *Tlr4*$^{+/+}$ and *Tlr4*$^{-/-}$ mice one week post-weaning. Summary of at least 2 independent experiments per condition. Summary of at least 2 independent experiments per condition. Statistics were calculated using 2-way ANOVA with multiple testing using the Benjamini, Krieger, and Yekutili method. *$P$ < 0.05, **$P$ < 0.01, ****$P$ < 0.0001

When examining ILC3s, we observed a significant increase in frequency of ILC3s in CMA-colonized mice compared to healthy-colonized and GF mice when TLR4 signaling

was sufficient (**Figure 29A**). Furthermore, this frequency was significantly decreased when TLR4 was deficient. Similar to what was seen in the ILC2s, the frequency of ILC3s was significantly higher in GF and CMA-colonized mice compared to healthy-colonized mice when TLR4 was deficient. The absolute numbers of ILC3s were not different between genotypes and colonization status, although CMA-colonized mice did have an increase in numbers (**Figure 29B**). The frequency of Th17 cells was significantly increased in TLR4-deficient GF mice compared their WT counterparts (**Figure 29C**). There was also an increase in Th17 cells in TLR4-deficient CMA-colonized mice compared to their WT counterparts. The absolute number of Th17 cells was not different between genotypes and colonization status (**Figure 29D**). Together, these data show that TLR4 signaling regulates the frequencies of ILC3s and Th17 cells in GF and CMA-colonized mice. In healthy-colonized mice, TLR4 signaling regulates ILC3 frequencies, but not Th17 frequencies.

In summary, early innate effectors (ILC2s and ILC3s) are induced in allergy-susceptible CMA-colonized mice and GF mice. Following sensitization, ILC2s are induced similarly in GF and CMA-colonized mice, while ILC3s are more highly induced in CMA-colonized mice. In the absence of TLR4 signaling, ILC2s are increased in both GF and CMA-colonized mice, while ILC3s are greatly reduced only in CMA-colonized mice, suggesting that innate type 3 inflammation is regulated by TLR4 in these mice. When TLR4 signaling is sufficient, healthy-colonized mice have reduced ILC2s and ILC3s compared to CMA-colonized mice. In agreement with previous findings (Bashir et al., 2004), when TLR4 signaling is deficient, all colonization statuses experience an increase in frequency of Th2 cells. Moreover, in allergy-susceptible GF and CMA-colonized mice,

there is an increased frequency of Th17 cells that is not observed in healthy-colonized mice. These data show that TLR4 regulates a complex network of type 2 and type 3 inflammatory cells of the innate and adaptive arms.

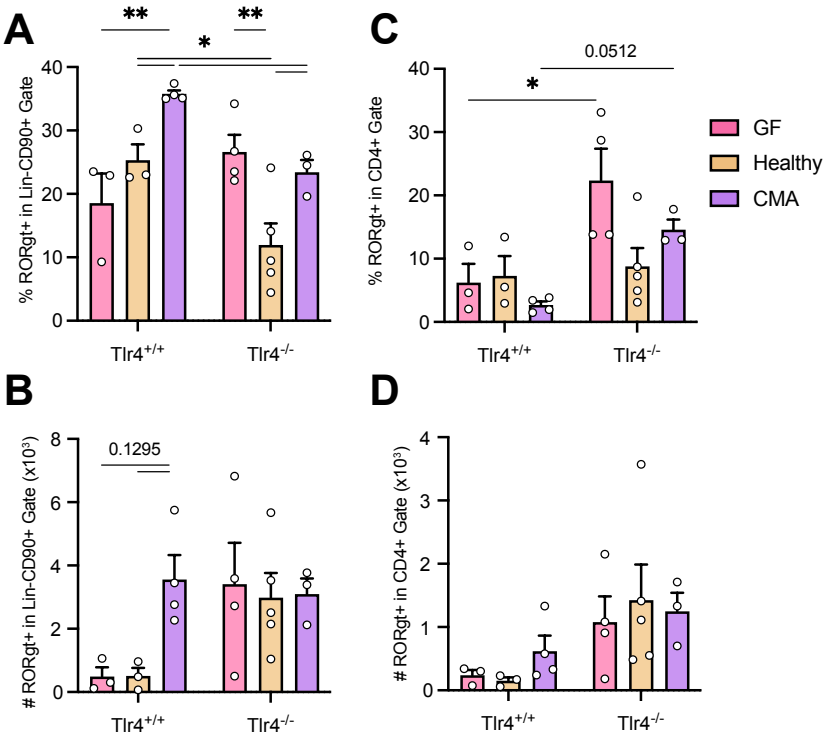


**Figure 29**: TLR4 signaling regulates innate and adaptive type 3 responses in sensitized CMA-colonized mice. Frequency and absolute numbers of **A-B)** ILC3s and **C-D)** Th17 cells in the ileal tissue of GF, healthy Donor 2-colonized, and CMA Donor 5-colonized *Tlr4*$^{+/+}$ and *Tlr4*$^{-/-}$ mice one week post-weaning. Summary of at least 2 independent experiments per condition. Summary of at least 2 independent experiments per condition. Statistics were calculated using 2-way ANOVA with multiple testing using the Benjamini, Krieger, and Yekutili method. *$P$ < 0.05, **$P$ < 0.01, ****$P$ < 0.0001

In this chapter, we show that in the ileum of Donor 5-colonized mice, TLR4 signaling in CD11c$^{+}$ cells specifically regulates Th17 cells and B cell responses, but not Tregs. Additionally, expression of antimicrobial defense genes in multiple immune cell subsets is regulated by TLR4 signaling in CD11c$^{+}$ cells. The Donor 5 microbiota is especially enriched in Bacteroidetes, a phylum previously associated with allergy. Finally, the CMA microbiota distinctly induces a mixed type 2/type 3 innate immune response upon sensitization with food antigen.

Analogous to experiments performed in global TLR4 knockout mice, rederivation of CD11c$^{cre}$TLR4$^{fl/fl}$ mice as GF confers advantages that the limitations of our previous

antibiotic-treated model could not address. Through these mice, we were able to determine the requirement of TLR4 signaling in $CD11c^+$ cells in the induction of IgA, Th17 cells, and antimicrobial genes in various of immune cell subsets by the CMA microbiota. Using microbial and dietary products, $CD11c^+$ cells act as a switch board for regulating intestinal immunity (Bang et al., 2021; Bachus et al., 2019). In the gut, dietary vitamin A is converted to retinoic acid and can form complexes with SAA-1 (Derebe et al., 2014). This complex can be endocytosed through interaction with low-density lipoprotein (LDL) receptor–related protein 1 (LRP1) on $CD11c^+$ cells, which then induces IL-17A by Th17 cells and IgA by B cells, but not $Foxp3^+$ Tregs, in the small intestine (Bang et al., 2021, Ivanov et al., 2009). As SAA-1 has been shown to opsonize bacteria through interaction with LPS (Cheng et al., 2018), endocytosis of SAA-1 via TLR4 on $CD11c^+$ cells could regulate similar immunological pathways, as observed in our results. These parallel findings bring into question the phenotypic influences SAA-1 has on $CD11c^+$ cells and the implications of that in mediating inflammatory responses. DCs stimulated with SAA promote IL-17A in T cells in vitro (Ather et al., 2011). However, the cytokine and transcriptional profile of $CD11c^+$ cells after stimulation with SAA-1, and how this mechanistically mediates T cell, B cell, and other immune cell responses in vivo, remains to be investigated. Interestingly, SAA can promote chemotactic activity in monocytes and immature DCs in vitro, which can have implications for the subsequent initiation of immune responses in vivo (Gouwy et al., 2015). Altogether, this data shows an important role for $CD11c^+$ cells in regulating some of the inflammatory responses induced by the CMA microbiota, which agrees with previously published mechanisms.

Rederivation of CD11c$^{cre}$TLR4$^{fl/fl}$ mice also allowed us to identify enriched bacteria in CMA-colonized mice without contamination from the SPF commensal microbiota. Through use of this gnotobiotic model, we were able to determine that Gram-negative bacteria, particularly Bacteroidetes, are specifically enriched in the CMA microbiota. Increased abundance of Bacteroidetes has been associated with increased prevalence of allergy in infant populations (Vatanen et al., 2016). Moreover, increased SAA-1 expression and Th17 cells have been correlated with increased abundance of Bacteroides in ileal biopsies from IBD patients (Tang et al., 2017). As *Saa1* has been shown to contribute to allergic inflammation (Smole et al., 2020), it is reasonable to suspect that induction of *Saa1* by a Bacteroidetes-enriched microbiota contributes to food allergies. Unexpectedly, colonization of mice with 1-4 Bacteroidetes species did not induce appreciable *Saa1* in ileal IECs. One possibility for why colonization with a small Bacteroidetes consortium may not induce *Saa1* is because the induction of *Saa1* requires a more complex microbiota. Microbial gut diversity can influence B cell and DC responses and alter the severity of intestinal inflammation (Cahenzli et al., 2013; Chen et al., 2017). Furthermore, interaction and communication between members of the microbiota can modulate the induction of atopic inflammation (Nakamura et al., 2020; Williams et al., 2019). Particular members of the CMA microbiota may play a specialized role in the overall community that favor the induction of *Saa1*, and quite possibly, the selected species used for the presented colonization studies may require other Bacteroidetes or non-Bacteroidetes to facilitate *Saa1* upregulation in the ileum epithelium. Another possibility for why *Saa1* was not induced may be that *Saa1* upregulation requires specific members of the CMA microbiota. Human-derived gut bacteria are uniquely adapted to

their host and can elicit diverse immunological responses that are species- and even strain-specific (Geva-Zatorsky et al., 2017; Yang et al., 2020; Britton et al., 2019). Although the Bacteroidetes isolates used in the presented data are human-derived, they may not possess the genetic elements present in the CMA microbiome that are necessary for the induction of *Saa1*. Future studies using isolates derived from the CMA microbiota, rather than a biobank, could illuminate the strain-specific contributions of the CMA microbiota in intestinal inflammation and *Saa1* induction. Overall, this data highlights the specific cellular contributions to inflammatory responses mediated by the CMA microbiota and a phylum of bacteria that are most likely the contributors of said responses. This contributes to the observed mixed type 2/type 3 inflammation in CMA-colonized mice, which will be further discussed in the next chapter.

## Chapter 5. Discussion and Future Directions

### I. The CMA microbiota induces type 2/type 3 inflammation, which includes the upregulation of *Saa1*, induction of Tregs and Th17 cells, and production of fecal IgA

In the data presented herein, we employ multiple colonization models to show that the CMA Donor 5 microbiota induces a mixed inflammatory response in the ileum. This not only includes the induction of *Saa1* and *Reg3b*, but other inflammatory and mucosal genes, including *Il33*, *Il13ra, Il15*, *Il18*. Furthermore, as a part of this inflammatory response, increased Tregs and Th17 cells are induced, along with fecal IgA, in comparison to healthy-colonized mice. Prior to epithelial cell activation elicited by sensitization with a dietary antigen, the CMA microbiota orients the ileal mucosa toward a type 2/type 3 inflammatory response. Adding insult to injury, it is unsurprising that upon cow's milk consumption, Donor 5 experienced severe symptoms with an intestinal mucosa that is already oriented toward inflammation. The atopic symptoms that Donor 5 suffered from within minutes after feeding (i.e., vomiting, urticaria), as well as the gastrointestinal inflammation (nodular hyperplasia, eosinophilic infiltration, intestinal bleeding) are likely the outcome of a vigorous allergen-specific response that has developed within the first months of the infant's life. In our study, we examine an early snapshot of the inflammatory responses that this microbiota induces.

In addition to the inflammatory transcriptional profile induced in the ileal mucosa, significantly elevated proportions, and numbers of Foxp3$^+$ Tregs, ROR$\gamma$t$^+$Foxp3$^+$ Tregs, and IL-17A$^+$ROR$\gamma$t$^+$ Th17 cells were specific to mice colonized with the CMA Donor 5

microbiota. *Saa1* is induced in the ileal epithelium by epithelial adherent bacteria and is downstream of the IL-23 signaling axis initiated by intestinal DCs in response to microbial stimulation (Sano et al., 2015). Induction of *Saa1* by the epithelium increases the production of IL-17A in Th17 cells and leads to the exacerbation of intestinal inflammation caused by this T cell subset (Atarashi et al., 2015; Lee et al., 2020). Concordantly, in our studies, the induction of effector Th17 cells was coregulated with the induction of *Saa1* by the CMA microbiota. Interestingly, Tregs were also highly induced in Donor 5-colonized mice. In the intestine, $Foxp3^+$ and $ROR\gamma t^+Foxp3^+$ Tregs maintain homeostasis by limiting inflammatory collateral damage while enacting effector functions to promote tolerance. Maintenance of these two Treg subsets is intricately regulated by the local microenvironment. IL-33, IL-15, and IL-18 directly regulate RORγt and Foxp3 expression in Tregs, favoring increased Foxp3 expression and enhancing Treg suppressor activity while dampening local inflammation (Alvarez et al., 2019; Tosiek et al., 2016; Harrison et al., 2015). In addition, the induction of $ROR\gamma t^+$ $Foxp3^+$ Tregs by the commensal microbiota makes this subset readily available for the suppression of type 2 and type 3 inflammation in the intestine (Ohnmacht et al., 2015; Sefik et al., 2015). With the production of SAA-1 favoring induction of Th17 cells, coupled with type 2 and type 3 inflammatory signals from the epithelium, the increased induction of Tregs is likely a compensatory mechanism to address inflammation within the local microenvironment.

Along with the induction of Tregs and Th17 cells, intestinal IgA was robustly produced in CMA Donor 5-colonized mice. IgA is the most abundant immunoglobulin isotype at mucosal surfaces and is regulated by the commensal microbiota (Mestecky et al., 1986; Hapfelmeier et al., 2010). Intestinal IgA plays an important role of establishing

symbiosis between the host and the microbiota, as well as limiting gut inflammation (Nakajima et al., 2018; Xiong et al., 2019). One mechanism by which IgA mediates symbiotic relationships is by binding intestinal microbes and limiting their interaction with the epithelium through agglutination and restriction of motility (Moor et al., 2017; Cullender et al., 2013). Upon binding of commensals and pathobionts, IgA regulates intestinal immunity by mediating controlled antigen sampling and uptake into the Peyer's patches by M cells (Forbes et al., 2008; Mathias et al., 2014; Rol et al., 2012). Because the production of IgA is significantly elevated in mice colonized with the Donor 5 microbiota in comparison to healthy colonized mice, and the CMA microbiota promotes intestinal inflammation, it is reasonable to suspect that IgA may be coating more bacteria in the CMA microbiota in an attempt to reestablish intestinal homeostasis. How this would affect the development of allergic responses to dietary antigens would be an interesting avenue of investigation. The current understanding of the contribution of IgA to food allergies is limited. It is assumed that IgA would suppress atopic responses to food, as IgA deficiency is associated with intestinal dysbiosis and atopy (Fadlallah et al., 2018; Janzi et al., 2009). Furthermore, antigenic exposure through dietary feeding promotes oral tolerance and induces cross-reactive IgA, while simultaneous exposure of dietary antigen and a mucosal adjuvant induces IgA that is highly antigen-specific (Pabst and Mowat, 2012; Zhang et al., 2020). As microbe-specific IgA is produced to quell intestinal inflammation induced by pathobionts (Xiong et al., 2019), dietary antigen-specific IgA could be produced in a similar fashion. In our system, the CMA microbiota has proinflammatory properties that may act as an adjuvant and increase allergic

susceptibility. The production of IgA could therefore be a mechanism to address inflammation induced by the microbiota, and potentially, dietary antigens.

## II. Inflammation induced by the CMA microbiota is regulated by TLR4 signaling in various cellular compartments

The intestinal inflammatory responses that are induced by the Donor 5 microbiota is dependent on TLR4 signaling in multiple cellular compartments. In CMA-colonized mice, we observed that the upregulation of *Saa1*, the induction of Th17 cells, and the production of intestinal IgA is specifically regulated by TLR4 signaling in $CD11c^+$ cells, while the induction of Tregs is regulated by TLR4 signaling in another cellular compartment (**Figures 14-16**). Furthermore, TLR4 signaling in epithelial cells also regulates *Saa1* expression (**Figure 7**). It is well documented in the literature that TLR4 signaling in different cell types specifically and differentially regulate allergic inflammation (McAlees et al., 2015; Hammad et al., 2009; Thomas et al., 2018), further validating the distinct way multiple cellular compartments contribute to gut immunity in the presented results.

As the first point of contact for luminal antigens, the epithelium acts as “border patrol” to microbial and dietary products to foster intestinal tolerance and homeostasis. To maintain this homeostasis, luminal antigens are delivered to the lamina propria in a regulated fashion, and a spatial boundary between these antigens and the epithelium is created via the production of antimicrobial peptides and mucus (Vaishnava et al., 2011; Frantz et al., 2012; Rol et al., 2012). Importantly, epithelial detection of microbes through

TLR signaling regulates these crucial barrier functions. Reduction of TLR signaling in epithelial cells results in increased permeability, bacterial translocation, and inflammation (Vaishnava et al., 2008; Corr et al., 2014; Frantz et al., 2012). With the exception of insult or infection, the epithelium largely induces tolerogenic responses to luminal products. In the case of Donor 5-colonized mice, the intestinal microbiota induces the alarmin *Il33* and the acute phase protein *Saa1*, which informs cells in the lamina propria of local epithelial stress or damage (**Figure 8 and 10, Table 5**). $CD11c^+$ cells in the lamina propria induce type 2 and type 3 inflammation in response to epithelial-derived IL-33 and SAA1, respectively, through FcRγ and IL-23 signaling (Tjota et al., 2014; Sano et al., 2015). Though the expression of *Saa1* and *Reg3b* are both similarly regulated by TLR4 signaling in epithelial cells and $CD11c^+$ cells, the immunological implications of this may not be equal. In response to allergen sensitization and challenge, TLR4 signaling in the epithelial compartment regulates eosinophilic inflammation, while in $CD11c^+$ cells it regulates neutrophilic inflammation (McAlees et al., 2015, Hammad et al., 2009, Thomas et al., 2018). While TLR4 signaling in these compartments regulates distinct cellular responses during allergic sensitization, the canonical cytokines of allergic inflammation (IL-4, IL-5, and IL-13) were not differentially regulated in these studies. In other words, TLR4 signaling in epithelial cells or $CD11c^+$ cells do not solely regulate allergic inflammation, but rather the “accessories” of the inflammation. Although the dichotomy of these responses requires further study, these findings highlight an interesting avenue for future investigation of the cellular immunity that each compartment regulates in response to the Donor 5 microbiota. Moreover, the cellular compartment regulating Tregs remains unknown. Direct sensing of microbes by T cells could potentially regulate Treg induction,

as intrinsic TLR signaling in T cells promotes Treg expansion and suppressive function (Caramalho et al., 2003; Crellin et al., 2005). Nonetheless, these findings underscore the multicellular immunoregulatory atlas of TLR4 in response to an inflammatory microbiota.

### III. The CMA microbiota is enriched with Bacteroidetes, a phylum associated with atopy

Microbial analysis of ileal samples from mice colonized with the CMA Donor 5 microbiota and the healthy Donor 2 microbiota shows that the CMA microbiota has increased abundance of Gram-negative taxa, while the healthy microbiota has enrichment of allergy protective Clostridia (**Figures 20-22**). Particularly, the CMA microbiota has increased representation of Bacteroidetes. The Bacteroidetes are a major phylum of the mammalian intestinal ecosystem (Donaldson et al., 2018). Their diverse metabolic capabilities make them ideal competitors for intestinal nutrients and highly adaptable to the selective pressures imposed by the host diet and immune system (Salyers et al., 1997; Shepherd et al., 2018; Donaldson et al., 2018). While in many contexts they develop a symbiotic relationship with the host by promoting intestinal health, in other contexts they can contribute to intestinal inflammation. Some Bacteroidetes have been implicated in causing intestinal inflammation and pathology in IBD (Mills et al., 2022; Bloom et al., 2011). Interestingly, ileal biopsies from IBD patients have increased expression of *Saa1* which significantly correlates to increased abundance of *Bacteroides* (Tang et al., 2017). SAA-1 has been shown to bind LPS on cell membranes of Gram-negative bacteria, mediating their uptake by phagocytes (Cheng et al., 2018, Shah et al.,

2006). It is therefore plausible that in addition to mounting Th17 immunity in response to epithelial adhesion by bacteria, *Saa1* upregulation could be an innate mechanism to resolve an overwhelming load of Gram-negative bacteria, particularly Bacteroidetes, at the ileal mucosa. This makes sense, as SAA-1 is an acute phase protein highly up regulated in response to insult and injury (Sun and Ye, 2016). In alignment with this, SAA-1 can also induce alarmins like prostaglandin E2 and IL-33 (Lee et al., 2006; Smole et al., 2020), leading to subsequent inflammatory responses to address local injury. While the current data shows that a small consortium of Bacteroidetes does not induce *Saa1*, more intricate ecological and immunological interactions could be driving *Saa1* upregulation, which may only be present in a more complex microbial community. Thus, the inflammatory signature induced by the CMA microbiota could be due to the high abundance of diverse Bacteroidetes species in close proximity to the epithelium.

A previous study by Vatanen et al. reported that infants from Estonia and Finland with higher incidence of allergy and autoimmunity had increased abundance of Bacteroidetes in their feces compared to genetically similar infants in Russian Karelia, which had decreased incidence of these diseases (Vatanen et al., 2016). The authors of this study found that LPS from Bacteroidetes was hypoimmunogenic compared to LPS from *Escherichia coli*, which may contribute to allergies and autoimmunity through lack of development of endotoxin tolerance (Martin et al., 2001). Endotoxin tolerance is acquired in response to strong, frequent engagement of TLR4 by LPS (Wesselkamper et al., 2001). Early life exposure to high levels of LPS reduces subsequent susceptibility to allergy, while low exposure increases susceptibility (Eisenbarth et al., 2002; von Mutius et al., 2000). Signals from the microbiota prior to weaning induce transient intestinal

inflammation termed the “weaning reaction” (Al Nabhani et al., 2019). These early inflammatory responses, which consist of the induction of *Tnfa* and *Ifng*, are important for proper education and development of the immune system to prevent aberrant inflammation later in life. Because LPS from Bacteroidetes is hypoimmunogenic, weak TLR4 antagonism by the pool of LPS that is available from the CMA microbiota may be inadequate at inducing the weaning reaction, leading to pathological imprinting and increased susceptibility to allergic inflammation later in life. Thus, allergic susceptibility conferred by the CMA microbiota could be through the “flavor” of inflammatory responses induced in the ileum. While Proteobacteria are far more abundant in the ileal contents of CMA mice compared to Bacteroidetes, the Bacteroidetes have more diverse saccharolytic and mucolytic capabilities than Proteobacteria that would likely allow them to be in closer proximity to the epithelium and more readily weakly stimulate TLR4 signaling on the epithelium and $CD11c^{+}$ cells (Zafar and Saier, 2021). Moreover, Bacteroidetes species have been found to make up the majority of Gram-negative bacteria within the intestinal mucus layer, while Proteobacteria consist of a small percentage (Li et al., 2015b). Future experiments examining the microbiota and structure of LPS from ileal contents and mucosal scrapings can begin to shed light on the source of LPS needed for upregulation of *Saa1* in the epithelium. The induction of type 2/type 3 inflammation by the CMA microbiota favors atopy, but future studies may also examine the induction of “protective” proinflammatory signals.

IV. Upon sensitization with an allergen, the CMA microbiota induces an innate, mixed type 2/type 3 inflammatory response that does not occur in GF or healthy-colonized mice

Upon sensitization with BLG plus CT, ILC and T cell populations were differentially regulated in GF, healthy-colonized, and CMA-colonized mice (**Figures 27-29**). TLR4-sufficient healthy-colonized mice exhibit reduced ILC2s compared to GF and CMA-colonized mice, as well as an increased frequency of total T cells (**Figure 27**). This is in alignment with the protective effects of the healthy microbiota (Feehley et al., 2019). On the other hand, CMA-colonized and GF WT mice, which are more susceptible to anaphylaxis than healthy mice, exhibited similar frequencies of ILC2s. CMA-colonized mice had a higher number of ILC2s compared to GF mice which agrees with the observation that CMA-colonized mice have increased total ILCs. During these early responses, Th2 immunity has not fully developed in WT mice, as dictated by the low frequency and abundance of Th2 cells in all colonization conditions. With only two sensitizations, this is not unexpected, as we typically assay antigen-specific allergic responses after at least five sensitizations and allergen challenge (Feehley et al., 2019). Thus, during early allergic responses, both CMA-colonized and GF mice can initiate innate type 2 inflammation. However, unlike GF mice, CMA-colonized mice have increased induction of ILC3s. While ILC3s are important for maintaining intestinal homeostasis through myriad mechanisms (Zhou and Sonnenburg, 2019), they can act as potent inducers of epithelial SAA-1 and type 3 inflammation through IL-22-dependent mechanisms (Sano et al., 2015; Gunasekera et al., 2020; Eken et al., 2014). This would

suggest that CMA-colonized mice have a mixed type 2/type 3 intestinal inflammatory response that does not occur in GF mice upon sensitization. In experimental mouse models, this mixed type 2/type 3 inflammatory response exacerbates antigen-specific allergic inflammation (Nakajima et al., 2014; He et al., 2007). Therefore, our data suggests that while both CMA-colonized and GF mice are susceptible to allergic sensitization, the mechanisms by which they are susceptible are not the same. GF mice are prone to atopy due to the dysregulation of IgE (Cahenzli et al., 2013; Hong et al., 2019), while the CMA microbiota promotes inflammatory responses.

Abrogation of TLR4 signaling can increase allergic susceptibility (Bashir et al., 2004; Brandt et al., 2013b). When TLR4 signaling is deficient, GF and CMA-colonized mice have increases in ILC2s compared to when TLR4 was sufficient (**Figure 27**), confirming that the inability to signal through TLR4 further increases susceptibility to allergic sensitization. In addition to microbe-derived ligands, TLR4 can also recognize several endogenous ligands, such a hyaluronan, which can influence intestinal immune cell phenotypes in GF mice (Termeer et al., 2002). Furthermore, TLR4-deficient mice of all colonization statuses have increased frequency of Th2 cells compared to their WT counterparts (**Figure 28**). Unexpectedly, in comparison to their WT counterparts, healthy-colonized mice also have increased number of Th2 cells and ILC2s (**Figure 28**). However, coupled with sensitization, this may be due to healthy-colonized mice also having a TLR4-dependent increase in total ILCs and T cells, which is not observed in GF and CMA-colonized mice. Interestingly, CMA colonized mice have decreased ILC3s, but increased Th17 cells compared to their WT counterparts (**Figure 29**). This too may be an effect that is specific for the CMA microbiota coupled with sensitization. In response to epithelial

adherent bacteria, Treg-specific deletion of MyD88 signaling, a downstream adaptor of TLR4, reduces intestinal IgA production, increases barrier permeability, and dysregulates the balance between Tregs and Th17 cells, leading to increased Th17 induction (Wang et al., 2015). Global abrogation of TLR4 could thus disrupt the immunological balance in the intestine through microbiota-dependent and -independent mechanisms. This suggests that TLR4 signaling is regulating the balance between the innate and adaptive arms during the early phases of allergic sensitization.

## V. Closing remarks

As very few studies show a proactive role of a microbiota in mediating inflammatory responses to food antigen, this work is novel in its demonstration of a microbially-mediated induction of type 2/type 3 inflammation following sensitization with BLG. The inflammatory responses and pathology that accompanies food allergies is multifaceted, and thus, defining etiological determinants poses as a notable difficulty in the study of the disease. Through this work, we characterize an intestinal inflammatory response that is directly resultant of host-microbe interactions with the Donor 5 microbiota (see model in **Figure 30**). While Donor 5 exhibited intestinal inflammation that did not occur in Donors 6-8, the observation that SAA-1 is elevated in the serum of a subset of infants in the larger cohort (**Figure 2D**) suggests that the intestinal inflammation that is associated with Donor 5 may be relevant to other CMA infants. Being that food allergies and other atopic diseases elicit diverse immunological responses, the use of SAA-1 as a biomarker could characterize a specific type of inflammatory response that is microbially mediated, poises

the intestine toward type 2/type 3 immunity, and is rapidly intensified in an antigen-specific manner upon exposure to cow's milk. Because of the presented results, we now know the features of the early immune response induced by this microbiota that will be important to examine in subsequent food antigen-specific responses. Future work can examine the adaptive immunological responses that are regulated by TLR4 globally and specifically in $CD11c^{+}$ cells in the induction of allergic sensitization to food antigen using a full sensitization model. Such experiments would be important for understanding the root of inflammatory manifestations that present in CMA infants with high serum SAA-1 and elucidate the "accessories" of these inflammatory responses. In time, this could potentially lead to the utilization of more personalized clinical treatments for CMA patients with this type of allergic inflammation.

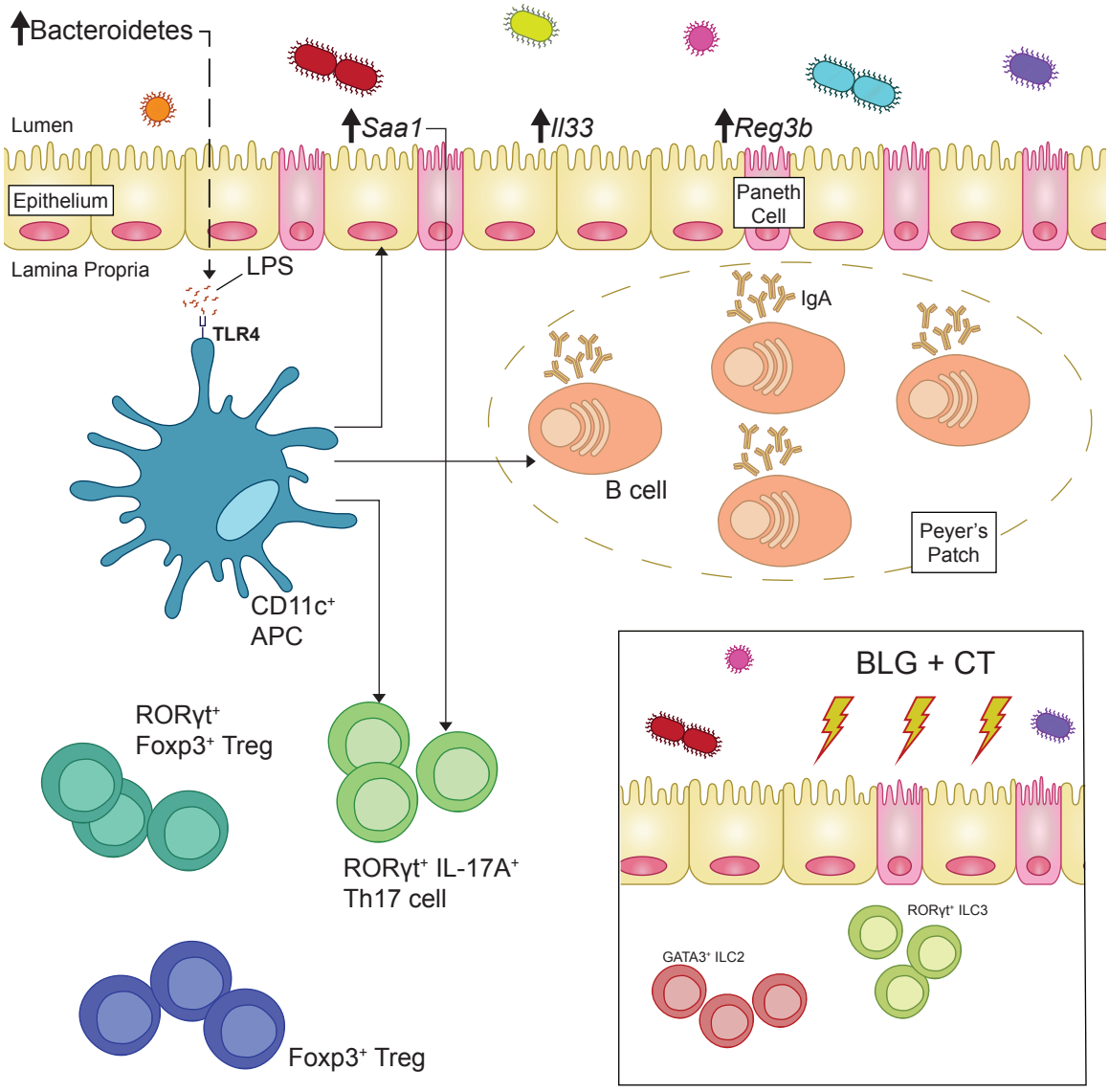


**Figure 30**: Model of intestinal inflammatory responses induced by the CMA Donor 5 microbiota. The CMA Donor 5 microbiota induces upregulation of inflammatory genes in the ileum epithelium which includes *Saa1*, *Reg3b*, *Il33*, and others that are related to type 2 and type 3 inflammatory responses. Colonization with the Donor 5 microbiota also induces Tregs, Th17 cells, and IgA production by B cells in the ileal lamina propria and Peyer's patches, respectively. Induction of inflammatory gene expression, Tregs, Th17 cells, and IgA is regulated by TLR4 signaling. Specifically, TLR4 signaling in $CD11c^+$ cells regulate epithelial inflammatory gene expression, IgA production, and induction of Th17 cells, but not Tregs. The Donor 5 microbiota is enriched with Gram-negative bacteria, particularly Bacteroidetes, which have previously been associated with allergy and *Saa* expression in the ileum. During the early stages of allergic sensitization, the Donor 5 microbiota induces an innate type 2/type 3 inflammatory response through the induction of ILC2s and ILC3s.

## References


Abdel-Gadir, A. *et al.* Microbiota therapy acts via a regulatory T cell MyD88/RORγt pathway to suppress food allergy. *Nat Med* **25**, 1164–1174 (2019).

Ajendra, J. *et al.* IL-17A both initiates, via IFNγ suppression, and limits the pulmonary type-2 immune response to nematode infection. *Mucosal Immunol* **13**, 958–968 (2020).

Al Nabhani, Z. *et al.* A Weaning Reaction to Microbiota Is Required for Resistance to Immunopathologies in the Adult. *Immunity* **50**, 1276-1288.e5 (2019).

Al-Ramli, W. *et al.* T(H)17-associated cytokines (IL-17A and IL-17F) in severe asthma. *J Allergy Clin Immunol* **123**, 1185–1187 (2009).

Allen, J. E. & Wynn, T. A. Evolution of Th2 immunity: a rapid repair response to tissue destructive pathogens. *PLoS Pathog* **7**, e1002003 (2011).

Alvarez, F. *et al.* The alarmins IL-1 and IL-33 differentially regulate the functional specialisation of Foxp3+ regulatory T cells during mucosal inflammation. *Mucosal Immunol* **12**, 746–760 (2019).

Araujo, M. I. *et al.* Inverse association between skin response to aeroallergens and Schistosoma mansoni infection. *Int Arch Allergy Immunol* **123**, 145–148 (2000).

Arrieta, M.-C. *et al.* Early infancy microbial and metabolic alterations affect risk of childhood asthma. *Sci Transl Med* **7**, 307ra152 (2015).

Atarashi, K. *et al.* Th17 Cell Induction by Adhesion of Microbes to Intestinal Epithelial Cells. *Cell* **163**, 367–380 (2015).

Ather, J.L., Ckless, K., Martin, R., Foley, K.L., Suratt, B.T., Boyson, J.E., Fitzgerald, K.A., Flavell, R.A., Eisenbarth, S.C., and Poynter, M.E. Serum amyloid A activates the NLRP3 inflammasome and promotes Th17 allergic asthma in mice. *J Immunol* **187**, 64–73 (2011).

Bachus, H. *et al.* Impaired Tumor-Necrosis-Factor-α-driven Dendritic Cell Activation Limits Lipopolysaccharide-Induced Protection from Allergic Inflammation in Infants. *Immunity* **50**, 225-240.e4 (2019).

Bae, M.-J. *et al.* Baicalein induces CD4(+)Foxp3(+) T cells and enhances intestinal barrier function in a mouse model of food allergy. *Sci Rep* **6**, 32225 (2016).

Bager, P. *et al.* Trichuris suis ova therapy for allergic rhinitis: a randomized, double-blind, placebo-controlled clinical trial. *J Allergy Clin Immunol* **125**, 123-130.e1–3 (2010).

Bang, Y.-J. *et al.* Serum amyloid A delivers retinol to intestinal myeloid cells to promote adaptive immunity. *Science* **373**, eabf9232 (2021).

Barnig, C. *et al.* Lipoxin A4 regulates natural killer cell and type 2 innate lymphoid cell activation in asthma. *Sci Transl Med* **5**, 174ra26 (2013).

Barrett, N. A. & Austen, K. F. Innate cells and T helper 2 cell immunity in airway inflammation. *Immunity* **31**, 425–437 (2009).

Bashir, M. E. H., Andersen, P., Fuss, I. J., Shi, H. N. & Nagler-Anderson, C. An enteric helminth infection protects against an allergic response to dietary antigen. *J Immunol* **169**, 3284–3292 (2002).

Bashir, M. E. H., Louie, S., Shi, H. N. & Nagler-Anderson, C. Toll-like receptor 4 signaling by intestinal microbes influences susceptibility to food allergy. *J Immunol* **172**, 6978–6987 (2004).

Bazil, V. *et al.* Structural relationship between the soluble and membrane-bound forms of human monocyte surface glycoprotein CD14. *Mol Immunol* **26**, 657–662 (1989).

Berin, M. C. & Wang, W. Reduced severity of peanut-induced anaphylaxis in TLR9-deficient mice is associated with selective defects in humoral immunity. *Mucosal Immunol* **6**, 114–121 (2013).

Bich, T. C. T. *et al.* Serum Amyloid A1: A Biomarker for Neutrophilic Airway Inflammation in Adult Asthmatic Patients. *Allergy Asthma Immunol Res* **14**, 40–58 (2022).

Blanchard, C. *et al.* Eotaxin-3 and a uniquely conserved gene-expression profile in eosinophilic esophagitis. *J Clin Invest* **116**, 536–547 (2006).

Bloom, S. M. *et al.* Commensal Bacteroides species induce colitis in host-genotype-specific fashion in a mouse model of inflammatory bowel disease. *Cell Host Microbe* **9**, 390–403 (2011).

Bodenhofer, U., Bonatesta, E., Horejš-Kainrath, C. & Hochreiter, S. msa: an R package for multiple sequence alignment. *Bioinformatics* **31**, 3997–3999 (2015).

Bolyen, E. *et al.* Reproducible, interactive, scalable and extensible microbiome data science using QIIME 2. *Nat Biotechnol* **37**, 852–857 (2019).

Bonnegarde-Bernard, A. *et al.* IKKβ in intestinal epithelial cells regulates allergen-specific IgA and allergic inflammation at distant mucosal sites. *Mucosal Immunol* **7**, 257–267 (2014).

Bourgonje, A. R. *et al.* A Combined Set of Four Serum Inflammatory Biomarkers Reliably Predicts Endoscopic Disease Activity in Inflammatory Bowel Disease. *Front Med (Lausanne)* **6**, 251 (2019).

Brandt, E. B. *et al.* Diesel exhaust particle induction of IL-17A contributes to severe asthma. *J Allergy Clin Immunol* **132**, 1194-1204.e2 (2013a).

Brandt, E. B., Gibson, A. M., Bass, S., Rydyznski, C. & Khurana Hershey, G. K. Exacerbation of allergen-induced eczema in TLR4- and TRIF-deficient mice. *J Immunol* **191**, 3519–3525 (2013b).

Britton, G. J. *et al.* Microbiotas from Humans with Inflammatory Bowel Disease Alter the Balance of Gut Th17 and RORγt+ Regulatory T Cells and Exacerbate Colitis in Mice. *Immunity* **50**, 212-224.e4 (2019).

Brough, H. A. *et al.* Early intervention and prevention of allergic diseases. *Allergy* **77**, 416–441 (2022).

Cahenzli, J., Köller, Y., Wyss, M., Geuking, M. B. & McCoy, K. D. Intestinal microbial diversity during early-life colonization shapes long-term IgE levels. *Cell Host Microbe* **14**, 559–570 (2013).

Callahan, B. J. *et al.* DADA2: High-resolution sample inference from Illumina amplicon data. *Nat Methods* **13**, 581–583 (2016).

Campbell, E., Hesser, L. A. & Nagler, C. R. B cells and the microbiota: a missing connection in food allergy. *Mucosal Immunol* **14**, 4–13 (2021).

Campos-Rodríguez, R. *et al.* Intermittent fasting favored the resolution of Salmonella typhimurium infection in middle-aged BALB/c mice. *Age (Dordr)* **38**, 13 (2016).

Cantalapiedra, C. P., Hernández-Plaza, A., Letunic, I., Bork, P. & Huerta-Cepas, J. eggNOG-mapper v2: Functional Annotation, Orthology Assignments, and Domain Prediction at the Metagenomic Scale. *Mol Biol Evol* **38**, 5825–5829 (2021).

Caramalho, I. *et al.* Regulatory T cells selectively express toll-like receptors and are activated by lipopolysaccharide. *J Exp Med* **197**, 403–411 (2003).

Cardona, V. *et al.* World allergy organization anaphylaxis guidance 2020. *World Allergy Organ J* **13**, 100472 (2020).

Cayrol, C. *et al.* Environmental allergens induce allergic inflammation through proteolytic maturation of IL-33. *Nat Immunol* **19**, 375–385 (2018).

Cervantes-Barragan, L. *et al.* Lactobacillus reuteri induces gut intraepithelial CD4+CD8αα+ T cells. *Science* **357**, 806–810 (2017).

Chan, J. K. *et al.* Alarmins: awaiting a clinical response. *J Clin Invest* **122**, 2711–2719 (2012).

Chen, F. *et al.* An essential role for TH2-type responses in limiting acute tissue damage during experimental helminth infection. *Nat Med* **18**, 260–266 (2012).

Chen, L. *et al.* NLRP12 attenuates colon inflammation by maintaining colonic microbial diversity and promoting protective commensal bacterial growth. *Nat Immunol* **18**, 541–551 (2017).

Chen, Y., Lun, A. T. L. & Smyth, G. K. From reads to genes to pathways: differential expression analysis of RNA-Seq experiments using Rsubread and the edgeR quasi-likelihood pipeline. *F1000Res* **5**, 1438 (2016).

Cheng, N., Liang, Y., Du, X. & Ye, R. D. Serum amyloid A promotes LPS clearance and suppresses LPS-induced inflammation and tissue injury. *EMBO Rep* **19**, e45517 (2018).

Cheng, Z., Taylor, B., Ourthiague, D. R. & Hoffmann, A. Distinct single-cell signaling characteristics are conferred by the MyD88 and TRIF pathways during TLR4 activation. *Sci Signal* **8**, ra69 (2015).

Chesné, J. *et al.* Prime role of IL-17A in neutrophilia and airway smooth muscle contraction in a house dust mite-induced allergic asthma model. *J Allergy Clin Immunol* **135**, 1643-1643.e3 (2015).

Cho, M. *et al.* Fibrinogen cleavage products and Toll-like receptor 4 promote the generation of programmed cell death 1 ligand 2-positive dendritic cells in allergic asthma. *J Allergy Clin Immunol* **142**, 530-541.e6 (2018).

Chow, J. C., Young, D. W., Golenbock, D. T., Christ, W. J. & Gusovsky, F. Toll-like receptor-4 mediates lipopolysaccharide-induced signal transduction. *J Biol Chem* **274**, 10689–10692 (1999).

Corr, S. C. *et al.* MyD88 adaptor-like (Mal) functions in the epithelial barrier and contributes to intestinal integrity via protein kinase C. *Mucosal Immunol* **7**, 57–67 (2014).

Crellin, N. K. *et al.* Human CD4+ T cells express TLR5 and its ligand flagellin enhances the suppressive capacity and expression of FOXP3 in CD4+CD25+ T regulatory cells. *J Immunol* **175**, 8051–8059 (2005).

Cullender, T. C. *et al.* Innate and adaptive immunity interact to quench microbiome flagellar motility in the gut. *Cell Host Microbe* **14**, 571–581 (2013).

Dabbagh, K., Dahl, M. E., Stepick-Biek, P. & Lewis, D. B. Toll-like receptor 4 is required for optimal development of Th2 immune responses: role of dendritic cells. *J Immunol* **168**, 4524–4530 (2002).

Dagher, R. *et al.* IL-33-ST2 axis regulates myeloid cell differentiation and activation enabling effective club cell regeneration. *Nat Commun* **11**, 4786 (2020).

De Filippis, F. *et al.* Specific gut microbiome signatures and the associated pro-inflamatory functions are linked to pediatric allergy and acquisition of immune tolerance. *Nat Commun* **12**, 5958 (2021).

de Los Reyes Jiménez, M. *et al.* An anti-inflammatory eicosanoid switch mediates the suppression of type-2 inflammation by helminth larval products. *Sci Transl Med* **12**, eaay0605 (2020).

DeLong, J. H. *et al.* Ara h 1-reactive T cells in individuals with peanut allergy. *J Allergy Clin Immunol* **127**, 1211-1218.e3 (2011).

Derebe, M. G. *et al.* Serum amyloid A is a retinol binding protein that transports retinol during bacterial infection. *Elife* **3**, e03206 (2014).

Doe, C. *et al.* Expression of the T helper 17-associated cytokines IL-17A and IL-17F in asthma and COPD. *Chest* **138**, 1140–1147 (2010).

Donaldson, G. P. *et al.* Gut microbiota utilize immunoglobulin A for mucosal colonization. *Science* **360**, 795–800 (2018).

Doron, I. *et al.* Mycobiota-induced IgA antibodies regulate fungal commensalism in the gut and are dysregulated in Crohn's disease. *Nat Microbiol* **6**, 1493–1504 (2021).

Eberl, G. Immunity by equilibrium. *Nat Rev Immunol* **16**, 524–532 (2016).

Eisenbarth, S. C. *et al.* Lipopolysaccharide-enhanced, toll-like receptor 4-dependent T helper cell type 2 responses to inhaled antigen. *J Exp Med* **196**, 1645–1651 (2002).

Eken, A., Singh, A. K., Treuting, P. M. & Oukka, M. IL-23R+ innate lymphoid cells induce colitis via interleukin-22-dependent mechanism. *Mucosal Immunol* **7**, 143–154 (2014).

Esaki, H. *et al.* Early-onset pediatric atopic dermatitis is TH2 but also TH17 polarized in skin. *J Allergy Clin Immunol* **138**, 1639–1651 (2016).

Fadlallah, J. *et al.* Microbial ecology perturbation in human IgA deficiency. *Sci Transl Med* **10**, eaan1217 (2018).

Feary, J. R. *et al.* Experimental hookworm infection: a randomized placebo-controlled trial in asthma. *Clin Exp Allergy* **40**, 299–306 (2010).

Feehley, T. *et al.* Healthy infants harbor intestinal bacteria that protect against food allergy. *Nat Med* **25**, 448–453 (2019).

Fitzgerald, K. A. *et al.* LPS-TLR4 signaling to IRF-3/7 and NF-kappaB involves the toll adapters TRAM and TRIF. *J Exp Med* **198**, 1043–1055 (2003).

Flannigan, K. L. *et al.* IL-17A-mediated neutrophil recruitment limits expansion of segmented filamentous bacteria. *Mucosal Immunol* **10**, 673–684 (2017).

Florsheim, E. B., Sullivan, Z. A., Khoury-Hanold, W. & Medzhitov, R. Food allergy as a biological food quality control system. *Cell* **184**, 1440–1454 (2021).

Forbes, S. J., Eschmann, M. & Mantis, N. J. Inhibition of Salmonella enterica serovar typhimurium motility and entry into epithelial cells by a protective antilipopolysaccharide monoclonal immunoglobulin A antibody. *Infect Immun* **76**, 4137–4144 (2008).

Frantz, A. L. *et al.* Targeted deletion of MyD88 in intestinal epithelial cells results in compromised antibacterial immunity associated with downregulation of polymeric immunoglobulin receptor, mucin-2, and antibacterial peptides. *Mucosal Immunol* **5**, 501–512 (2012).

Furuta, G. T. & Katzka, D. A. Eosinophilic Esophagitis. *N Engl J Med* **373**, 1640–1648 (2015).

Ganz, T. Defensins: antimicrobial peptides of innate immunity. *Nat Rev Immunol* **3**, 710–720 (2003).

Gao, L. *et al.* Neonatal LPS Administered Before Sensitization Reduced the Number of Inflammatory Monocytes and Abrogated the Development of OVA-Induced Th2 Allergic Airway Inflammation. *Front Immunol* **12**, 725906 (2021).

García, L. N., Leimgruber, C., Nicola, J. P., Quintar, A. A. & Maldonado, C. A. Neonatal endotoxin stimulation is associated with a long-term bronchiolar epithelial expression of innate immune and anti-allergic markers that attenuates the allergic response. *PLoS One* **15**, e0226233 (2020).

Gehring, U. *et al.* Asthma and allergic symptoms in relation to house dust endotoxin: Phase Two of the International Study on Asthma and Allergies in Childhood (ISAAC II). *Clin Exp Allergy* **38**, 1911–1920 (2008).

Gertie, J. A. *et al.* Oral anaphylaxis to peanut in a mouse model is associated with gut permeability but not with Tlr4 or Dock8 mutations. *J Allergy Clin Immunol* **149**, 262–274 (2022).

Geva-Zatorsky, N. *et al.* Mining the Human Gut Microbiota for Immunomodulatory Organisms. *Cell* **168**, 928-943.e11 (2017).

Gittler, J. K. *et al.* Progressive activation of T(H)2/T(H)22 cytokines and selective epidermal proteins characterizes acute and chronic atopic dermatitis. *J Allergy Clin Immunol* **130**, 1344–1354 (2012).

Gollwitzer, E. S. *et al.* Lung microbiota promotes tolerance to allergens in neonates via PD-L1. *Nat Med* **20**, 642–647 (2014).

Gonzalez-Espinosa, C. *et al.* Preferential signaling and induction of allergy-promoting lymphokines upon weak stimulation of the high affinity IgE receptor on mast cells. *J Exp Med* **197**, 1453–1465 (2003).

Goodridge, H. S. *et al.* In vivo exposure of murine dendritic cell and macrophage bone marrow progenitors to the phosphorylcholine-containing filarial nematode glycoprotein ES-62 polarizes their differentiation to an anti-inflammatory phenotype. *Immunology* **113**, 491–498 (2004).

Gouwy, M. *et al.* Serum amyloid A chemoattracts immature dendritic cells and indirectly provokes monocyte chemotaxis by induction of cooperating CC and CXC chemokines. *Eur J Immunol* **45**, 101–112 (2015).

Gracz, A. D., Puthoff, B. J. & Magness, S. T. Identification, isolation, and culture of intestinal epithelial stem cells from murine intestine. *Methods Mol Biol* **879**, 89–107 (2012).

Gunasekera, D. C. *et al.* The development of colitis in Il10-/- mice is dependent on IL-22. *Mucosal Immunol* **13**, 493–506 (2020).

Gupta, R. S. *et al.* The Public Health Impact of Parent-Reported Childhood Food Allergies in the United States. *Pediatrics* **142**, e20181235 (2018).

Gurish, M. F. *et al.* IgE enhances parasite clearance and regulates mast cell responses in mice infected with Trichinella spiralis. *J Immunol* **172**, 1139–1145 (2004).

Haberman, Y. et al. Pediatric Crohn disease patients exhibit specific ileal transcriptome and microbiome signature. *J Clin Invest* **124**, 3617–3633 (2014).

Hadebe, S. *et al.* Microbial Ligand Costimulation Drives Neutrophilic Steroid-Refractory Asthma. *PLoS One* **10**, e0134219 (2015).

Halim, T. Y. F. *et al.* Group 2 innate lymphoid cells license dendritic cells to potentiate memory TH2 cell responses. *Nat Immunol* **17**, 57–64 (2016).

Hammad, H. *et al.* House dust mite allergen induces asthma via Toll-like receptor 4 triggering of airway structural cells. *Nat Med* **15**, 410–416 (2009).

Hapfelmeier, S. *et al.* Reversible microbial colonization of germ-free mice reveals the dynamics of IgA immune responses. *Science* **328**, 1705–1709 (2010).

Harrison, O. J. *et al.* Epithelial-derived IL-18 regulates Th17 cell differentiation and Foxp3$^{+}$ Treg cell function in the intestine. *Mucosal Immunol* **8**, 1226–1236 (2015).

He, R., Oyoshi, M. K., Jin, H. & Geha, R. S. Epicutaneous antigen exposure induces a Th17 response that drives airway inflammation after inhalation challenge. *Proc Natl Acad Sci U S A* **104**, 15817–15822 (2007).

Hong, S.-W. *et al.* Food antigens drive spontaneous IgE elevation in the absence of commensal microbiota. *Sci Adv* **5**, eaaw1507 (2019).

Hsia, B. J. *et al.* Trif-dependent induction of Th17 immunity by lung dendritic cells. *Mucosal Immunol* **8**, 186–197 (2015).

Hviid, A., Svanström, H. & Frisch, M. Antibiotic use and inflammatory bowel diseases in childhood. *Gut* **60**, 49–54 (2011).

Hyatt, D. *et al.* Prodigal: prokaryotic gene recognition and translation initiation site identification. *BMC Bioinformatics* **11**, 119 (2010).

Inclan-Rico, J. M. & Siracusa, M. C. First Responders: Innate Immunity to Helminths. *Trends Parasitol* **34**, 861–880 (2018).

Irvin, C. *et al.* Increased frequency of dual-positive TH2/TH17 cells in bronchoalveolar lavage fluid characterizes a population of patients with severe asthma. *J Allergy Clin Immunol* **134**, 1175-1186.e7 (2014).

Ito, T. *et al.* TSLP-activated dendritic cells induce an inflammatory T helper type 2 cell response through OX40 ligand. *J Exp Med* **202**, 1213–1223 (2005).

Ivanov, I. I. *et al.* Induction of intestinal Th17 cells by segmented filamentous bacteria. *Cell* **139**, 485–498 (2009).

Iwasaki, A. & Medzhitov, R. Regulation of adaptive immunity by the innate immune system. *Science* **327**, 291–295 (2010).

Iweala, O. I. & Nagler, C. R. The Microbiome and Food Allergy. *Annu Rev Immunol* **37**, 377–403 (2019).

Janzi, M. *et al.* Selective IgA deficiency in early life: association to infections and allergic diseases during childhood. *Clin Immunol* **133**, 78–85 (2009).

Jeon, H. *et al.* Pathogenic Mechanism of Der p 38 as a Novel Allergen Homologous to RipA and RipB Proteins in Atopic Dermatitis. *Front Immunol* **12**, 646316 (2021).

Jia, Y.-P. *et al.* TLR2/TLR4 activation induces Tregs and suppresses intestinal inflammation caused by Fusobacterium nucleatum in vivo. *PLoS One* **12**, e0186179 (2017).

Josefowicz, S. Z. *et al.* Extrathymically generated regulatory T cells control mucosal TH2 inflammation. *Nature* **482**, 395–399 (2012).

Judd, L. M. *et al.* Elevated IL-33 expression is associated with pediatric eosinophilic esophagitis, and exogenous IL-33 promotes eosinophilic esophagitis development in mice. *Am J Physiol Gastrointest Liver Physiol* **310**, G13-25 (2016).

Just, A. C. *et al.* Prenatal exposure to butylbenzyl phthalate and early eczema in an urban cohort. *Environ Health Perspect* **120**, 1475–1480 (2012).

Kim, B. S. *et al.* Basophils promote innate lymphoid cell responses in inflamed skin. *J Immunol* **193**, 3717–3725 (2014).

Kim, M. H. *et al.* IL-17A-Producing Innate Lymphoid Cells Promote Skin Inflammation by Inducing IL-33-Driven Type 2 Immune Responses. *J Invest Dermatol* **140**, 827-837.e9 (2020).

King, C. L. *et al.* Mice with a targeted deletion of the IgE gene have increased worm burdens and reduced granulomatous inflammation following primary infection with Schistosoma mansoni. *J Immunol* **158**, 294–300 (1997).

Kinnebrew, M. A. *et al.* Interleukin 23 production by intestinal CD103(+)CD11b(+) dendritic cells in response to bacterial flagellin enhances mucosal innate immune defense. *Immunity* **36**, 276–287 (2012).

Krishnamoorthy, N. *et al.* Neutrophil cytoplasts induce TH17 differentiation and skew inflammation toward neutrophilia in severe asthma. *Sci Immunol* **3**, eaao4747 (2018).

Kudo, M. *et al.* IL-17A produced by αβ T cells drives airway hyper-responsiveness in mice and enhances mouse and human airway smooth muscle contraction. *Nat Med* **18**, 547–554 (2012).

Lajoie, S. *et al.* Complement-mediated regulation of the IL-17A axis is a central genetic determinant of the severity of experimental allergic asthma. *Nat Immunol* **11**, 928–935 (2010).

Lambrecht, B. N. & Hammad, H. The immunology of the allergy epidemic and the hygiene hypothesis. *Nat Immunol* **18**, 1076–1083 (2017).

Layland, L. E. *et al.* Schistosoma mansoni-mediated suppression of allergic airway inflammation requires patency and Foxp3+ Treg cells. *PLoS Negl Trop Dis* **7**, e2379 (2013).

Layunta, E., Jäverfelt, S., Dolan, B., Arike, L. & Pelaseyed, T. IL-22 promotes the formation of a MUC17 glycocalyx barrier in the postnatal small intestine during weaning. *Cell Rep* **34**, 108757 (2021).

Lee, H. Y., Jo, S. H., Lee, C., Baek, S.-H. & Bae, Y.-S. Differential production of leukotriene B4 or prostaglandin E2 by WKYMVm or serum amyloid A via formyl peptide receptor-like 1. *Biochem Pharmacol* **72**, 860–868 (2006).

Lee, J.-Y. *et al.* Serum Amyloid A Proteins Induce Pathogenic Th17 Cells and Promote Inflammatory Disease. *Cell* **183**, 2036–2039 (2020).

Li, D., Liu, C.-M., Luo, R., Sadakane, K. & Lam, T.-W. MEGAHIT: an ultra-fast single-node solution for large and complex metagenomics assembly via succinct de Bruijn graph. *Bioinformatics* **31**, 1674–1676 (2015a).

Li, H. *et al.* The outer mucus layer hosts a distinct intestinal microbial niche. *Nat Commun* **6**, 8292 (2015b).

Li, H. *et al.* Mucosal or systemic microbiota exposures shape the B cell repertoire. *Nature* **584**, 274–278 (2020).

Liao, Y., Smyth, G. K. & Shi, W. The R package Rsubread is easier, faster, cheaper and better for alignment and quantification of RNA sequencing reads. *Nucleic Acids Res* **47**, e47 (2019).

Lindemans, C. A. *et al.* Interleukin-22 promotes intestinal-stem-cell-mediated epithelial regeneration. *Nature* **528**, 560–564 (2015).

Liu, J. *et al.* Local Group 2 Innate Lymphoid Cells Promote Corneal Regeneration after Epithelial Abrasion. *Am J Pathol* **187**, 1313–1326 (2017).

Liu, N., Ohnishi, N., Ni, L., Akira, S. & Bacon, K. B. CpG directly induces T-bet expression and inhibits IgG1 and IgE switching in B cells. *Nat Immunol* **4**, 687–693 (2003).

Liu, Y. *et al.* TLR4 regulates RORγt+ regulatory T-cell responses and susceptibility to colon inflammation through interaction with Akkermansia muciniphila. *Microbiome* **10**, 98 (2022).

Lopetuso, L. R. *et al.* IL-33 promotes recovery from acute colitis by inducing miR-320 to stimulate epithelial restitution and repair. *Proc Natl Acad Sci U S A* **115**, E9362–E9370 (2018).

Lu, S. *et al.* IL-17A, but not IL-17F, is indispensable for airway vascular remodeling induced by exaggerated Th17 cell responses in prolonged ovalbumin-challenged mice. *J Immunol* **194**, 3557–3566 (2015).

Lv, J. *et al.* Airway epithelial TSLP production of TLR2 drives type 2 immunity in allergic airway inflammation. *Eur J Immunol* **48**, 1838–1850 (2018).

Maric, J. *et al.* Cytokine-induced endogenous production of prostaglandin D2 is essential for human group 2 innate lymphoid cell activation. *J Allergy Clin Immunol* **143**, 2202-2214.e5 (2019).

Maric, J. *et al.* Prostaglandin E2 suppresses human group 2 innate lymphoid cell function. *J Allergy Clin Immunol* **141**, 1761-1773.e6 (2018).

Marichal, T. *et al.* A beneficial role for immunoglobulin E in host defense against honeybee venom. *Immunity* **39**, 963–975 (2013).

Marinaro, M. *et al.* Mucosal adjuvant effect of cholera toxin in mice results from induction of T helper 2 (Th2) cells and IL-4. *J Immunol* **155**, 4621–4629 (1995).

Martin, M., Katz, J., Vogel, S. N. & Michalek, S. M. Differential induction of endotoxin tolerance by lipopolysaccharides derived from Porphyromonas gingivalis and Escherichia coli. *J Immunol* **167**, 5278–5285 (2001).

Mathias, A., Pais, B., Favre, L., Benyacoub, J. & Corthésy, B. Role of secretory IgA in the mucosal sensing of commensal bacteria. *Gut Microbes* **5**, 688–695 (2014).

McAlees, J. W. *et al.* Distinct Tlr4-expressing cell compartments control neutrophilic and eosinophilic airway inflammation. *Mucosal Immunol* **8**, 863–873 (2015).

McKinley, L. *et al.* TH17 cells mediate steroid-resistant airway inflammation and airway hyperresponsiveness in mice. *J Immunol* **181**, 4089–4097 (2008).

McSorley, H. J. *et al.* Suppression of type 2 immunity and allergic airway inflammation by secreted products of the helminth Heligmosomoides polygyrus. *Eur J Immunol* **42**, 2667–2682 (2012).

Medzhitov, R., Preston-Hurlburt, P. & Janeway, C. A. A human homologue of the Drosophila Toll protein signals activation of adaptive immunity. *Nature* **388**, 394–397 (1997).

Mestecky, J., Russell, M. W., Jackson, S. & Brown, T. A. The human IgA system: a reassessment. *Clin Immunol Immunopathol* **40**, 105–114 (1986).

Metsälä, J. *et al.* Mother's and offspring's use of antibiotics and infant allergy to cow's milk. *Epidemiology* **24**, 303–309 (2013).

Mills, R. H. *et al.* Multi-omics analyses of the ulcerative colitis gut microbiome link Bacteroides vulgatus proteases with disease severity. *Nat Microbiol* **7**, 262–276 (2022).

Minutti, C. M. *et al.* Local amplifiers of IL-4Rα-mediated macrophage activation promote repair in lung and liver. *Science* **356**, 1076–1080 (2017).

Molofsky, A. B. *et al.* Interleukin-33 and Interferon-γ Counter-Regulate Group 2 Innate Lymphoid Cell Activation during Immune Perturbation. *Immunity* **43**, 161–174 (2015).

Moor, K. *et al.* High-avidity IgA protects the intestine by enchaining growing bacteria. *Nature* **544**, 498–502 (2017).

Moro, K., Ealey, K. N., Kabata, H. & Koyasu, S. Isolation and analysis of group 2 innate lymphoid cells in mice. *Nat Protoc* **10**, 792–806 (2015).

Mortimer, K. *et al.* Dose-ranging study for trials of therapeutic infection with Necator americanus in humans. *Am J Trop Med Hyg* **75**, 914–920 (2006).

Motomura, Y. *et al.* Basophil-derived interleukin-4 controls the function of natural helper cells, a member of ILC2s, in lung inflammation. *Immunity* **40**, 758–771 (2014).

Msallam, R. *et al.* Fetal mast cells mediate postnatal allergic responses dependent on maternal IgE. *Science* **370**, 941–950 (2020).

Murphy, K., Weaver, C. & Berg, L. Janeway's Immunobiology. (Norton, W. W. & Company, Inc., 2022).

Nagao-Kitamoto, H. *et al.* Interleukin-22-mediated host glycosylation prevents Clostridioides difficile infection by modulating the metabolic activity of the gut microbiota. *Nat Med* **26**, 608–617 (2020).

Nakajima, A. *et al.* IgA regulates the composition and metabolic function of gut microbiota by promoting symbiosis between bacteria. *J Exp Med* **215**, 2019–2034 (2018).

Nakajima, S. *et al.* IL-17A as an inducer for Th2 immune responses in murine atopic dermatitis models. *J Invest Dermatol* **134**, 2122–2130 (2014).

Nakamura, Y. *et al.* Staphylococcus Agr virulence is critical for epidermal colonization and associates with atopic dermatitis development. *Sci Transl Med* **12**, eaay4068 (2020).

Nik, A. M. & Carlsson, P. Separation of intact intestinal epithelium from mesenchyme. *Biotechniques* **55**, 42–44 (2013).

Noda, S. *et al.* The Asian atopic dermatitis phenotype combines features of atopic dermatitis and psoriasis with increased TH17 polarization. *J Allergy Clin Immunol* **136**, 1254–1264 (2015).

Nowarski, R. *et al.* Epithelial IL-18 Equilibrium Controls Barrier Function in Colitis. *Cell* **163**, 1444–1456 (2015).

Nutten, S. Atopic dermatitis: global epidemiology and risk factors. *Ann Nutr Metab* **66 Suppl 1**, 8–16 (2015).

O'Neill, L. A. J., Golenbock, D. & Bowie, A. G. The history of Toll-like receptors - redefining innate immunity. *Nat Rev Immunol* **13**, 453–460 (2013).

Obata-Ninomiya, K. *et al.* The skin is an important bulwark of acquired immunity against intestinal helminths. *J Exp Med* **210**, 2583–2595 (2013).

Ohnmacht, C. *et al.* The microbiota regulates type 2 immunity through RORγt$^{+}$ T cells. *Science* **349**, 989–993 (2015).

Okai, S. *et al.* High-affinity monoclonal IgA regulates gut microbiota and prevents colitis in mice. *Nat Microbiol* **1**, 16103 (2016).

Olszak, T. *et al.* Microbial exposure during early life has persistent effects on natural killer T cell function. *Science* **336**, 489–493 (2012).

Ozseker, F. *et al.* Serum amyloid A (SAA) in induced sputum of asthmatics: a new look to an old marker. *Int Immunopharmacol* **6**, 1569–1576 (2006).

Pabst, O. & Mowat, A. M. Oral tolerance to food protein. *Mucosal Immunol* **5**, 232–239 (2012).

Pate, C. A. et al. Asthma Surveillance - United States, 2006-2018. MMWR *Surveill Summ* **70**, 1–32 (2021).

Pénard-Morand, C. *et al.* Long-term exposure to close-proximity air pollution and asthma and allergies in urban children. *Eur Respir J* **36**, 33–40 (2010).

Perrier, C., Thierry, A.-C., Mercenier, A. & Corthésy, B. Allergen-specific antibody and cytokine responses, mast cell reactivity and intestinal permeability upon oral challenge of sensitized and tolerized mice. *Clin Exp Allergy* **40**, 153–162 (2010).

Peterson, L. W. & Artis, D. Intestinal epithelial cells: regulators of barrier function and immune homeostasis. *Nat Rev Immunol* **14**, 141–153 (2014).

Piggott, D. A. *et al.* MyD88-dependent induction of allergic Th2 responses to intranasal antigen. *J Clin Invest* **115**, 459–467 (2005).

Pochanke, V. *et al.* Identification and characterization of a novel antigen from the nematode Nippostrongylus brasiliensis recognized by specific IgE. *Eur J Immunol* **37**, 1275–1284 (2007).

Profet, M. The function of allergy: immunological defense against toxins. *Q Rev Biol* **66**, 23–62 (1991).

Radermecker, C. *et al.* Locally instructed CXCR4hi neutrophils trigger environment-driven allergic asthma through the release of neutrophil extracellular traps. *Nat Immunol* **20**, 1444–1455 (2019).

Rak, G. D. *et al.* IL-33-Dependent Group 2 Innate Lymphoid Cells Promote Cutaneous Wound Healing. *J Invest Dermatol* **136**, 487–496 (2016).

Ramu, S. *et al.* Allergens produce serine proteases-dependent distinct release of metabolite DAMPs in human bronchial epithelial cells. *Clin Exp Allergy* **48**, 156–166 (2018).

Rezende, R. M. & Weiner, H. L. History and mechanisms of oral tolerance. *Semin Immunol* **30**, 3–11 (2017).

Rol, N., Favre, L., Benyacoub, J. & Corthésy, B. The role of secretory immunoglobulin A in the natural sensing of commensal bacteria by mouse Peyer's patch dendritic cells. *J Biol Chem* **287**, 40074–40082 (2012).

Rollenske, T. *et al.* Parallelism of intestinal secretory IgA shapes functional microbial fitness. *Nature* **598**, 657–661 (2021).

Russell, S. L. *et al.* Early life antibiotic-driven changes in microbiota enhance susceptibility to allergic asthma. *EMBO Rep* **13**, 440–447 (2012).

Ryu, J.-H. *et al.* Distinct TLR-mediated pathways regulate house dust mite-induced allergic disease in the upper and lower airways. *J Allergy Clin Immunol* **131**, 549–561 (2013).

Salimi, M. *et al.* A role for IL-25 and IL-33-driven type-2 innate lymphoid cells in atopic dermatitis. *J Exp Med* **210**, 2939–2950 (2013).

Salimi, M. *et al.* Cysteinyl leukotriene E4 activates human group 2 innate lymphoid cells and enhances the effect of prostaglandin D2 and epithelial cytokines. *J Allergy Clin Immunol* **140**, 1090-1100.e11 (2017).

Salyers, A. A., Vercellotti, J. R., West, S. E. & Wilkins, T. D. Fermentation of mucin and plant polysaccharides by strains of Bacteroides from the human colon. *Appl Environ Microbiol* **33**, 319–322 (1977).

Sano, T. *et al.* An IL-23R/IL-22 Circuit Regulates Epithelial Serum Amyloid A to Promote Local Effector Th17 Responses. *Cell* **163**, 381–393 (2015).

Sawada, Y. *et al.* Prostaglandin E2 (PGE2)-EP2 signaling negatively regulates murine atopic dermatitis-like skin inflammation by suppressing thymic stromal lymphopoietin expression. *J Allergy Clin Immunol* **144**, 1265-1273.e9 (2019).

Schmid-Grendelmeier, P. *et al.* Eosinophils express functional IL-13 in eosinophilic inflammatory diseases. *J Immunol* **169**, 1021–1027 (2002).

Schumann, R. R. *et al.* Structure and function of lipopolysaccharide binding protein. *Science* **249**, 1429–1431 (1990).

Schwartz, C. *et al.* Basophil-mediated protection against gastrointestinal helminths requires IgE-induced cytokine secretion. *Proc Natl Acad Sci U S A* **111**, E5169-5177 (2014).

Schwartz, L. B., Irani, A. M., Roller, K., Castells, M. C. & Schechter, N. M. Quantitation of histamine, tryptase, and chymase in dispersed human T and TC mast cells. *J Immunol* **138**, 2611–2615 (1987).

Schwartz, L. B., Lewis, R. A., Seldin, D. & Austen, K. F. Acid hydrolases and tryptase from secretory granules of dispersed human lung mast cells. *J Immunol* **126**, 1290–1294 (1981).

Schwarze, J. *et al.* Antigen-specific immunoglobulin-A prevents increased airway responsiveness and lung eosinophilia after airway challenge in sensitized mice. *Am J Respir Crit Care Med* **158**, 519–525 (1998).

Schwarzer, M. *et al.* Diet Matters: Endotoxin in the Diet Impacts the Level of Allergic Sensitization in Germ-Free Mice. *PLoS One* **12**, e0167786 (2017).

Scott, I. C. *et al.* Interleukin-33 is activated by allergen- and necrosis-associated proteolytic activities to regulate its alarmin activity during epithelial damage. *Sci Rep* **8**, 3363 (2018).

Sefik, E. *et al.* Individual intestinal symbionts induce a distinct population of RORγ$^{+}$ regulatory T cells. *Science* **349**, 993–997 (2015).

Segal, D. M., Taurog, J. D. & Metzger, H. Dimeric immunoglobulin E serves as a unit signal for mast cell degranulation. *Proc Natl Acad Sci U S A* **74**, 2993–2997 (1977).

Shah, C., Hari-Dass, R. & Raynes, J. G. Serum amyloid A is an innate immune opsonin for Gram-negative bacteria. *Blood* **108**, 1751–1757 (2006).

Shen, H., Tesar, B. M., Walker, W. E. & Goldstein, D. R. Dual signaling of MyD88 and TRIF is critical for maximal TLR4-induced dendritic cell maturation. *J Immunol* **181**, 1849–1858 (2008).

Shepherd, E. S., DeLoache, W. C., Pruss, K. M., Whitaker, W. R. & Sonnenburg, J. L. An exclusive metabolic niche enables strain engraftment in the gut microbiota. *Nature* **557**, 434–438 (2018).

Shibata, N. *et al.* Lymphoid tissue-resident Alcaligenes LPS induces IgA production without excessive inflammatory responses via weak TLR4 agonist activity. *Mucosal Immunol* **11**, 693–702 (2018).

Shim, J.-U. *et al.* Flagellin suppresses experimental asthma by generating regulatory dendritic cells and T cells. *J Allergy Clin Immunol* **137**, 426–435 (2016).

Smits, H. H. *et al.* Cholera toxin B suppresses allergic inflammation through induction of secretory IgA. *Mucosal Immunol* **2**, 331–339 (2009).

Smole, U. *et al.* Serum amyloid A is a soluble pattern recognition receptor that drives type 2 immunity. *Nat Immunol* **21**, 756–765 (2020).

Snelgrove, R. J. *et al.* Alternaria-derived serine protease activity drives IL-33-mediated asthma exacerbations. *J Allergy Clin Immunol* **134**, 583-592.e6 (2014).

Sokol, C. L., Barton, G. M., Farr, A. G. & Medzhitov, R. A mechanism for the initiation of allergen-induced T helper type 2 responses. *Nat Immunol* **9**, 310–318 (2008).

Spadaro, G., Giurato, G., Stellato, C., Marone, G. & Casolaro, V. Basophil degranulation in response to IgE ligation is controlled by a distinctive circadian clock in asthma. *Allergy* **75**, 158–168 (2020).

Spencer, L. A., Porte, P., Zetoff, C. & Rajan, T. V. Mice genetically deficient in immunoglobulin E are more permissive hosts than wild-type mice to a primary, but not secondary, infection with the filarial nematode Brugia malayi. *Infect Immun* **71**, 2462–2467 (2003).

Starkl, P. *et al.* IgE antibodies, FcεRIα, and IgE-mediated local anaphylaxis can limit snake venom toxicity. *J Allergy Clin Immunol* **137**, 246-257.e11 (2016).

Steel, N. et al. TGFβ-activation by dendritic cells drives Th17 induction and intestinal contractility and augments the expulsion of the parasite Trichinella spiralis in mice. *PLoS Pathog* **15**, e1007657 (2019).

Stefka, A. T. et al. Commensal bacteria protect against food allergen sensitization. *PNAS* **111**, 13145–13150 (2014).

Sujino, T. *et al.* Tissue adaptation of regulatory and intraepithelial $CD4^+$ T cells controls gut inflammation. *Science* **352**, 1581–1586 (2016).

Sun, L. & Ye, R. D. Serum amyloid A1: Structure, function and gene polymorphism. *Gene* **583**, 48–57 (2016).

Sutherland, T. E. *et al.* Chitinase-like proteins promote IL-17-mediated neutrophilia in a tradeoff between nematode killing and host damage. *Nat Immunol* **15**, 1116–1125 (2014).

Tan, A. M. *et al.* TLR4 signaling in stromal cells is critical for the initiation of allergic Th2 responses to inhaled antigen. *J Immunol* **184**, 3535–3544 (2010).

Tang, H. *et al.* The T helper type 2 response to cysteine proteases requires dendritic cell-basophil cooperation via ROS-mediated signaling. *Nat Immunol* **11**, 608–617 (2010).

Tang, M. S. *et al.* Integrated Analysis of Biopsies from Inflammatory Bowel Disease Patients Identifies SAA-1 as a Link Between Mucosal Microbes with TH17 and TH22 Cells. *Inflamm Bowel Dis* **23**, 1544–1554 (2017).

Termeer, C. *et al.* Oligosaccharides of Hyaluronan activate dendritic cells via toll-like receptor 4. *J Exp Med* **195**, 99–111 (2002).

Thio, C. L.-P., Lai, A. C.-Y., Chi, P.-Y., Webster, G. & Chang, Y.-J. Toll-like receptor 9-dependent interferon production prevents group 2 innate lymphoid cell-driven airway hyperreactivity. *J Allergy Clin Immunol* **144**, 682-697.e9 (2019).

Thomas, S. Y. *et al.* MyD88-dependent dendritic and epithelial cell crosstalk orchestrates immune responses to allergens. *Mucosal Immunol* **11**, 796–810 (2018).

Thorne, P. S. *et al.* Endotoxin exposure is a risk factor for asthma: the national survey of endotoxin in United States housing. *Am J Respir Crit Care Med* **172**, 1371–1377 (2005).

Tjota, M. Y. *et al.* Signaling through FcRγ-associated receptors on dendritic cells drives IL-33-dependent TH2-type responses. *J Allergy Clin Immunol* **134**, 706-713.e8 (2014).

Tosiek, M. J., Fiette, L., El Daker, S., Eberl, G. & Freitas, A. A. IL-15-dependent balance between Foxp3 and RORγt expression impacts inflammatory bowel disease. *Nat Commun* **7**, 10888 (2016).

Trompette, A. *et al.* Allergenicity resulting from functional mimicry of a Toll-like receptor complex protein. *Nature* **457**, 585–588 (2009).

Tsai, P.-Y. *et al.* IL-22 Upregulates Epithelial Claudin-2 to Drive Diarrhea and Enteric Pathogen Clearance. *Cell Host Microbe* **21**, 671-681.e4 (2017).

Upadhyay, V. *et al.* Lymphotoxin regulates commensal responses to enable diet-induced obesity. *Nat Immunol* **13**, 947–953 (2012).

Vaishnava, S. *et al.* The antibacterial lectin RegIIIgamma promotes the spatial segregation of microbiota and host in the intestine. *Science* **334**, 255–258 (2011).

Vaishnava, S., Behrendt, C. L., Ismail, A. S., Eckmann, L. & Hooper, L. V. Paneth cells directly sense gut commensals and maintain homeostasis at the intestinal host-microbial interface. *Proc Natl Acad Sci U S A* **105**, 20858–20863 (2008).

van den Biggelaar, A. H. *et al.* Decreased atopy in children infected with Schistosoma haematobium: a role for parasite-induced interleukin-10. *Lancet* **356**, 1723–1727 (2000).

Vatanen, T. *et al.* Variation in Microbiome LPS Immunogenicity Contributes to Autoimmunity in Humans. *Cell* **165**, 1551 (2016).

Voehringer, D. Protective and pathological roles of mast cells and basophils. *Nat Rev Immunol* **13**, 362–375 (2013).

Volpi, C. *et al.* High doses of CpG oligodeoxynucleotides stimulate a tolerogenic TLR9-TRIF pathway. *Nat Commun* **4**, 1852 (2013).

von Mutius, E. *et al.* Exposure to endotoxin or other bacterial components might protect against the development of atopy. *Clin Exp Allergy* **30**, 1230–1234 (2000).

Wang, Q., Garrity, G. M., Tiedje, J. M. & Cole, J. R. Naive Bayesian classifier for rapid assignment of rRNA sequences into the new bacterial taxonomy. *Appl Environ Microbiol* **73**, 5261–5267 (2007).

Wang, S. *et al.* MyD88 Adaptor-Dependent Microbial Sensing by Regulatory T Cells Promotes Mucosal Tolerance and Enforces Commensalism. *Immunity* **43**, 289–303 (2015).

Wang, Y. & McCusker, C. Neonatal exposure with LPS and/or allergen prevents experimental allergic airways disease: development of tolerance using environmental antigens. *J Allergy Clin Immunol* **118**, 143–151 (2006).

Watanabe, N. *et al.* Human thymic stromal lymphopoietin promotes dendritic cell-mediated CD4+ T cell homeostatic expansion. *Nat Immunol* **5**, 426–434 (2004).

Weller, P. F. & Spencer, L. A. Functions of tissue-resident eosinophils. *Nat Rev Immunol* **17**, 746–760 (2017).

Wernroth, M.-L. *et al.* Early Childhood Antibiotic Treatment for Otitis Media and Other Respiratory Tract Infections Is Associated With Risk of Type 1 Diabetes: A Nationwide Register-Based Study With Sibling Analysis. *Diabetes Care* **43**, 991–999 (2020).

Wesche, H., Henzel, W. J., Shillinglaw, W., Li, S. & Cao, Z. MyD88: an adapter that recruits IRAK to the IL-1 receptor complex. *Immunity* **7**, 837–847 (1997).

Wesemann, D. R. & Nagler, C. R. The Microbiome, Timing, and Barrier Function in the Context of Allergic Disease. Immunity **44**, 728–738 (2016).

Wesselkamper, S. C., Chen, L. C., Kleeberger, S. R. & Gordon, T. Genetic variability in the development of pulmonary tolerance to inhaled pollutants in inbred mice. *Am J Physiol Lung Cell Mol Physiol* **281**, L1200-1209 (2001).

Wiesner, D. L. *et al.* Club Cell TRPV4 Serves as a Damage Sensor Driving Lung Allergic Inflammation. *Cell Host Microbe* **27**, 614-628.e6 (2020).

Willart, M. A. M. *et al.* Interleukin-1α controls allergic sensitization to inhaled house dust mite via the epithelial release of GM-CSF and IL-33. *J Exp Med* **209**, 1505–1517 (2012).

Williams, M. R. *et al.* Quorum sensing between bacterial species on the skin protects against epidermal injury in atopic dermatitis. *Sci Transl Med* **11**, eaat8329 (2019).

Wills-Karp, M. Neutrophil ghosts worsen asthma. *Sci Immunol* **3**, eaau0112 (2018).

Wilson, M. S. *et al.* Suppression of allergic airway inflammation by helminth-induced regulatory T cells. *J Exp Med* **202**, 1199–1212 (2005).

Wilson, R. H. *et al.* The Toll-like receptor 5 ligand flagellin promotes asthma by priming allergic responses to indoor allergens. *Nat Med* **18**, 1705–1710 (2012).

Wojno, E. D. T. *et al.* The prostaglandin $D_2$ receptor CRTH2 regulates accumulation of group 2 innate lymphoid cells in the inflamed lung. *Mucosal Immunol* **8**, 1313–1323 (2015).

Wright, S. D., Ramos, R. A., Tobias, P. S., Ulevitch, R. J. & Mathison, J. C. CD14, a receptor for complexes of lipopolysaccharide (LPS) and LPS binding protein. *Science* **249**, 1431–1433 (1990).

Xiong, E. *et al.* MZB1 promotes the secretion of J-chain-containing dimeric IgA and is critical for the suppression of gut inflammation. *Proc Natl Acad Sci U S A* **116**, 13480–13489 (2019).

Yamamoto, M. *et al.* Essential role for TIRAP in activation of the signalling cascade shared by TLR2 and TLR4. *Nature* **420**, 324–329 (2002).

Yamamoto, M. *et al.* Role of adaptor TRIF in the MyD88-independent toll-like receptor signaling pathway. *Science* **301**, 640–643 (2003).

Yang, C. *et al.* Fecal IgA Levels Are Determined by Strain-Level Differences in Bacteroides ovatus and Are Modifiable by Gut Microbiota Manipulation. *Cell Host Microbe* **27**, 467-475.e6 (2020).

Yarur, A. J. *et al.* Serum Amyloid A as a Surrogate Marker for Mucosal and Histologic Inflammation in Patients with Crohn's Disease. *Inflamm Bowel Dis* **23**, 158–164 (2017).

Yu, D.-H. *et al.* Postnatal epigenetic regulation of intestinal stem cells requires DNA methylation and is guided by the microbiome. *Genome Biol* **16**, 211 (2015).

Zafar, H. & Saier, M. H. Gut Bacteroides species in health and disease. *Gut Microbes* **13**, 1–20 (2021).

Zaiss, M. M. *et al.* The Intestinal Microbiota Contributes to the Ability of Helminths to Modulate Allergic Inflammation. *Immunity* **43**, 998–1010 (2015).

Zhang, B. *et al.* Divergent T follicular helper cell requirement for IgA and IgE production to peanut during allergic sensitization. *Sci Immunol* **5**, (2020).

Zhang, Z. *et al.* β-Glucan exacerbates allergic asthma independent of fungal sensitization and promotes steroid-resistant TH2/TH17 responses. *J Allergy Clin Immunol* **139**, 54-65.e8 (2017).

Zhou, W. & Sonnenberg, G. F. Activation and Suppression of Group 3 Innate Lymphoid Cells in the Gut. *Trends Immunol* **41**, 721–733 (2020).

Zhou, Y. *et al.* Metascape provides a biologist-oriented resource for the analysis of systems-level datasets. *Nat Commun* **10**, 1523 (2019).